Bearing Capacity for Foundation near Slope

Kai Wing Ip

A Thesis

in

The Department

Of

Building, Civil and Environment Engineering

Presented in Partial Fulfillment of the Requirements
For Degree of Master of Applied Science at
Concordia University
Montreal, Quebec, Canada

November 2005

Your file Votre référence
ISBN: 0-494-14249-9
Our file Notre référence
ISBN: 0-494-14249-9

ABSTRACT

The bearing capacity of the foundation is a primary concern in the field of foundation engineering. The self weight of the structure and the applied loads are transferred to the soil safely and economically. The load at which the shear failure of the soil occurs is called the ultimate bearing capacity of the foundation.

Quite often, structures are built on or near a slope. This is due to land limitation, such as for bridges or for architectural purposes. The ultimate bearing capacity of the foundations for these buildings is significantly affected by the presence of the slope. Design of foundations under these conditions is complex and the information available in the literature is limited.

A numerical model was developed to simulate the case of strip foundation near slope, using the finite element technique together with the program "PLAXIS". The parameters believed to govern this behavior were examined individually to determine their effect on the ultimate bearing capacity of a strip footing. The superposition method was used in the analyses to calculate the bearing capacity factors, N_c, N_q, and N_γ, independently. The results produced by the present numerical model were compared with the available experimental data.

An analytical model was also developed for the problem stated to predict the ultimate bearing capacity of a strip footing. Design theory, design procedure and design charts are presented for practical use.

ACKNOWLEDGEMENT

I WOULD LIKE TO GIVE MY HIGHEST SINCERE THANKFULNESS TO MY THESIS SUPERVISOR, DR. ADEL M. HANNA. HIS KNOWLEDGE AND EXPERIENCE IN GEOTECHNICAL ENGINEERING HAS GREATLY AIDED IN MY RESEARCH PROJECT. WITHOUT HIS GUIDANCE, PATIENCE AND ENCOURAGEMENT, I WOULD NOT HAVE BEEN ABLE TO MAKE MY DREAM COME TRUE OF WRITING THIS MASTER'S THESIS.

I ALSO WANT TO THANK MY PARENTS MR. TAK SANG IP AND MRS. KIT YU IP CHAN, AND MY FIANCÉE DONNA YIP. THEIR FINANCIAL AND SPIRITUAL SUPPORT HAD AIDED ME IN THE PROCESS OF WRITING THIS THESIS. I HAVE BEEN ABLE TO FINISH MY STUDY AT AN ADVANCED ACADEMIC LEVEL.

TABLE OF CONTENT

FIGURES

TABLES

Symbols

α	=	Angle of slope
β	=	Angle of equivalent free surface with respected to horizontal surface
γ, kN/m^3	=	Unit weight of soil
ϕ	=	Angle of friction of soil
θ	=	Angle of radial shear zone
b	=	Distance from the edge of slope
B	=	Width of footing
c, kN/m^2	=	Cohesion parameter of soil
D_f	=	Depth of footing below ground surface
N_c	=	Bearing Capacity Factor due to cohesion of soil
N_q	=	Bearing Capacity Factor due to overburden pressure
N_γ	=	Bearing Capacity Factor due to weight of soil below the footing
N_{cq}	=	Bearing Capacity Factor due to effect of cohesion and overburden pressure
$N_{\gamma q}$	=	Bearing Capacity Factor due to effect of weight of soil and overburden pressure
R_c	=	Reduction Factor of Bearing Capacity Factor N_c
R_q	=	Reduction Factor of Bearing Capacity Factor N_q
R_γ	=	Reduction Factor of Bearing Capacity Factor N_γ
R_{D_f}	=	Coefficient of Reduction for the loss of soil mass due to the present of slope
q_u, kN/m/m	=	Ultimate Bearing Capacity per unit width per unit length

CHAPTER 1

INTRODUCTION

The bearing capacity of the foundations is a primary concern in the field of foundation engineering. The self weight of the structure and the applied loading such as: dead load, live load, wind load etc. are to be transferred to the soil safely and economically. The load at which the shear failure of the soil beneath the foundation occurs is called the ultimate bearing capacity of the foundation. The magnitude of the ultimate bearing capacity depends on the mechanical characteristics of the soil and the physical characteristics of the footing. In practice, a reasonable factor of safety is applied to the ultimate values to produce the allowable values for these foundations, depending on the uncertainty of soil behavior and the loading conditions.

Quite often, structures are built on or near a slope. This is due to land limitation or for architectural purposes. In these cases design requirements stipulate that in additional for the foundations to transfer the load safely to the underlain soil strata but also the stability of the slope after incorporating the foundations load must remain intact. Occasionally engineers are required to determine the location and depth of foundations to be built on or near slope. In these cases, design of shallow foundations becomes more complicate in modeling and accordingly in satisfying both safety and economy of these foundations.

The objective of this thesis is to present a critical review of the available literature on foundations near or in slope. A numerical model will be developed using Finite Element technique to simulate the problem stated. Sensitivity analyses will be conducted

to determine the parameters believed to govern this behavior. A superposition method is developed to calculate the bearing capacity factors, N_c, N_q, and N_γ, independently. Design theory is presented for practicing use.

CHAPTER 2

LITERATURE REVIEW

2.1 GENERAL

The ultimate bearing capacity of a foundation is defined as the maximum load that the ground can sustain. Under the working load, the foundation will experience vertical movement in the ground or settlement. When the working load reaches the ultimate bearing capacity q_u, the supporting soil will undergo a sudden shear failure.

Theories for the ultimate bearing capacity of shallow foundations were developed by employing one of the following four analytical techniques:

1. Slip line methods
2. Limit equilibrium methods
3. Limit analysis methods
4. Finite element methods.

The slip line method involves the construction of a family of shear or slip lines in the vicinity of the footing load. These slip lines represent the directions of the maximum shear stresses. The plastic slip line is bounded by rigid regions. In plane-strain cases, the normal and shear stresses along the slip line can be determined by solving the two differential equations of the plastic equilibrium and the one for yield condition.

The limit equilibrium methods were utilized by Terzaghi (1943) and Meyerhof (1951) to develop theories of bearing capacity of shallow foundations. They can best be described as approximate approaches to constructing the slip line field. The solution requires that assumptions be made regarding the shape of the failure surface and the normal stress distribution along such surface. The stress distribution usually satisfies the

yield condition and the equations of static equilibrium. Using the method of trial and error, it was possible to find the most critical location of the slip line. While, limit equilibrium method utilizes the basic philosophy of failure surface assumption, it gives no consideration to soil kinematics and equilibrium conditions. Nevertheless, the method has been the widely used owing to its simplicity and reasonably good predictions.

The limit analysis method considers the soil stress-strain relationship in an idealized manner. This idealization, termed normality or the flow rule, establishes the limit theorems on which limit analysis is based. The method offers upper and lower bound to the true solution of the problem given. The upper bound solution is calculated from a kinematically admissible velocity field that satisfies the velocity boundary condition. The lower bound solution is determined from a statically admissible stress field that satisfies the stress boundary condition, is in equilibrium, which does not violates the failure condition. If the two solutions coincide, then the methods give the true solution.

2.2 BEARING CAPACITY THEORY FOR STRIP FOUNDATION ON HORIZONTAL SURFACE

The bearing capacity of foundations on horizontal surface is calculated using the superposition method, suggested by Terzaghi (1943), in which the contributions to the bearing capacity from different soil and loading parameters are summed, as represented by the following expression:

$$q_u = cN_c + qN_q + \frac{1}{2}\gamma BN_\gamma \tag{2.1}$$

Where q_u is the maximum pressure, which can be sustained by the footing, q is the overburden or surcharge at the foundation base and N_c, N_q and N_γ are the bearing capacity factors represent the contribution of the soil cohesion, surcharge loading, and soil weight respectively.

Terzaghi (1943) proposed a theory for determination of the ultimate bearing capacity of shallow rough rigid continuous foundation supported by a homogenous, isotropic soil. He defined a shallow foundation as a foundation for which the width of the foundation, B, is equal to or less than it embedded depth. The failure surface in soil at the ultimate load as assumed by Terzaghi is shown in Figure 2.1.

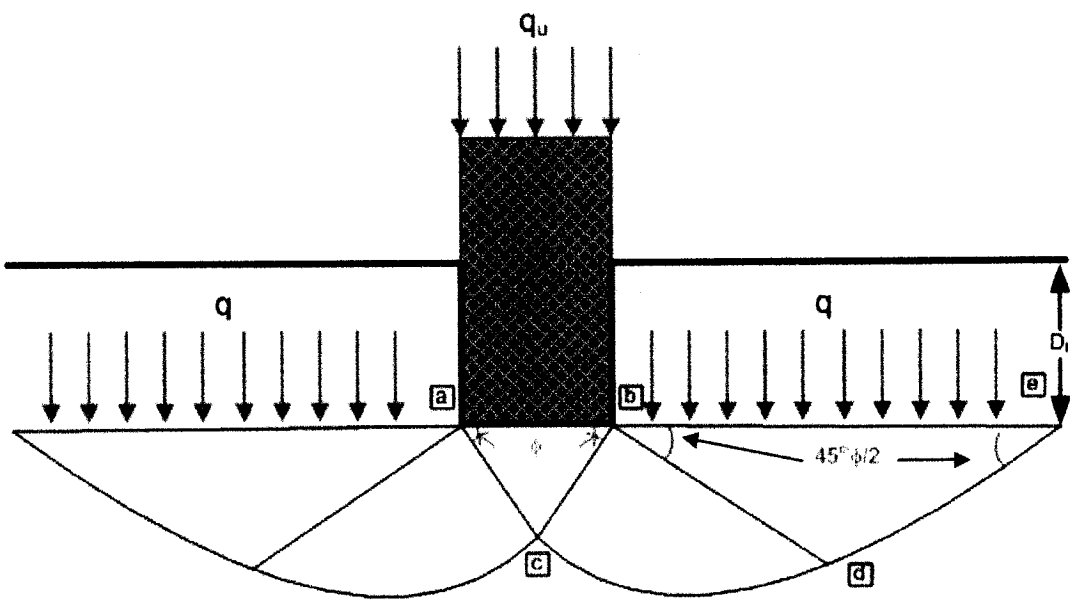

Figure 2.1. Failure plane of Terzaghi's Theory for Shallow Foundation

The wedge *abc* is the elastic zone that is located immediately below the bottom of the footing. In this region, the resistance against sliding is caused by the weight of the soil. The angle $\angle abc$ and $\angle bac$ are assumed to be equal to$\phi°$. Wedge *bcd* is the radial shear

zone with *cd* being an arc that is interpolated by a function $r_o = r_1 e^{\theta \tan\phi^\circ}$. Wedge *bde* is the Rankine passive pressure zone. The soil above the foundation base is replaced by an equivalent surcharge *q*. The slip lines in this zone intersect the surcharge at $45^\circ - \phi^\circ/2$ with horizontal.

The ultimate bearing capacity of the foundation can be easily determined by considering the faces *ac* and *bc* of the triangular elastic zone and determine the passive force on each face required to cause failure. Since the passive force is due to surcharge (*q*), cohesion (*c*), unit weight of the soil (γ), and the angle of shear resistance (ϕ°), superposition method was applying to develop the bearing capacity factors although the solution is not exact. The bearing capacity factors, N_c, N_q and N_γ, are given in terms of angle of shear resistance ϕ° as following:

$$N_q = \frac{e^{2(3\pi/4-\phi/2)\tan\phi}}{2\cos^2(45+\phi/2)}$$

$$N_c = \cot\phi\left(N_q - 1\right) \qquad \ldots (2.2a, b, c)$$

$$N_\gamma = \frac{1}{2}K_p \tan^2\phi - \frac{\tan\phi}{2}$$

Meyerhof (1951) presented a theory to predict the bearing capacity of foundations on horizontal surface, based on limit equilibrium method of analysis. The failure surface at ultimate load under strip footing as assumed by Meyerhof is shown in Figure 2.2.

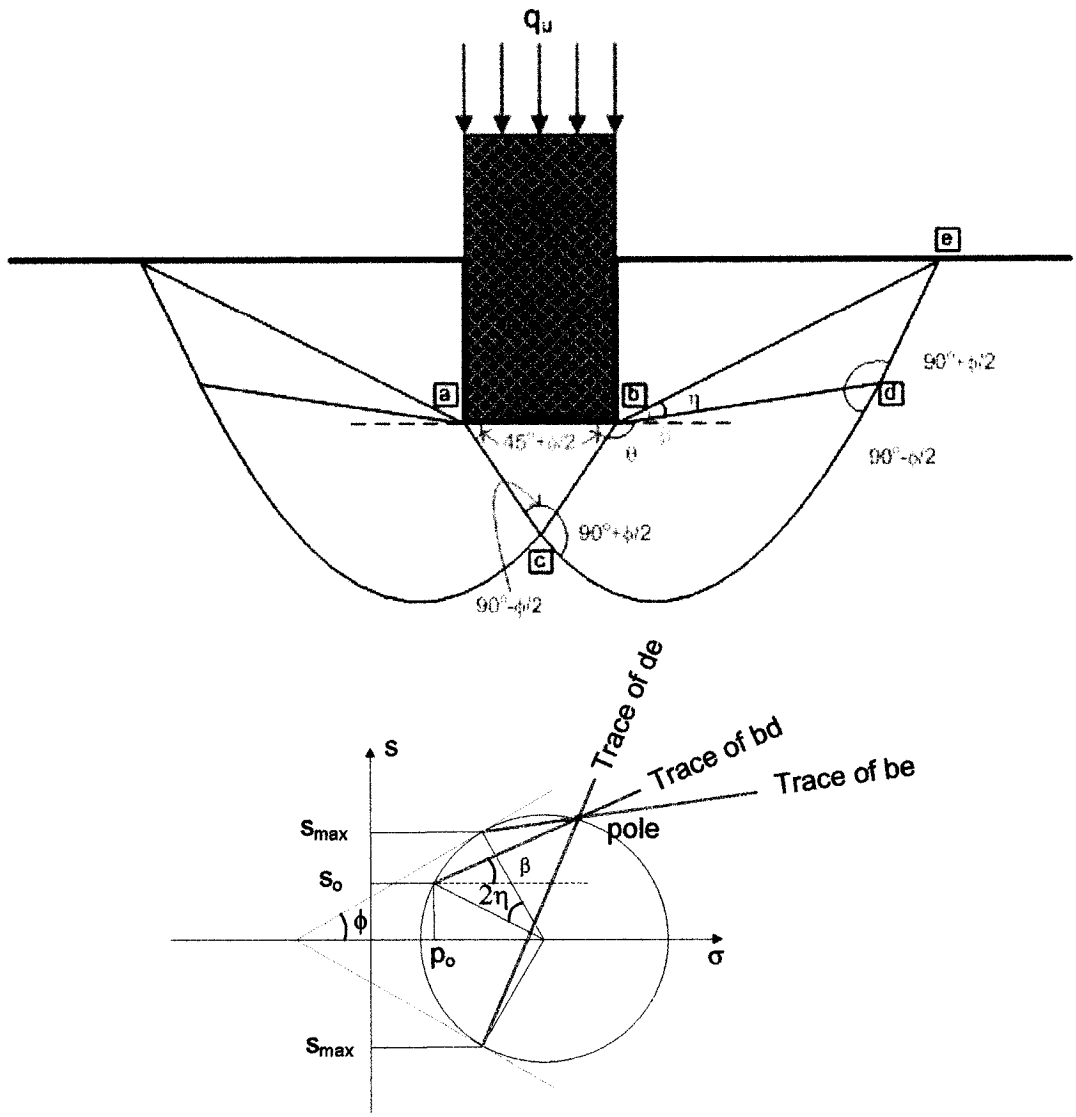

Figure 2.2. (a) Failure plane of Meyerhof's Theory for Shallow Foundation
(b) Mohr-Columb Envelope

The wedge *abc* is the elastic zone that is located immediately below the bottom of the footing. In this region, the resistance against sliding is caused by the weight of the soil. The angle $\angle abc$ and $\angle bac$ are assumed to be equal to $45^o + \phi^o/2$ according to active earth pressure theory. Wedge *bcd* is the radial shear zone with *cd* being an arc that is interpolated by a function $r_o = r_1 e^{\theta \tan\phi^o}$. This assumption fits to the practical result that is obtained from the field. Wedge *bde* is a mixed shear zone in which the shear varies

between the limits of radial and plane shear depending on the depth and roughness of the foundation. The plane *be* is referred to as an equivalent free surface. Unlike Terzaghi's theory that the soil above the foundation is assumed to be equal to an equivalent surcharge, Meyerhof considered the shear stress, s_o, along the failure surface. However, the contribution of s_o remains unknown (Figure 2.2) since it depends on the degree of mobilization of the shear strength of the soil. (η=45°-ϕ?2 for immobilized and η=0° for fully mobilized)

Meyerhof employed Terzaghi's equation of bearing capacity and derived the bearing capacity factors as following:

$$q = cN_c + p_o N_q + \frac{1}{2}\gamma B N_\gamma \qquad \ldots (2.3)$$

Where,

$$N_c = \left\{\cot\phi\left[\frac{(1+\sin\phi)e^{2\theta\tan\phi}}{(1-\sin\phi)\sin(2\eta+\phi)} - 1\right]\right\}$$

$$N_q = \left[\frac{(1+\sin\phi)e^{2\theta\tan\phi}}{(1-\sin\phi)\sin(2\eta+\phi)} - 1\right] \qquad \ldots (2.4a, b, c)$$

$$N_\gamma = \left[\frac{4P_{p\gamma}\sin(45^\circ+\phi/2)}{\gamma B^2} - \frac{1}{2}\tan(45^\circ+\phi/2)\right]$$

$$\theta = 135^\circ + \beta - \eta - \frac{\phi}{2}$$

The term p_o in Equation 2.3 is magnitude of normal stress acting on the equivalent free surface (line $\overline{be}$ of Figure 2.2). To predict the ultimate bearing capacity the degree of mobilization of the equivalent-free surface need to be assumed in order to determine the angle β^o, η and the corresponding normal stress p_o. The bearing capacity factors can be calculated from Equation 2.4a thru 2.4c.

Meyerhof (1963) presented a more general form to the bearing capacity theory to take into consideration the effect of foundation shape, load inclination and the depth of the foundation as follows:

$$q = cN_c\lambda_{cs}\lambda_{ci}\lambda_{cd} + \gamma D_f N_q \lambda_{qs}\lambda_{qi}\lambda_{qd} + \frac{1}{2}\gamma B N_\gamma \lambda_{\gamma s}\lambda_{\gamma i}\lambda_{\gamma d} \quad \ldots (2.5)$$

where

$\lambda_{cs}, \lambda_{qs}, \lambda_{\gamma s}$ = Shape Factor

$\lambda_{cd}, \lambda_{qd}, \lambda_{\gamma d}$ = Depth Factors

$\lambda_{ci}, \lambda_{qi}, \lambda_{\gamma i}$ = Inclined Load Factors

N_c, N_q & N_γ = for surface foundation condition

Table 2.1. Shape, Depth and Inclination factors given by Meyerhof (1963)

Shape Factors	For ϕ^o=0° $\lambda_{cs} = 1 + 0.2\frac{B}{L}$ $\lambda_{qs} = \lambda_{\gamma s} = 1$	For ϕ^o>10° $\lambda_{cs} = 1 + 0.2\frac{B}{L}\tan^2\left(45^o + \frac{\phi}{2}\right)$ $\lambda_{qs} = \lambda_{\gamma s} = 1 + 0.1\frac{B}{L}\tan^2\left(45^o + \frac{\phi}{2}\right)$
Depth Factors	For ϕ^o=0° $\lambda_{cs} = 1 + 0.2\frac{D_f}{B}$ $\lambda_{qs} = \lambda_{\gamma s} = 1$	For ϕ^o>10° $\lambda_{cd} = 1 + 0.2\frac{D_f}{B}\tan^2\left(45^o + \frac{\phi}{2}\right)$ $\lambda_{qd} = \lambda_{\gamma d} = 1 + 0.1\frac{D_f}{B}\tan^2\left(45^o + \frac{\phi}{2}\right)$
Inclination Factors	$\lambda_{ci} = \lambda_{qi} = \left(1 - \frac{\psi^\circ}{90^\circ}\right)^2$ $\lambda_{\gamma i} = \left(1 - \frac{\psi^\circ}{\phi^\circ}\right)^2$	

2.3 BEARING CAPACITY THEORY FOR STRIP FOUNDATIONS NEAR SLOPE

Meyerhof (1957) indicated that for a foundation located on or near the slope, the plastic zone on the side of the slope is relatively smaller than those of similar foundation on leveled ground and thus the ultimate bearing capacity of the foundation is correspondingly reduced. He presented a solution (Figure 2.3) for the ultimate bearing capacity of rough strip foundation on or near slopes that combined with those from stability analysis to form the equation as following:

$$q_{u,slope} = cN_{cq} + \frac{1}{2}\gamma BN_{\gamma q} \quad \ldots (2.6)$$

Where N_{cq} is a coefficient represents the combined effect of the cohesion of the soil and the overburden pressure and $N_{\gamma q}$ is a coefficient represents the combined effect of the shear resistance of the soil below the foundation and the overburden pressure. The above equation is applicable to foundations on or near a slope having a distance b from the top of the slope. Meyerhof provided design charts for the bearing capacity factors, N_{cq} and $N_{\gamma q}$.

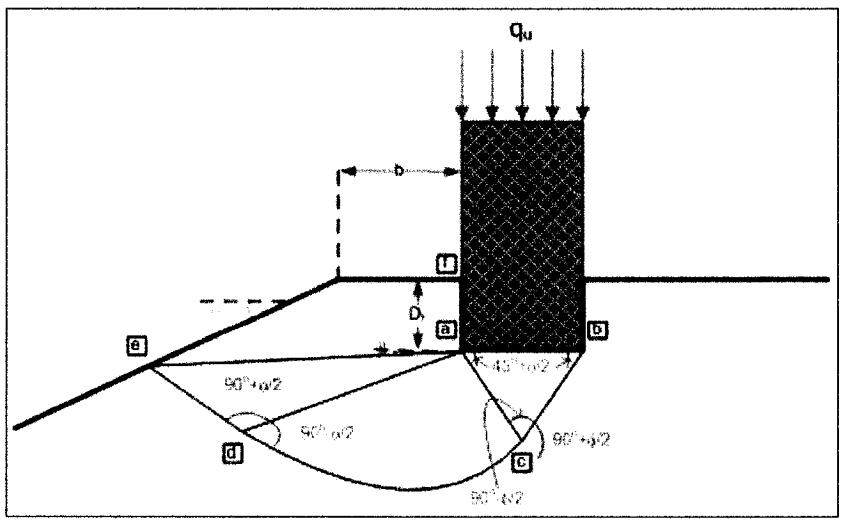

Figure 2.3. Failure plane, Meyerhof's Theory for shallow foundation near slope (1957).

It can be noted that the bearing factors depends on the distance of the foundation from the top of the slope, b, the angle of slope, $\alpha°$, the angle of shearing resistance of the soil, $\phi°$, and the depth/width ratio, D_f/B, of the foundation. While these factors decrease with increasing $\alpha°$, they will increase rapidly with the increase of the distance b. Beyond a distance of 2 to 6 times the foundation width, which depends on $\alpha°$ and D_f/B ratio, the bearing capacity becomes independent of the angle of slope and follows the theory of a foundation on leveled ground. Figure 2.4 shows the bearing capacity factor for slope having purely cohesive soil and purely cohesionless soil.

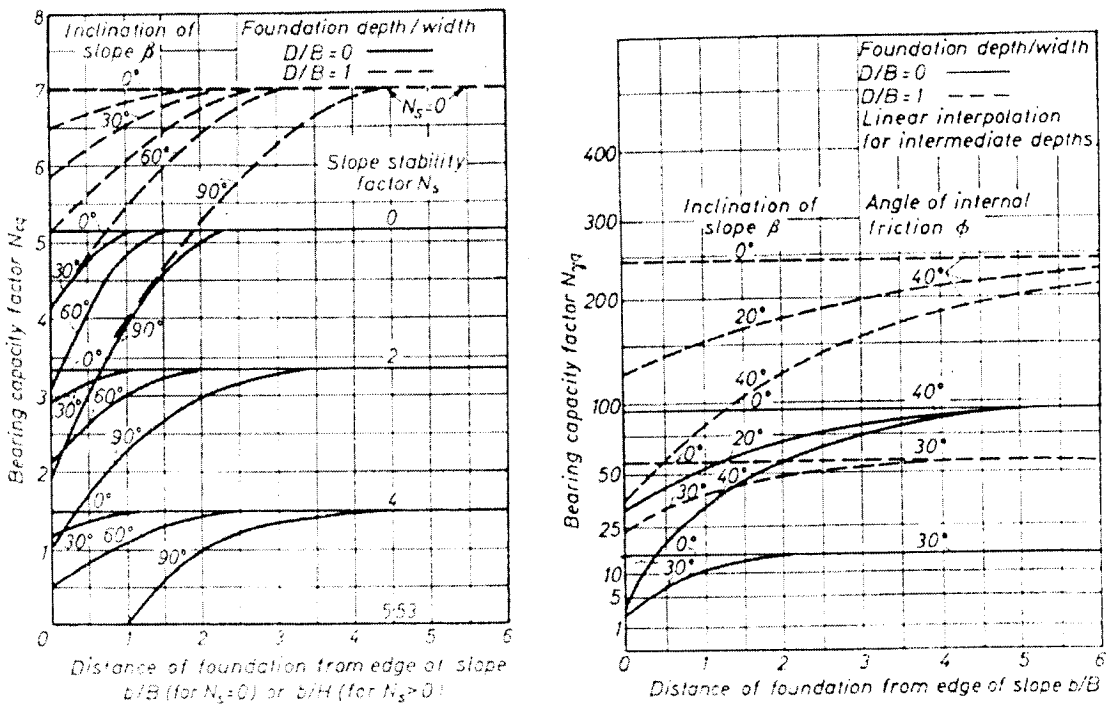

Figure 2.4. Bearing capacity factors for foundation near slope (after Meyerhof, 1957)

Shields, Bauer, Deschenes and Barsvary (1977) have conducted series of tests to compute the bearing capacity factor $N_{\gamma q}$ for a footing in cohesionless slope. The tests were conducted in a large sand box measuring 15m in length, 2m in width and 2.2 meter in height. A slope of 2 horizontal to 1 vertical was chosen because it was the standard slope of the approach fills in the Province of Ontario. The slope was made of sand at two densities, which represent compact (ϕ^{o}=37°-45°) and dense sand (ϕ^{o}=41°-50°). The angle of shear resistance of the soil sample was determined by plane-strain test, triaxial test and direct shear box. Shield et al reported that the angle ϕ° obtained by plane-strain would be best represent the actual shear strength developed in the footing. However the experimental work showed that this assumption was valid only for surface footing on dense sand. For other cases, angle ϕ° given by triaxial test or triaxial+10% (suggested by Meyerhof, 1963, to correct for the plane strain condition) give a reasonable fit between the theoretical and experimental bearing capacity. Table 2.2 shows the value of ϕ° of two sand samples.

Table 2.2 Values of angle of shear resistance used by Shield et al.

Test	**Compact Sand**	**Dense Sand**
Triaxial	37°	41°
Triaxial +10%	41°	45°
Plane-Strain	45°	48°
Direct Shear Box	45°	50°

In these experiments, footing of 0.3m in width and 2m in length located on the top of slope was loaded up to failure. The ultimate bearing capacity was recorded and the bearing capacity factors were calculated according to Meyerhof's equation (1957). Shields et al. found that the Meyerhof's theory (1957) overestimates the magnitude of the

bearing capacity. However at shallow depths close to the edge of the slope the theory are closer to the actual bearing capacity. Shields et al. presented design charts presented in Figure 2.5.

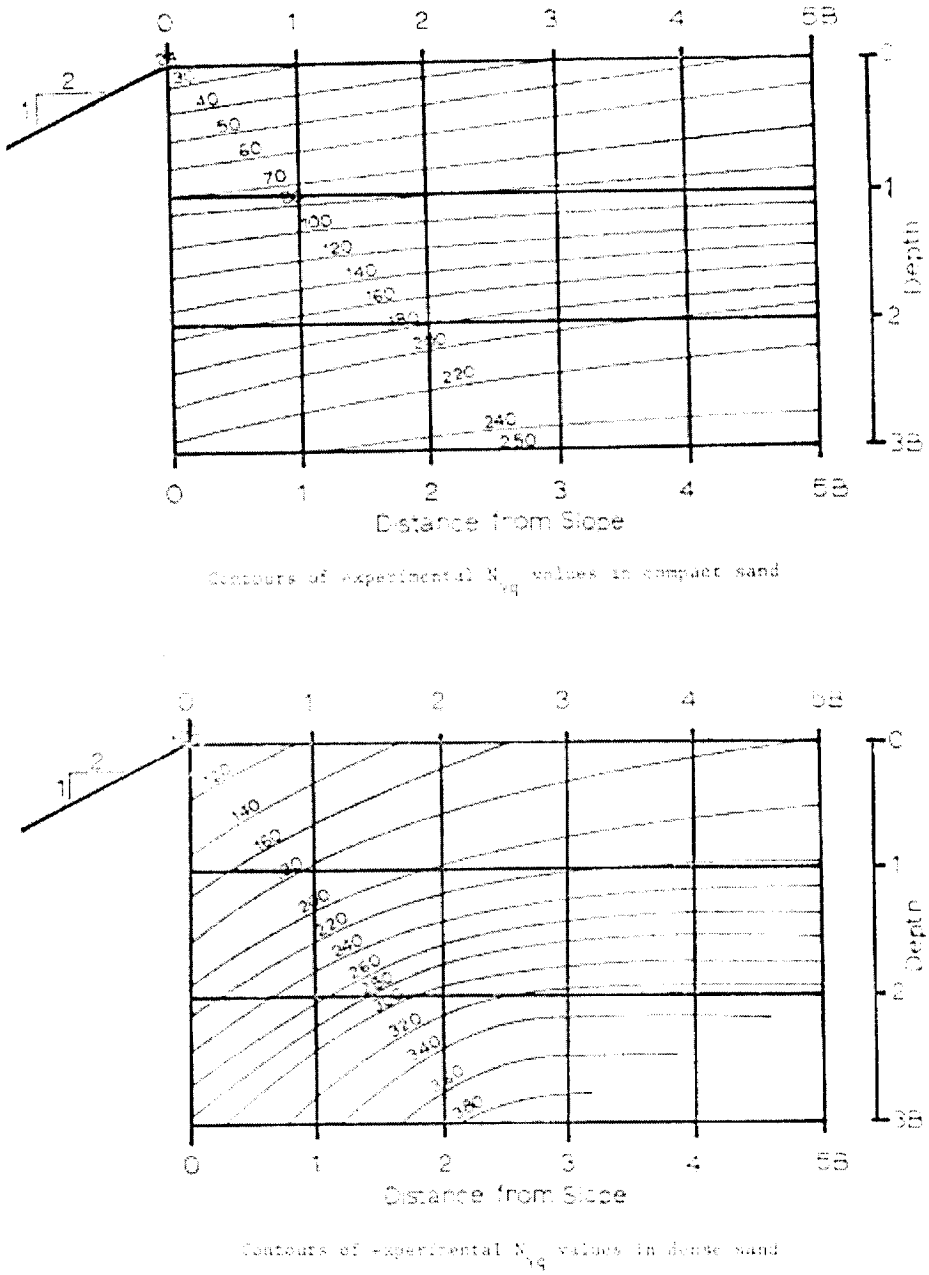

Figure 2.5. Bearing capacity factor $N_{\gamma q}$ (after Shields et al. 1977)

Andrews (1986) showed that most of the existing analyses for footings in slope, assume a non-failing zone of soil immediately beneath the footing, with the elastic zone being symmetric on either side of the footing. In contrast with the symmetry that is seen beneath footing on ground level, photographs from physical models on slopes (Peynircioglu 1948, Giroud and Tran 1971 and Kimura et al 1985) show that the failure zone are asymmetric. The failure on the side of slope is larger than the zone on the side of ground level surface. Kimura et al (1985) show that only a single wedge is formed underneath the footing, not two smaller wedges as presented in the literature. The detailed geometry of the wedge is not immediately detected and it has to be determined by trial and error. Figure 2.6 shows the geometry of the asymmetric non-failure plane beneath the footing and the typical prediction of the elastic wedge for $\phi°$=30° and 40°.

Graham, Andrews, and Shields (1987) presented an analytical method of stress characteristic for determination of the bearing capacity of a footing adjacent to cohesionless slope, particularly taking into account the stress condition immediately beneath the footing. This method allows more careful modeling of the boundary and field condition for the failure mechanism in sand mass. The solution combined the differential equation for stress transmission in plane-strain with Coulomb-Mohr relationship. The failure wedge of the soil below the foundation, suggested by Andrew (1986) was adopted. The shape and stress distribution of the failure plane extended from the failure wedge were developed as the analysis proceeds (Figure 2.7) and thus assuming the critical surfaces was not necessary. Graham et al. assumed that the effect of progressive failure on the bearing capacity of the footing can be neglected. That is at the ultimate load, the peak strength is mobilized simultaneously along the potential failure plane. It is also

assumed that the material is isotropic. The predicted values of the bearing capacity factors with the parameters representing the physical characteristics of the footing are shown in Figure 2.8

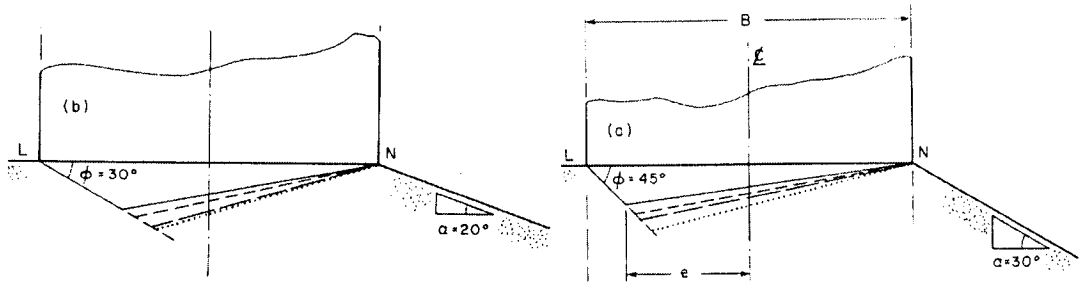

Figure 2.6. Typical result (after Andrew, 1986)

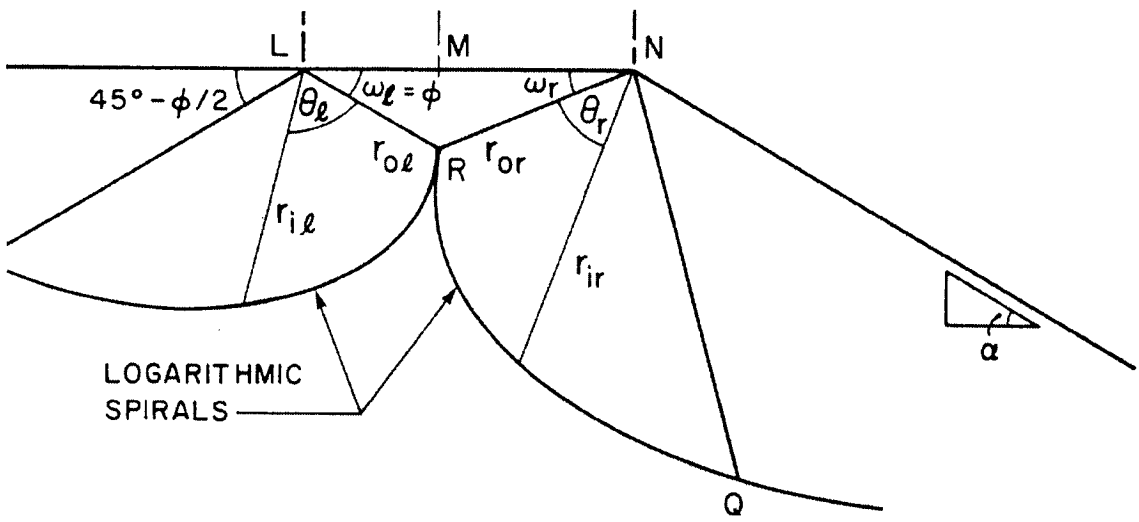

Figure 2.7. Geometry of the asymmetric failure mechanism (after Graham et al, 1987)

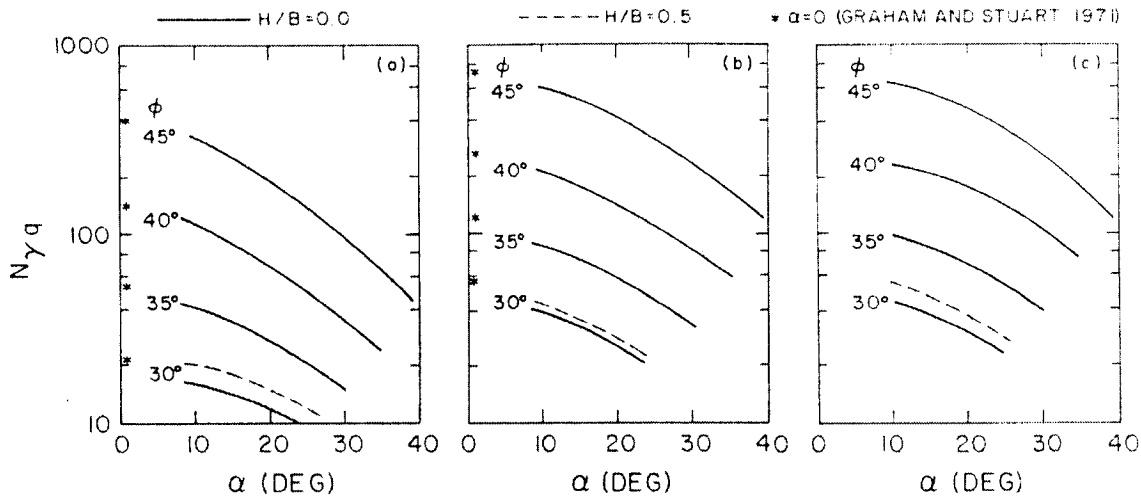

Predicted $N_{\gamma q}$-values: (*a*) $D/B = 0$; (*b*) $D/B = 0.5$; (*c*) $D/B = 1.0$. ($H/B = 0.0, 0.5$.)

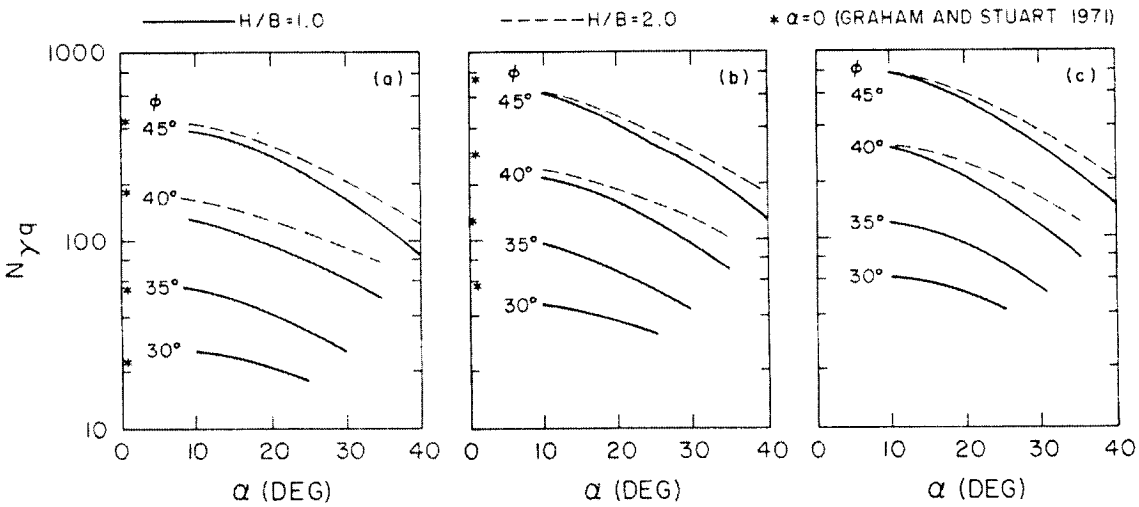

Predicted $N_{\gamma q}$-values: (*a*) $D/B = 0$; (*b*) $D/B = 0.5$; (*c*) $D/B = 1.0$. ($H/B = 1.0, 2.0$.)

Figure 2.8 Bearing capacity factors (after Graham, et al., 1987)

Tatsuoka, Huang and Morimoto (1989) claimed that the solution given by Graham et al. (1987) is mathematically corrected. However in general the behavior of sand is far different from a perfectly plastic material. Furthermore, the effect of progressive failure is significant for the case of dense sand - that is the peak load reaches

before the failure plane is fully developed. Hence, if peak strength is assumed to be mobilized along the slip line, the bearing capacity may be overestimated. In this case the assumption made by Graham et al. (1987) may lead to unsafe solution.

Gemperline (1988) proposed an empirical equation for the determination of the bearing capacity factors for footing at the top of a cohesionless slope based on the result of 215 centrifuge tests on a prototype slope model. This equation would enable foundation engineers to determine the bearing capacity factor $N_{\gamma q}$ for footing of different size and shape located in the region of a slope.

The tests were carried out with two practical slopes of 2 horizontal to 1 vertical and 1.5 horizontal to 1 vertical, sand with nine different values of shear resistance, and various *b/B* (distance from the top of slope to footing width), *D/B* (embedded depth to footing width), and B/L ratio (width/length of the footing). Based on 215 tests, Gemperline proposed an empirical formula for determining the bearing capacity factor $N_{\gamma q}$ that is used in Meyerhof's theory as follows:

$$q_u = \frac{1}{2}\gamma B N_{\gamma q} \qquad \ldots (2.7)$$

Where:

$$N_{\gamma q} = f_\phi \times f_B \times f_{D/B} \times f_{B/L} \times f_{D/B,B/L} \times f_{\beta,b/B} \times f_{\beta,b/D,D/B} \times f_{\beta,b/B,B/L} \qquad \ldots (2.8)$$

Where ϕ= angle of shear resistance

β= angle of slope

Furthermore

$$f_\phi = 10^{(0.1159\phi - 2.386)} \qquad \ldots (2.9a)$$

$$f_B = 10^{(.34 - .2\log_{10} B)} \qquad \ldots (2.9b)$$

$$f_{D/B} = 1 + 0.65(D/B) \qquad \ldots (2.9c)$$

$$f_{B/L} = 1 - 0.27(B/L) \quad \ldots (2.9d)$$

$$f_{D/B,B/L} = 1 + 0.39(D/L) \quad \ldots (2.9e)$$

$$f_{\beta,b/B} = 1 - 0.8\left[1 - (1 - \tan\beta)^2\right]\left\{2/\left[2 + (b/B)^2 \tan\beta\right]\right\} \quad \ldots (2.9f)$$

$$f_{\beta,b/D,D/B} = 1 + 0.6(B/L)\left[1 - (1 - \tan\beta)^2\right]\left\{2/\left[2 + (b/B)^2 \tan\beta\right]\right\} \quad \ldots (2.9g)$$

$$f_{\beta,b/B,B/L} = 1 + 0.33(D/B)\tan\beta\left\{2/\left[2 + (b/B)^2 \tan\beta\right]\right\} \quad \ldots (2.9h)$$

Saran, Sud, and Handa (1989) presented analytical solutions to predict the ultimate bearing capacity of footing adjacent to slope using two different analytical approaches: limit equilibrium and limit analysis.

In the limit equilibrium approach, footing was assumed to be a shallow strip footing having rough base and the soil above the base was replaced by an equivalent uniform surcharge, which implies that the soil above the footing has no shear resistance. The failure mechanism on the side of slope was assumed and the shear strength of the soil on the other side was not fully mobilized. The failure region is divided into two zones, (Figure 2.9). Zone I represents an elastic region and zone II a combination of radial and passive shear bounded by a logarithmic spiral arc. The shear stress on the flat side is characterized by mobilization factor m and its shear resistance is expressed as $\tau = m(c + \sigma \tan\phi)$. The degree of mobilization is calculated by determining the equilibrium of the elastic wedge (Zone I) and of the radial and passive shear zone (Zone III) with different value of m. A common value of m represents the mobilization of the failure plane on the side of flat ground. Superposition method was used to compute the bearing capacity factors N_c, N_q and N_γ, independently as following:

$$N_c = \frac{P_{pc} + P_{pmc}}{cB} + \frac{(1+m)\sin\phi\sin\phi_m}{\sin(\phi+\phi_m)}$$

$$N_q = \frac{P_{pq} + P_{pmq}}{\gamma D_f B} \qquad \ldots (2.10a, b, c)$$

$$N_\gamma = \frac{2P_{p\gamma} + 2P_{pm\gamma}}{\gamma B^2}$$

Where: the subscript "$_m$" represents the passive earth pressure.

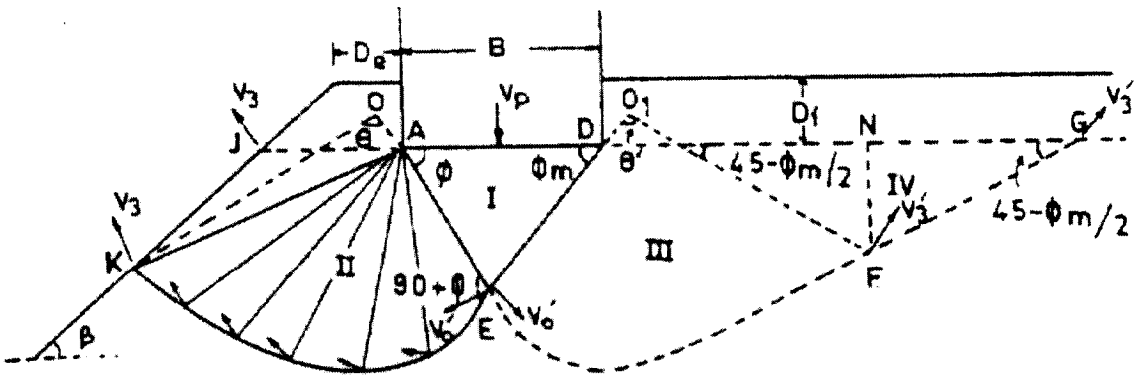

Figure 2.9. Assumed failure mechanism (after Saran et al. 1989)

In the limit analyses approach, the failure mechanism was taken similar to that adopted in the limit equilibrium analysis and is kinematically admissible with no geometric changes during plastic flow. The soil mass is assumed to be ideally plastic and no plastic strain occurs in plane strain condition. Coulomb's yield criterion is valid. A constant degree of shear stress mobilization occurs throughout the failure mechanism. The bearing capacity equation in the limit analysis is obtained by equating the total rate of energy dissipated to the total rate of work done and is given as following:

$$N_c = \frac{2\sin\phi_m \sin\phi}{\sin(\phi+\phi_m)} + \sec\phi \frac{\sin\phi_m}{\sin(\phi+\phi_m)}\left[\frac{e^{2\theta\tan\phi}-1}{\tan\phi}\right]$$
$$+\sec\phi_m \frac{\sin\phi}{\sin(\phi+\phi_m)}\left[\frac{e^{2(135-\phi_m/2)\tan\phi_m}-1}{\tan\phi_m}\right] \quad \ldots (2.11a)$$
$$+\sec\phi_m \frac{\sin\phi}{\sin(\phi+\phi_m)}\left[\frac{\sin(45-\phi_m/2)\cos\phi_m e^{2(135-\phi_m/2)\tan\phi_m}}{\cos(180+\phi_m/2)}\right]$$

$$N_q = \left(\frac{b}{B}+\frac{1}{2}\frac{D_f}{B\tan\beta}\right)\sec\phi e^{\theta\tan\phi}\cos(180-\theta-\phi)+ \quad \ldots (2.11b)$$
$$2\sec\phi_m \frac{\sin\phi}{\sin(\phi+\phi_m)} e^{2(135-\phi_m/2)\tan\phi_m}\cos^2\left(45-\frac{\phi_m}{2}\right)$$

$$N_\gamma = \frac{\sin^2\phi_m \sec\phi}{\sin^2(\phi+\phi_m)(9\tan^2\phi+1)}\left\{e^{3\theta\tan\phi}[3\tan\phi\cos(\theta+\phi)+\sin(\theta+\phi)]-4\sin\phi\right\}$$
$$+\cos(180-\theta+\phi)\left[\left(\frac{b+\frac{D_f}{\tan\beta}}{B}\right)^2 \frac{\sin(180-\theta-\phi)\sin\beta}{\sin(\beta+\theta+\phi-180)}\right]\sec\phi e^{\theta\tan\phi}$$
$$+\sec\phi_m \frac{\sin^2\phi}{\sin^2(\phi+\phi_m)(9\tan^2\phi_m+1)}\left\{e^{3(135-\phi_m/2)\tan\phi_m}[3\tan\phi_m\cos(135+\phi_m/2)+\sin(135+\phi_m/2)]-4\sin\phi_m\right\}$$
$$+2\sec\phi_m \frac{\sin\phi}{\sin(\phi+\phi_m)}\sin(45-\phi_m/2)e^{3(135-\phi_m/2)\tan\phi_m}\cos^2(45-\phi_m/2)-\frac{\sin\phi\sin\phi_m}{\sin(\phi+\phi_m)}$$
$$\ldots (2.11c)$$

Garnier, Ganepa, Corte and Bakir (1994) proposed an experimental study on strip foundation near slope to evaluate the coefficient of reduction of bearing capacity due to slope effect. Three slope models of 3 vertical to 2 horizontal, 2 vertical to 1 horizontal and 3 vertical to 1 horizontal were prepared with cohesionless material having angle of shear resistance being equal to 40.5°. The width of the strip footing was 0.9 meter and was placed on the ground surface near the slope, so that surface foundation condition was considered. Loads were applied on the model footing at difference distance

from the edge of slope. The peak load at the time of failure was measured and the coefficient of reduction of bearing capacity was calculated as the percentage of the reference peak load (flat surface model). These results were plotted in Figure 2.10.

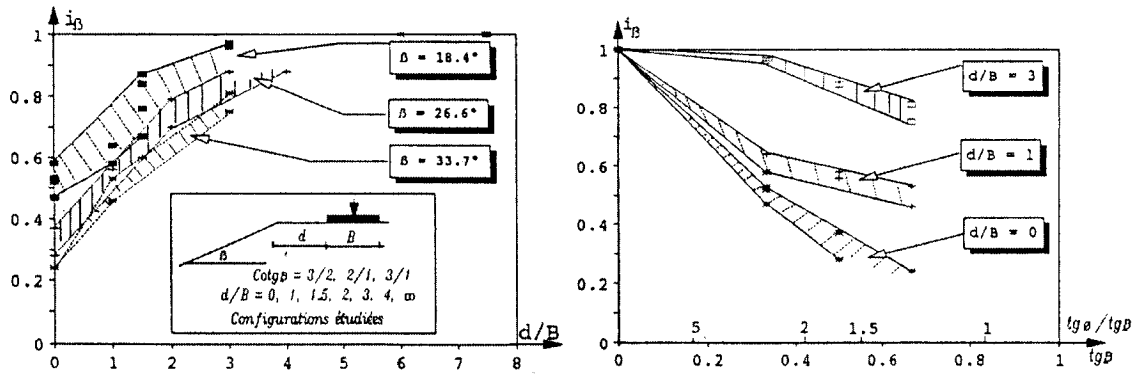

Figure 2.10. Reduction coefficient i_β for bearing capacity factor $N_{\gamma q}$ (after Garnier et al. 1994). Note that the terms $tg\phi$ and $tg\beta$ represent the function of $tan(\phi)$ and $tan(\beta)$ respectively.

For different slope model (3/2, 2/1 and 3/1), it was found that the bearing capacity of the footing was not practically different from the value of distance/width ratio (b/B) greater than 6 due to the effect of slope. For the identical distance from the slope, the coefficient of reduction decreases when the angle of slope increases. Based on the results of these tests, the coefficient of reduction was found to be always greater than 0.2 even with a test model having steeper slope (3 vertical to 2 horizontal).

Figure 2.11 shows the coefficient of reduction for three cases of footing location (b/B=0, 1 and 3). It shows clearly that the effect due to the value of angle of slope is significant when b/B is smaller than 3. It can be also noted that for footing at the edge of the slope the reduction varies nearly linearly with respected to $tan(\beta)$.

An expression for the coefficient of reduction for bearing capacity of foundations near slope was proposed as follows:

$$i_\beta = 1 - \left[1.8\tan\beta^\circ - 0.9\tan^2\beta^\circ\right]\left(1 - \frac{b}{6B}\right) \qquad \text{for b/B} < 6$$

$$i_\beta = 1 \qquad \text{for b/B} > 6 \qquad \ldots (2.12)$$

The failure mechanism of the soil under the footing model was observed and schematically presented in Figure 2.11. Zone I is the elastic triangular wedge developed underneath the footing base. Zone II is the radial shear zone having arc followed approximate log-spiral function. Zone III is the mixed shear zone extend from the log-spiral arc in Zone II. The angle of the slip line to the horizontal in this zone was found to be zero when the footing was at or closer to the edge of the slope. It increases with the increase of the distance between the footing and the edge of the slope. It was also observed that the elastic wedge underneath the footing was slight asymmetric compared to those of horizontal surface. As the footing was far away from the edge of slope, this zone became symmetric.

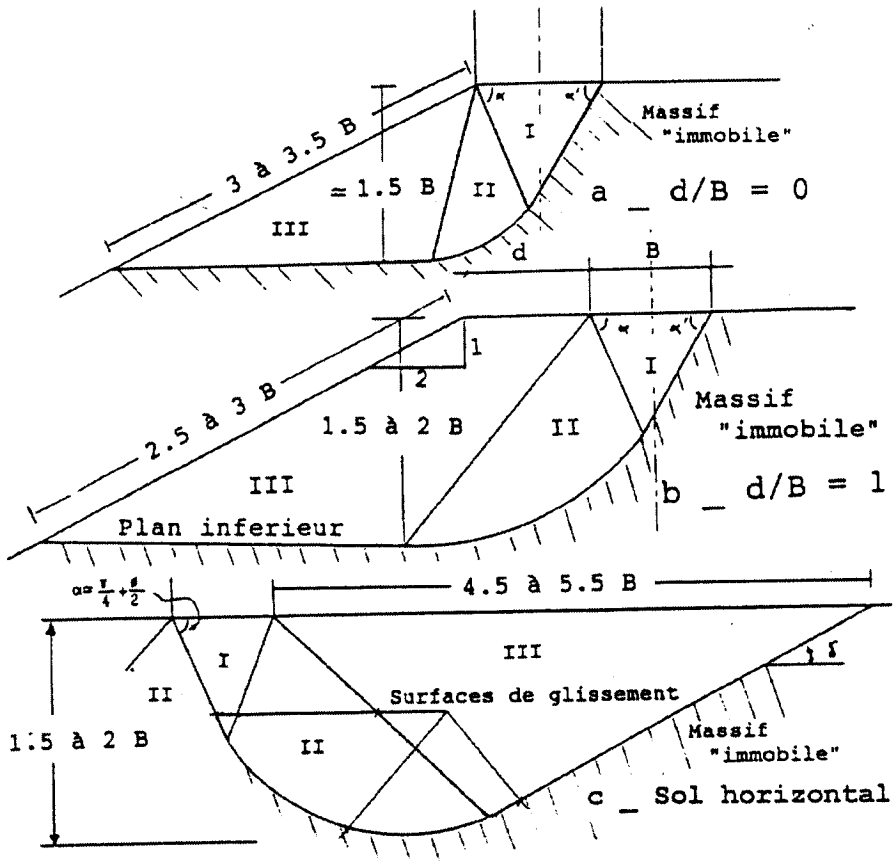

Figure 2.11. Schematic failure mechanism (Garnier et al. 1994)

2.4 DISCUSSIONS

Theories of Meyerhof (1957) and Graham et al (1987), and the experimental work from Shields et al. (1977), Gemperline (1988) and Garnier et al. (1994) provided the design chart needed to predict the magnitude of $N_{\gamma q}$. However these values are only valid for a limited range of footing location and embedded depth. Method of Gemperline has provided a mathematical solution, which is valid for different size and different horizontal and vertical location of the footing. The experimental work of Meyerhof (1957) and Shield et al. showed that soil with different value of $\phi°$ leads to bearing capacity with respect to the distance of the footing.

While most of the theories developed for foundations near slope are for cohesionless material, Meyerhof presented a solution for the case of pure cohesive soil ($\phi°$=0°). Thus for cohesive-frictional material, Equation 2.6 may not be capable to predict the ultimate bearing capacity of footing on these materials.

The solutions of Saran et al. (1989) are valid only for D_f/B=0 to 1 and b/B = 0 to1. For other footing locations and embedded depths, the values of bearing capacity factors are not accurately predicted.

The purpose of this thesis is to develop a numerical model to simulate the case of shallow, strip foundation near a slope. The model should be capable to measure the ultimate bearing capacity of these footing and accordingly the coefficient for bearing capacity factors N_c, N_q, and N_γ. Coefficient of reduction in bearing capacity factors will be introduced to take into account the effect of slope in the general bearing capacity theory for shallow foundation. Sensitivities analysis will be conducted on the governing parameters. Design charts are presented.

CHAPTER 3

NUMERICAL MODEL

3.1 GENERAL

A numerical model was developed using the Finite Element technique and the computer program "PLAXIS". PLAXIS was developed in 1987 in Netherland. This powerful program covers most of the problem in geotechnical engineering. It is capable to simulate the geometry of the foundation, as well as the soil and the loading conditions. Solutions produced by finite element method of analyses are widely acceptable in current industry.

The objective is to evaluate the bearing capacity of a strip footing near the slope; specifically, to determine the contribution of b/B (distance from edge of slope to foundation width) & angle of slope $\alpha°$ on the bearing capacity of these footings. Accordingly, a strip footing was considered near a slope having a maximum angle of slope limited to 30° (Meyerhof 1957). The footing was tested at different ratio of b/B.

3.2 PROBLEM DEFINITION

In common practice, a foundation has a form of a long, rectangular concrete block (strip footing) standing on or embedded in the ground. The force acting on the footing is uniform along the footing length. As the result, a two-dimensional finite element model is sufficient to develop the problem for the case of a continuous footing near the slope. This model assumes that the angle of slope is uniform across the footing length. The displacement and strain in the direction of footing length are zero; however the normal stresses are taken into account.

By trial and error using the upper and lower limit of soil parameters and footing location, the effective area extended up to 7 meters in the horizontal direction and 5 meters in the vertical direction. Beyond these distances, the total displacements as well as effective stresses were nearly unchanged. For conservative reason, the soil cluster of 25m width by 7m depth with a top of the slope at 10m from the left constituted the model under investigation.

To perform finite element calculation, the model was divided into finite number of triangular elements. A 15-node, triangular element was used in the finite element mesh. They are accurate elements that have produced high quality stress results for problem of soil collapsing. It provided a fourth order interpolation for displacements and the numerical integration involves twelve stress points. A denser mesh was generated along the footing-soil interfaces and the horizontal surface adjacent to the slope because the deformation of these areas is relatively more critical. The deformation of the soil at failure can be accurately measured. Figure 3.1 presents a sample of a finite element mesh of the numerical model defined in computer program.

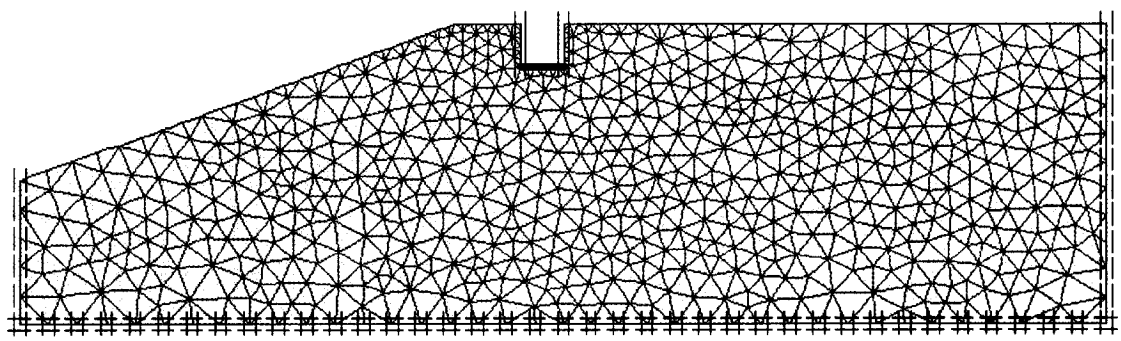

Figure 3.1. Finite Element Mesh.

3.2.1 Boundary Condition

In this model, the boundaries for the finite element mesh are shown in Figure 3.2. In this Figure, the line 0-4 and 3-2 are the "virtual" boundaries of the slope. In reality, the inclined surface extends infinitely to the left direction and the horizontal surface extends infinitely to the right direction. It should be mentioned here that these boundaries were chosen to be far from the zone, where the failure mechanism will take place and the stresses remained unchanged during loading. To simulate this scenario and limit the size of the model in finite element method, these two edges were defined in such a way that no horizontal movement, u_x=0, was allowed (horizontal fixity) and thus the model's consistency was satisfied. The same concept was applied on the bottom edge except that both horizontal and vertical movement, u_x and u_y, are zero (horizontal and vertical fixity).

In case of the footing having the embedded depth greater than zero, the slope model becomes inconsistent due to the unstable cluster edges (edges 5-11 and 6-12). These edges collapse immediately after the loading is applied. In reality, the soil at the side edges of the block-like footing has no horizontal movement. To simulate this scenario and satisfy the consistency, horizontal fixity was defined on both edges.

The footing in this model is a rigid rough strip footing had a dimension of 0.5, 1 and 1.5 m width, B. The footing was considered weightless. The following table shows the properties of the model footing used in the present investigation.

EA	5000000 kN/m
EI	8500 kN.m^2/m
Equivalent depth, d	.143m
Poisson Ratio, ν	0.3
Unit weight, w	0 kN/m/m

Table 3.1. Footing Properties

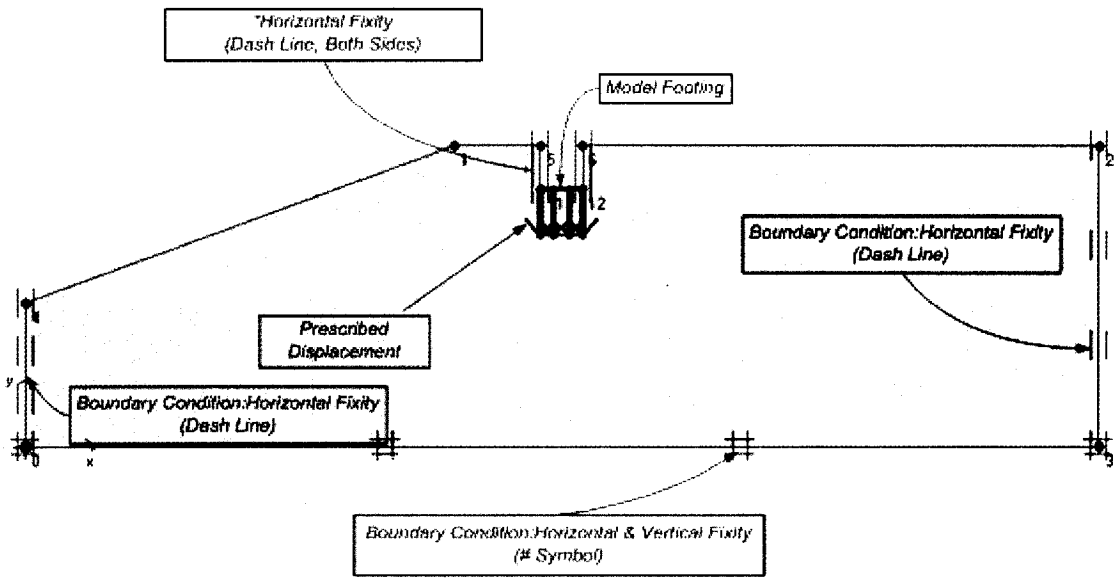

Figure 3.2. Boundary condition for the numerical model.

3.2.2 Constitutive Laws

The strength characteristic of the soil is modeled using Mohr-Coulomb failure criteria. This model is widely used in geotechnical engineering, especially in dealing with foundation problem. The Mohr-Coulomb failure criterion is defined in terms of cohesion and angle of shearing resistance (c and $\phi°$), together with a material density. These parameters are well known in engineering practice and it can be easily obtained from the results of laboratory tests. In addition, the following assumptions are made:

1. Soil is a elastic-plastic material
2. Stiffness, E, does not depend significantly on the stress level, which means that it remains constant throughout testing.
3. Cohesion, c, does not vary with depth.
4. Soil is homogenous and isotropic.

The soil parameters with their standard units and the soil properties are listed below. Note that in this model the soil was introduced as a rigid material thus general shear failure was expected.

E	: Young's Modulus	13000 kN/m^2
ν	: Poisson's ratio	0.3
ϕ	: Angle of Friction	5° to 50°
c	: Cohesion	0 and 5 kN/m^2
ψ	: Angle of Dilantancy	0°
γ	: Unit weight of model soil	18 kN/m^3

Table 3.2. Soil parameters.

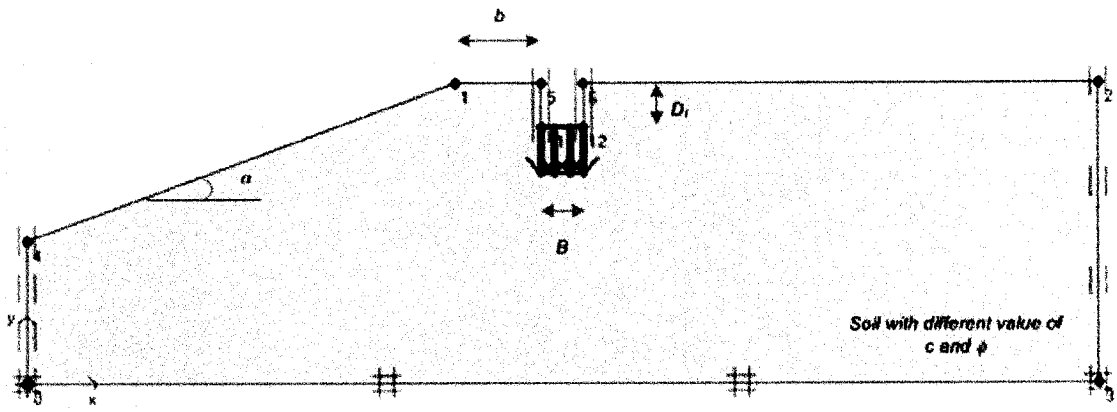

Figure 3.3. Geometry of the problem

Figure 3.3 presents the configuration of the problem under investigation and the corresponding variables that were assigned in the numerical model. $\alpha°$ represents the angle of slope of the model. The tests were conducted with different value of the angle $\alpha°$ in order to evaluate the variation of the bearing capacity factors due to slope effect. B represents the width of the footing and b represents the distance of the footing from the edge of slope. Note that the distance b was measured, according to Meyerhof's theory,

between the top of slope and the footing edge which face to the side of slope. D_f represents the embedded depth of the footing.

3.3 TEST PROCEDURE

The parameters $\alpha°$, b/B, D_f, c, $\phi°$, and γ are the input data of the finite element model. Six slope models with $\alpha°$ equal to 5°, 10°, 15°, 20°, 25° and 30° were considered. The case of $\alpha°$ equal to 0° was taken as the case of foundation on surfaced ground. For each slope model, the footing was placed in different location in horizontal direction. This location was based on the b/B ratio, which was assigned to be equal to 0, 1, 2, 3, 4 and 6. The variation of the ultimate bearing capacity with respect to the location of footing in horizontal direction can be observed. Note that a footing width of one meter were defined to run all tests with different soil parameters; a width of 0.5 and 1.5 meter were defined to run the tests with D_f=0m and selective soil parameters. For every case the embedment depth of the footing was assigned to be equal to 0, 0.5 and 1.0 in order to evaluate the bearing capacity factor due to overburden pressure. In this investigation a total of 108 tests were performed. In addition, two designate slope problems with different soil and footing parameter were defined. The purpose is to verify if the proposed analytical model satisfies the typical foundation problem. The characteristic of these test models are tabulated in Table 3.3.

46 sets of test soil ($\phi°$=5° to 50°) were entered into each test model. Note that the slope angle $\alpha°$ remained equal or less than the angle of shearing resistance $\phi°$ of the soil to maintain the stability of the slope. Figure 3.4 summarizes the value of input parameters that were assigned in the test model.

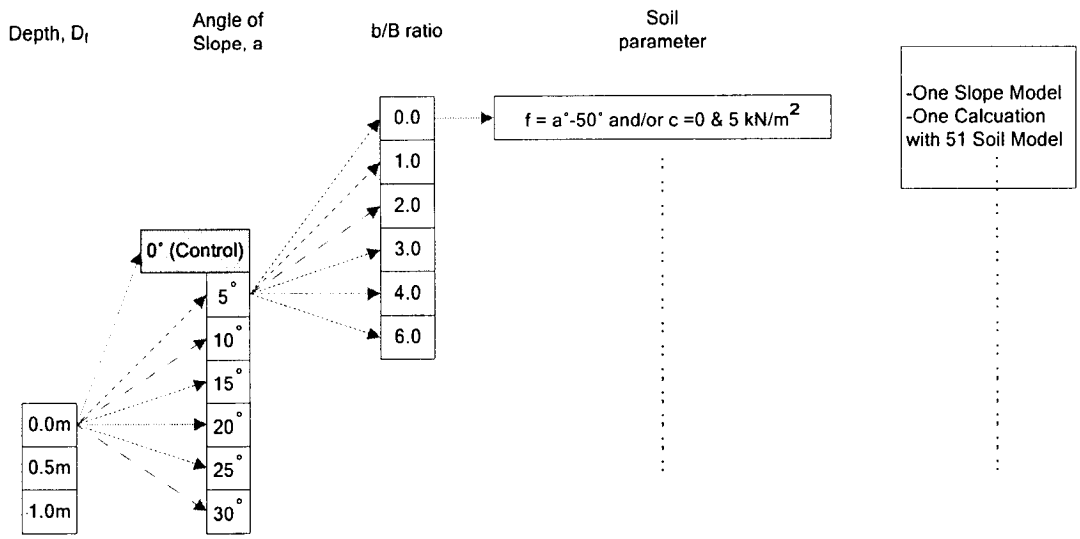

Figure 3.4. Input parameters for the determination of bearing capacity factors.

Table 3.3. Cases considered

	#1	#2
ϕ	α° to 50°	α° to 50°
c	10 kN/m^2	25 kN/m^2
γ	18 kN/m^3	
D_f	2	0.5
B	1	1.5
b/B	0, 3, and 6	

Superposition method was used to determine the ultimate bearing capacity due to cohesion, overburden pressure and shear resistance below the footing. For example, to calculate the ultimate bearing capacity due to shear resistance below the footing, q_{u,N_γ} the cohesion of soil "c" and the embedment depth of the footing "Df" were assigned a value of zero. Thus the Equation 2.1 can be simplified as following:

$$q_u = cN_c + \gamma DN_q + \frac{1}{2}\gamma BN_\gamma = (0)N_c + \gamma(0)N_q + \frac{1}{2}\gamma BN_\gamma = \frac{1}{2}\gamma BN_\gamma = q_{u,N_\gamma} \quad \ldots \quad (3.1a)$$

To determine the ultimate bearing capacity due to cohesion, the unit weight of soil γ and the embedment depth of the footing "D_f" were assigned a value of zero. Thus the Equation 2.1 can be simplified as following:

$$q_u = cN_c + \gamma D N_q + \frac{1}{2}\gamma B N_\gamma = cN_c + (0)(0)N_q + \frac{1}{2}(0)BN_\gamma = cN_c = q_{u,N_c} \quad \ldots (3.1b)$$

Finally, to determining the ultimate bearing capacity due to overburden pressure the following equation was used:

$$q_u = q_{u,N_c} + q_{u,N_q} + q_{u,N_\gamma} = cN_c + \gamma D N_q + \frac{1}{2}\gamma B N_\gamma = (0)N_c + \gamma(D_f)N_q + \frac{1}{2}\gamma B N_\gamma = q_{u,N_q} + q_{u,N_\gamma} \quad \ldots (3.1c)$$

Where q_u is the ultimate load and q_{u,N_γ} has been determined previously. The q_{u,N_q} can now be determined by subtracting q_{u,N_γ} from q_u.

Two types of loading system can be defined in numerical model: prescribed displacement and distributed force. Both systems provide similar result. In this investigation, prescribed displacement was used to apply the load on the footing. As a result of the prescribed displacement, the corresponding resultant force at the center of the footing was recorded. The program repeats this step by increasing the vertical displacement until the soil reached failure. The resultant force at that time was used to identify the ultimate bearing capacity of the footing.

For each test, the soil parameter (c, $\phi°$, and γ), the intermediate prescribed displacement and the corresponding resultant force were recorded regularly until in the foundation has reached failure. Figure 3.5 shows displacements vs. resultant force. It can be noted from this figure that the maximum resultant force or the ultimate bearing capacity can be found at the first local maximum of the curve. This value was reported herein as the ultimate load.

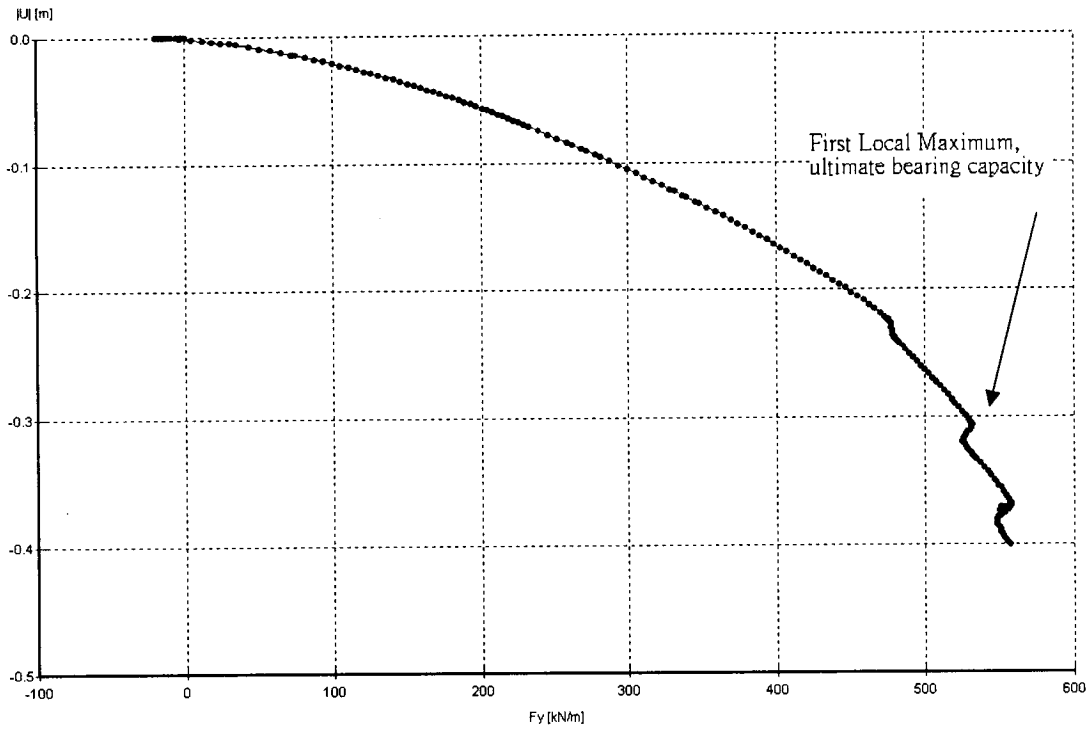

Figure 3.5. Displacement vs. resultant force

3.4 TYPICAL OUTPUT

The size and shape of failure plane below the foundation can illustrate physically the influence of the slope angle on the deduced bearing capacity. In order to clearly demonstrate the differences in the failure plane due to the effect of slope angle $\alpha°$, *b/B* ratio, as well as the soil properties ($\phi°$ and *c*), the case of soil with $\phi° = 30°$ and 40° with two different physical characteristics of the foundation are chosen for comparison. The deduced failure mechanisms are shown in Figures 3.6 through 3.15. Note that no displacement was found on or near the boundary of the numerical model. This concludes that no additional stress was generated by this constraint near the boundaries.

It can be noted that if the foundation is located close to the edge of the slope, the soil below the foundation tends to move toward the slope, since it has less shear resistance. In Figure 3.6a and 3.6b, the influence area concentrates mainly on the side of

the slope. The failure slip line follows similar log-spiral shape, but its degree of curvature is less than that for horizontal surface. According to the failure plane suggested by Meyerhof, the depth of failure plane in the case of foundation on horizontal surface extends approximately one time the footing width ($1B$). In the test model (i.e.: Figure 3.6b) however, the depth the failure plane extends approximately $2B$. This is due to the fact that the soil in the vicinity of the slope is less confined and accordingly, it can move relatively freely far away and deeply from the footing. This causes the degree of curvature becoming lower in this situation.

When the foundation is located $2B$ from the edge of the slope, the ultimate bearing capacity of the foundation increases as expected. The slope model (Figure 3.8b) shows that the displacement of the soil occurs slightly on the side of ground surface. The depth of the failure plane reduces to $1.5B$. It illustrates the fact that the degree of confinement on the side of the slope increases and part of the stress due to the footing begins being governed by soil on the side of the ground surface.

By locating the footing further away from the edge of slope, the influence of the slope is vanishing. Figure 3.9b and 3.10b show that no displacement occurs on and pass through the slope surface. The failure plane becomes symmetric, which illustrates that the stress is spread on both side of the footing. Also, its depth reduces to approximately $1B$, which is similar to the case of footing on the horizontal surface.

The reduction in ultimate bearing capacity due to inclination can be illustrated by slope model with $\alpha°=10°$ and $\alpha°=30°$.

As mentioned in previous section, the curvature of the failure surface becomes more linear and the slip line extends to the slope surface when the foundation is located

near the slope. This is found to be more significant when steeper slope presents. In Figure 3.6d, the failure surface follows straight line rather that spiral curve. In Figure 3.6c, in which $\phi°$=30°, such situation becomes more obvious, as slope will remain stable as long as $\alpha° < \phi°$. If the angle $\phi°$ is equal to or less than angle of slope $\alpha°$, slope sliding occurs on the slope surface (shallow slope failure) under certain circumstance such as external force acting on the top of the slope. It can be concluded that for such steep slope, the foundation fails under shallow slope failure rather than foundation failure.

The increase in the angle of the slope increases the required distance b where the bearing capacity becomes independent of the slope. Figure 3.9b and 3.9d illustrate the required distance b with respect to $\alpha°$. For $\alpha°$ =10°, soil displacement occurs far away from the slope while there is still some displacements occurring on the slope when $\alpha°$ =30°.

When the foundation is located at a shallow depth from the ground surface, the effect of the slope inclination is more significant.

When the footing is built at D_f=0 m (Figure 3.6a), the failure surface extend to the slope surface at approximately 2.25 times foundation width (2.25B). While when D_f =1.0 m (Figure 3.11a), such extension increases to approximate 4.5B. For the same slope model ($\alpha°$=10°), when the footing is located 4B from the edge of slope b, (Figure 3.9b and 3.14b) the failure surface extends approximately 2B from the center of the footing and the point intersecting the ground surface is located 2B from the edge of slope. On the other hand, when D_f=1.0, the failure surface extends approximately 4B from the edge of the footing and it just passed the edge of the slope. This implies that, for a given slope

and distance from the slope, surface foundation may have little or no effect of slope but foundation with shallow depth of D_f may have relatively higher degree of slope effect.

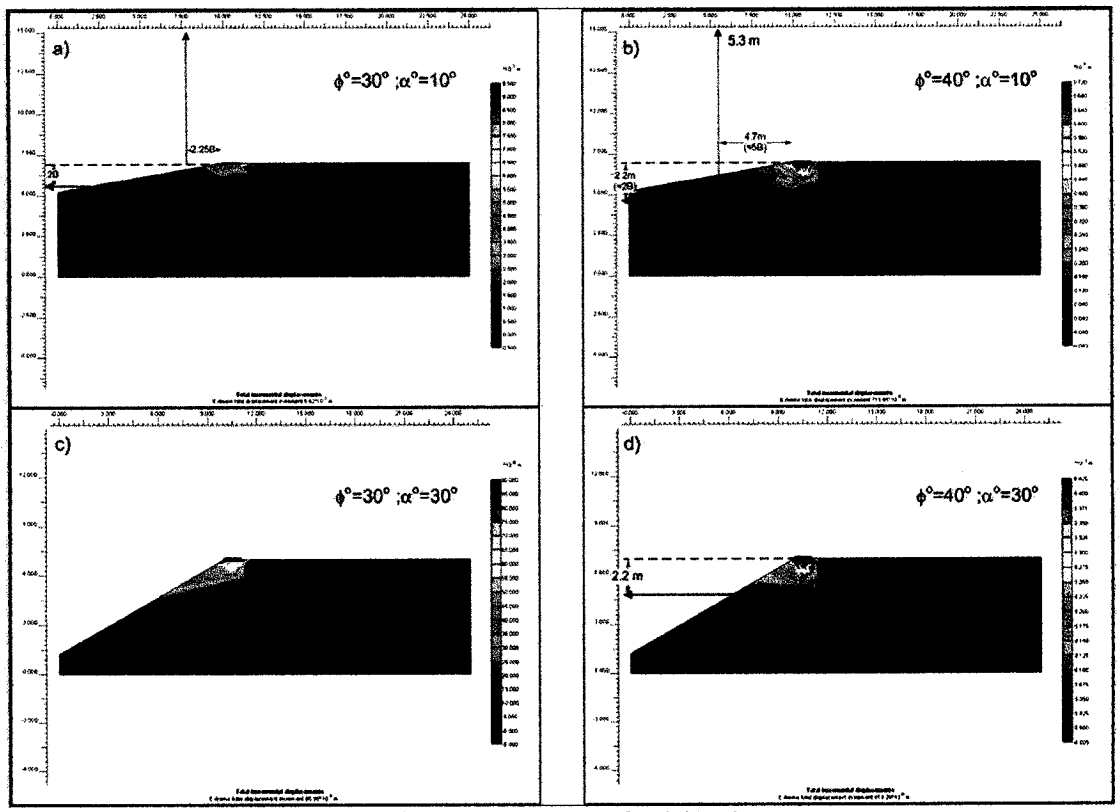

Figure 3.6 Output for b/B=0

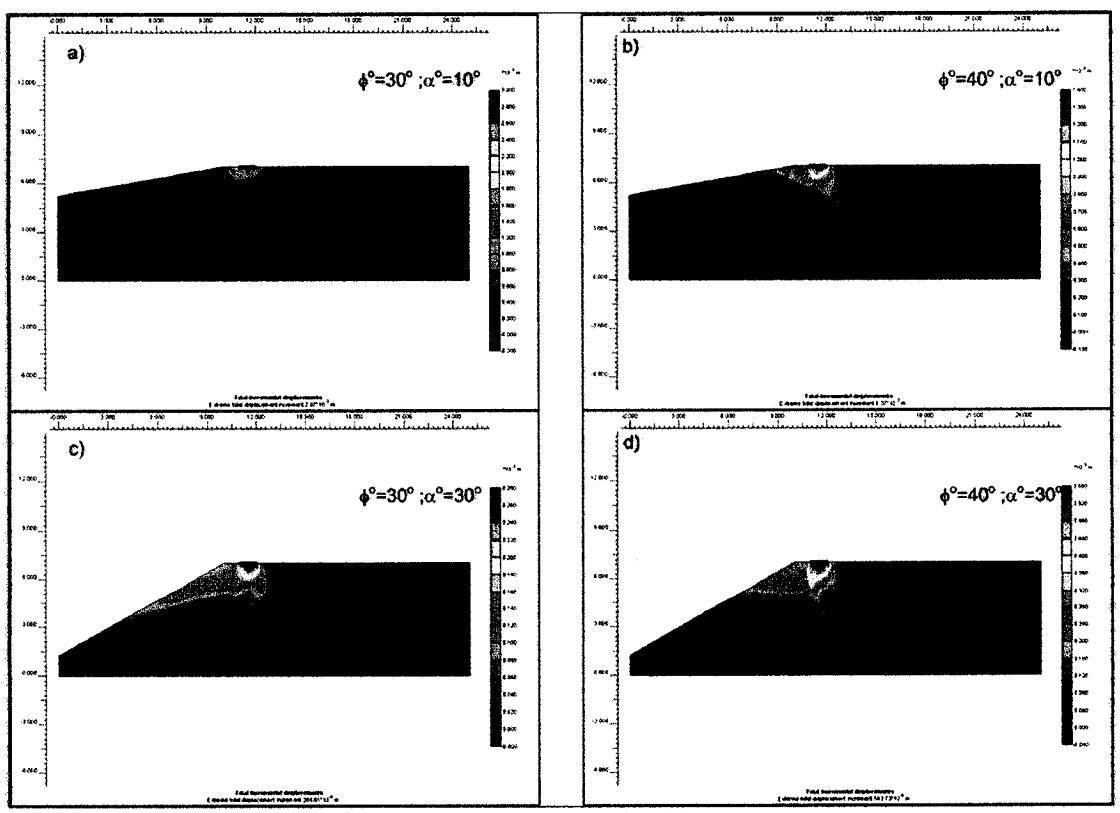

Figure 3.7 Output for b/B=1

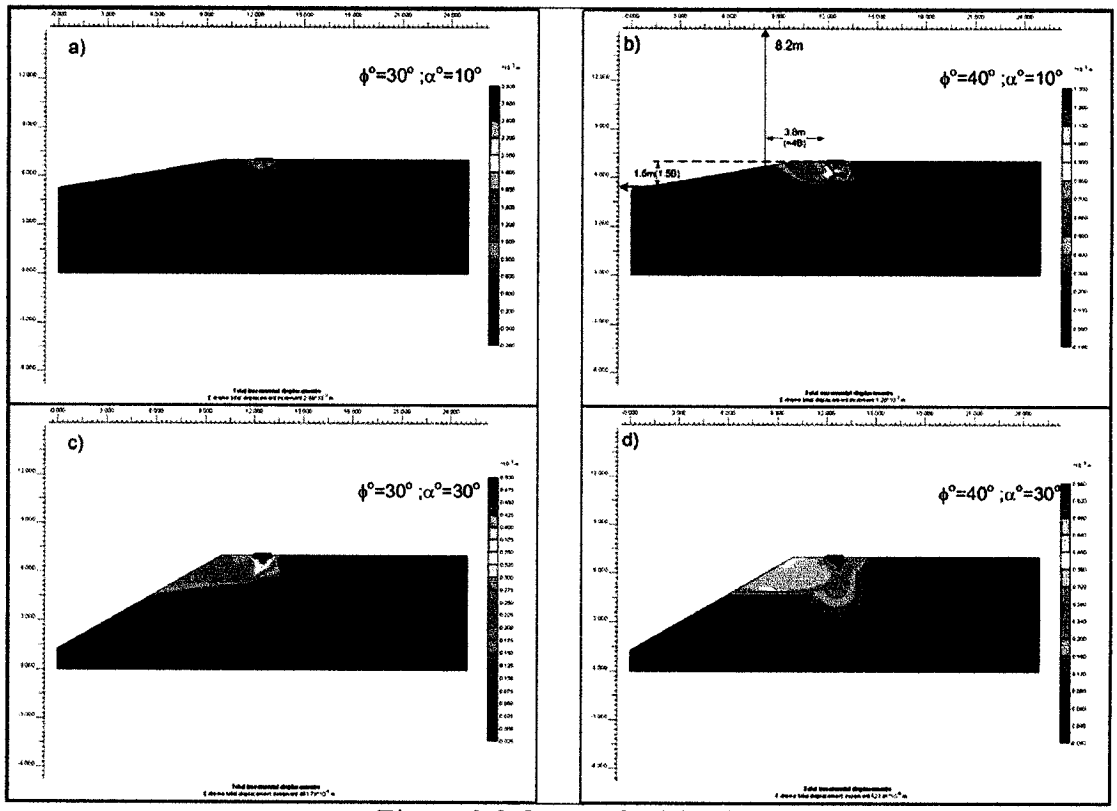

Figure 3.8 Output for b/B=2

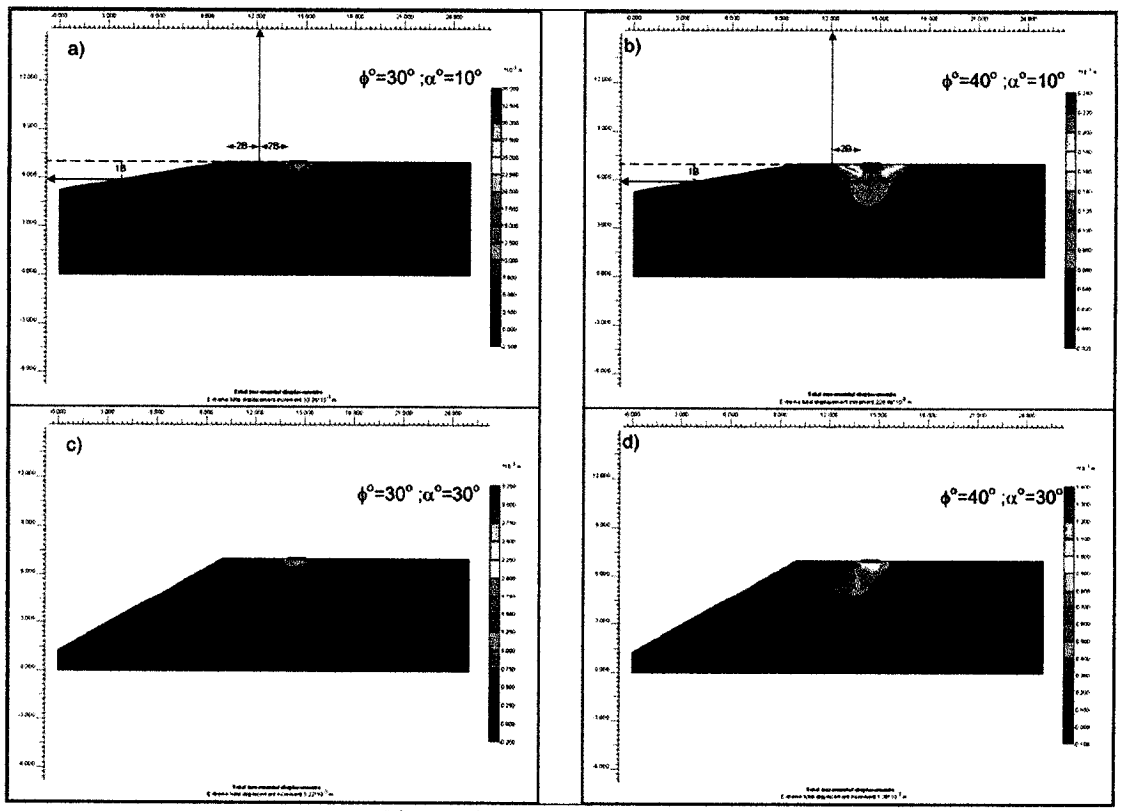

Figure 3.9 Output for b/B=4

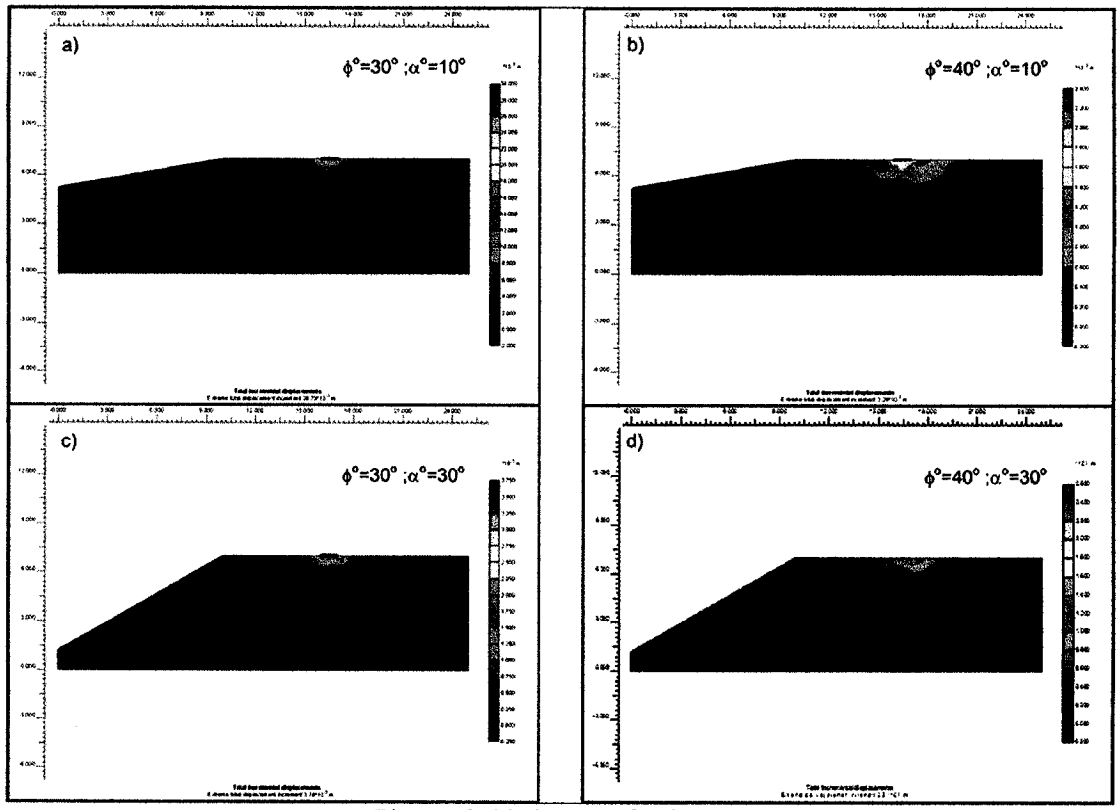

Figure 3.10 Output for b/B=6

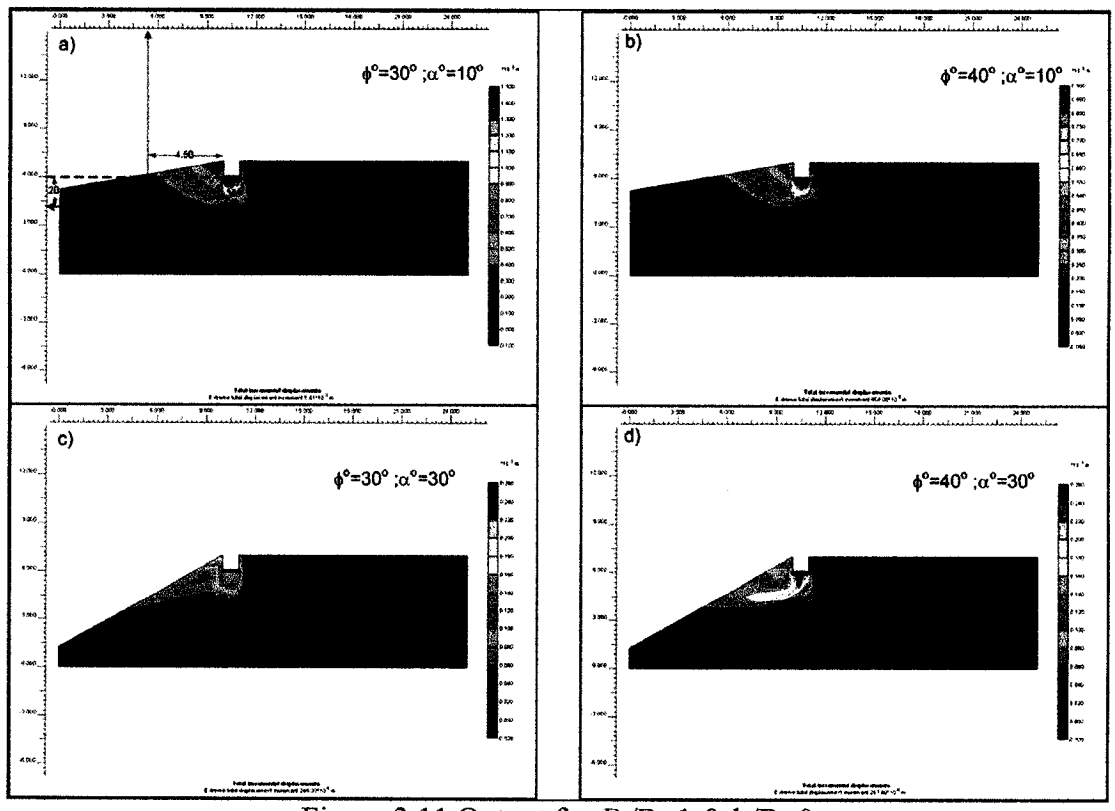

Figure 3.11 Output for D_f/B=1 & b/B=0

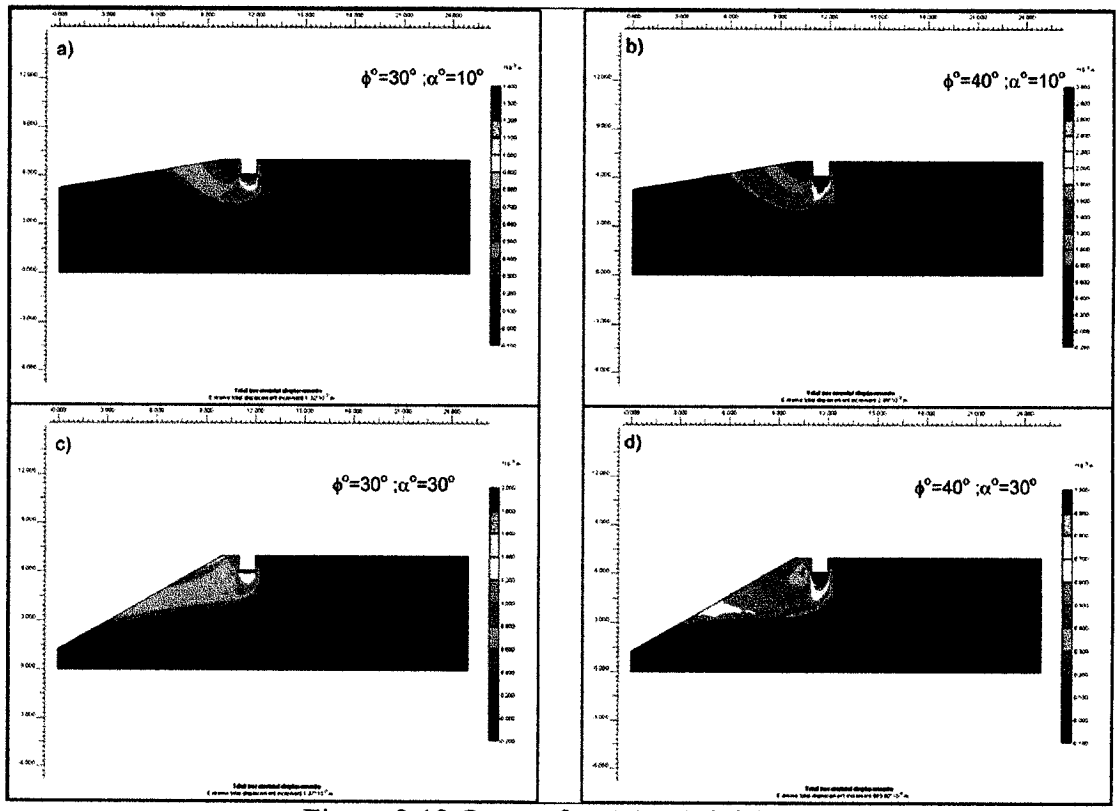

Figure 3.12 Output for D_f/B=1 & b/B=1

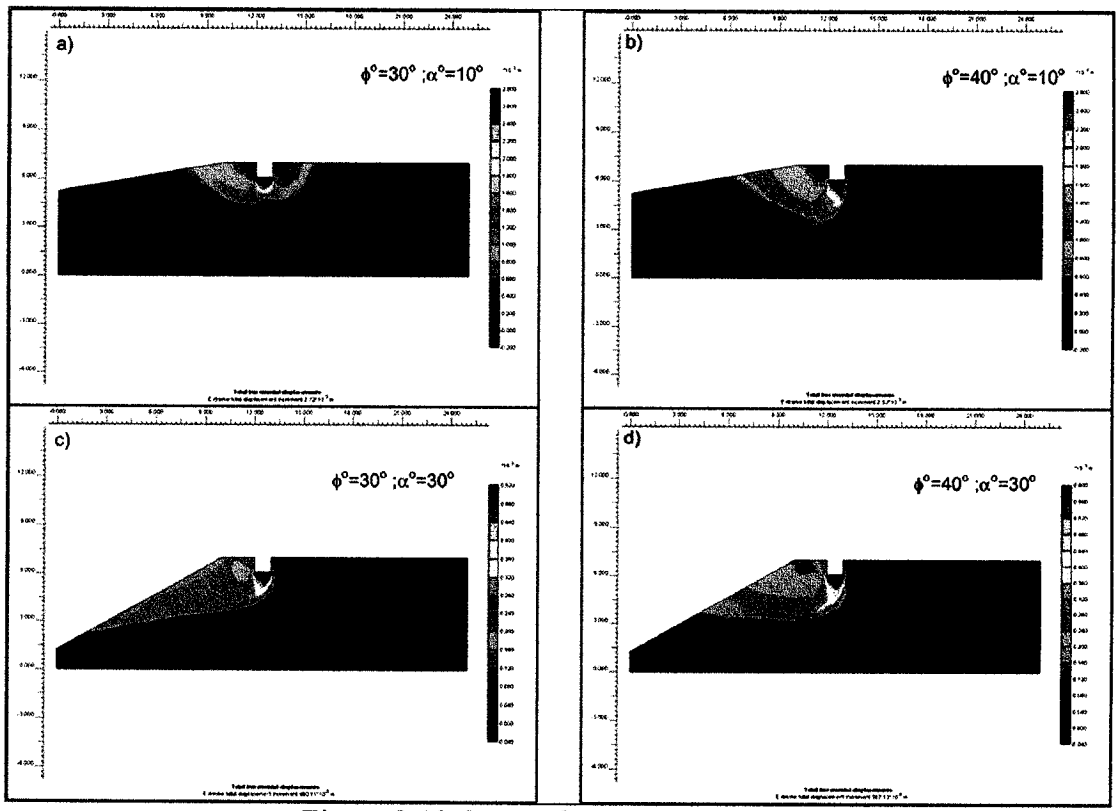

Figure 3.13 Output for D_f/B=1 & b/B=2

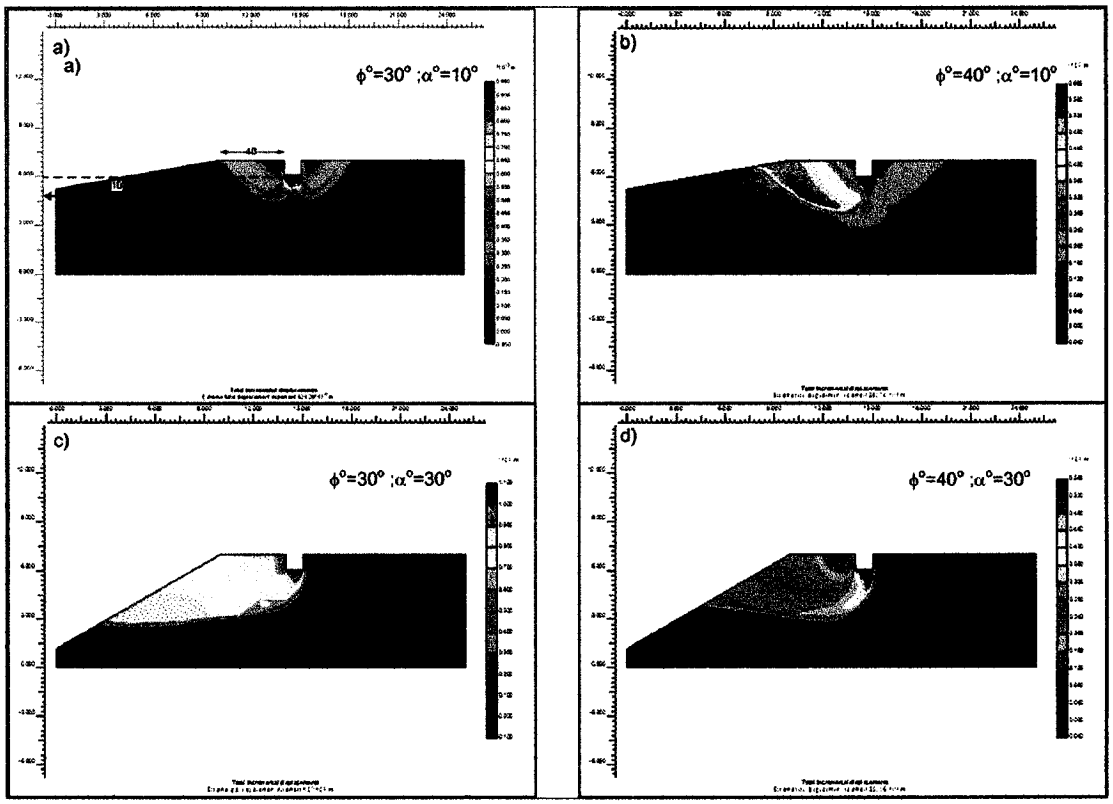

Figure 3.14 Output for D_f/B=1 & b/B=4

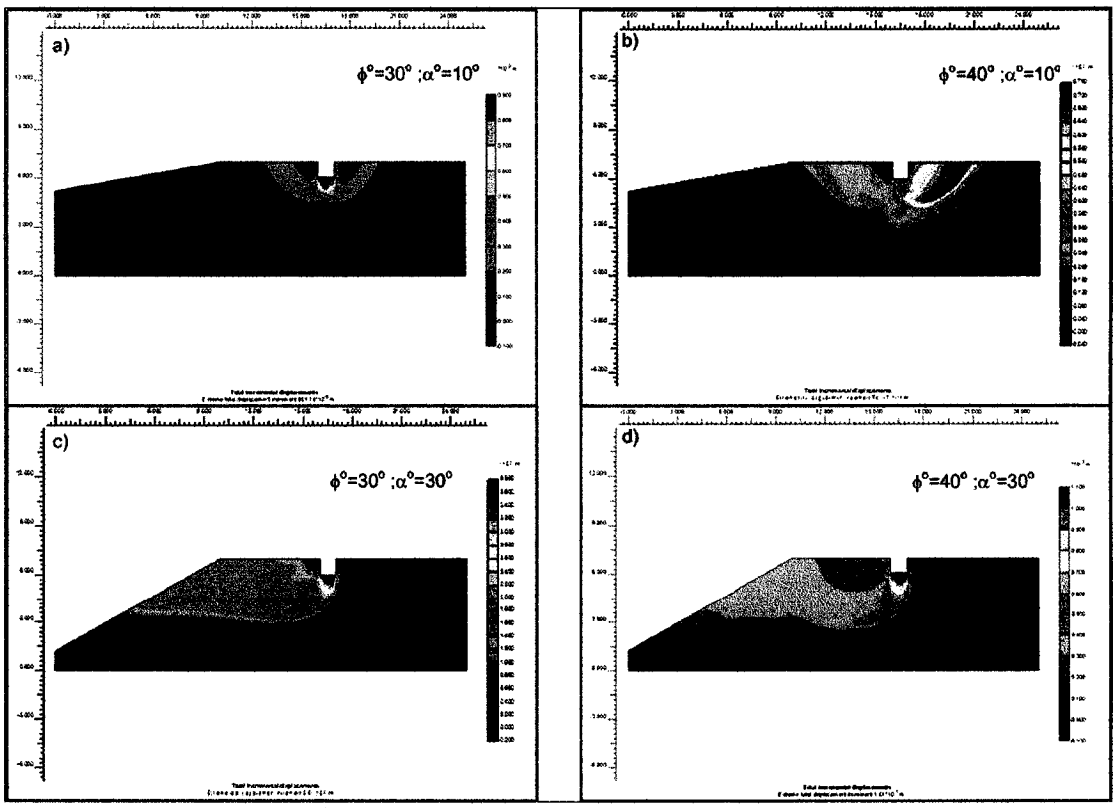

Figure 3.15 Output for D_f/B=1 & b/B=6

CHAPTER 4

RESULT AND ANALYSIS

4.1 RESULT PRODUCED BY THE NUMERICAL MODEL

The testing program on footings near slope deduced from the present numerical model is summarized in Table 4.1 and typical results are given in Table 4.2. The complete set of results is given in Appendix A (Table A.1 to A.5). The results of the case of horizontal surface ($\alpha°=0°$) are given in Table A.6. The results for the case of footings near slope having B=0.5 and 1.5m are given in Table A.7 and for the cases of D_f>B and D_f<B are given in Table A.8.

Table 4.1. Summary of the testing program.

Table	Test No.	α°	B, m	D_f, m	D_f/B	b, m	b/B	γ, kN/m^3	c, kN/m^2	ϕ°
A.1	1-1	5°	1	0	0	0 - 6	0 - 6	18	0	5° to 50°
	1-2	10°								10° to 50°
	1-3	15°								15° to 50°
	1-4	20°								20° to 50°
	1-5	25°				0 - 8	0 - 8			25° to 50°
	1-6	30°								30° to 50°
A.2	2-1	5°	1	0.5	0.5	0 - 6	0 - 6			5° to 50°
	2-2	10°								10° to 50°
	2-3	15°								15° to 50°
	2-4	20°								20° to 50°
	2-5	25°				0 - 8	0 - 8			25° to 50°
	2-6	30°								30° to 50°
A.3	3-1	5°	1	1	1	0 - 6	0 - 6			5° to 50°
	3-2	10°								10° to 50°
	3-3	15°								15° to 50°
	3-4	20°								20° to 50°
	3-5	25°				0 - 8	0 - 8			25° to 50°
	3-6	30°								30° to 50°
A.4	4-1	5°	1	0	0	0 - 6	0 - 6	0	5	5° to 50°
	4-2	10°								10° to 50°
	4-3	15°								15° to 50°
	4-4	20°								20° to 50°
	4-5	25°								25° to 50°
	4-6	30°				0 - 8	0 - 8			30° to 50°
A.5	5-1	5°	1	1	1	0 - 6	0 - 6			5° to 50°
	5-2	10°								10° to 50°
	5-3	15°								15° to 50°
	5-4	20°								20° to 50°
	5-5	25°								25° to 50°
	5-6	30°				0 - 8	0 - 8			30° to 50°
A.6	6-1	0°	1	0	0	-	-	0	5	5° to 50°
	6-2			0	0			18	0	
	6-3			1	1			18	0	
A.7	7-1	5°	0.5	0	0	0 - 6	0 - 12	18	0	5° to 50°, increment by 5°
	7-2	15°								15° to 50°, increment by 5°
	7-3	30°								30° to 50°, increment by 5°
	8-1	5°	1.5				0 - 4			5° to 50°, increment by 5°
	8-2	15°								15° to 50°, increment by 5°
	8-3	30°								30° to 50°, increment by 5°
A.8	9-1	5°	1	2	2	0 - 6	0 - 6	18	10	5° to 50°, increment by 5°
	9-2	15°								15° to 50°, increment by 5°
	9-3	30°								30° to 50°, increment by 5°
	10-1	5°	1.5	0.5	0.33	0 - 6	0 - 4		25	5° to 50°, increment by 5°
	10-2	15°								15° to 50°, increment by 5°
	10-3	30°								30° to 50°, increment by 5°

Table 4.2. Typical results deduced from the numerical model.

Test	α°	B	D_f	D_f/B	b	b/B	γ, kN/m^3	c, kN/m^2	ϕ°	q_u, $kN/m/m$
6-1	0°	1	0	0	-	-	0	5	30°	149.0
									37°	259.3
									40°	387.5
									45°	695.6
									48°	1008.1
6-2							18	0	30°	145.8
									37°	516.5
									40°	946.9
									45°	2656.9
									48°	5176.9
6-3			1	1					30°	423.8
									37°	1385.5
									40°	2499.9
									45°	6130.9
									48°	10833.4
1-4	20°	1	0	0	0.0	0	18	0	40°	307.1
					3.0	3				548.1
					6.0	6				777.4
2-4			0.5	0.5	0.0	0				454.0
					3.0	3				868.4
					6.0	6				1366.3
3-4			1	1	0.0	0				685.6
					3.0	3				1306.9
					6.0	6				2020.4
4-4			0	0	0.0	0	0	5		215.7
					3.0	3				281.9
					6.0	6				351.5
5-4			1	1	0.0	0				361.5
					3.0	3				439.3
					6.0	6				507.0

Table 4.2. Typical results deduced from the numerical model. (Cont'd)

Test	α°	B	D_f	D_f/B	b	b/B	γ, kN/m^3	c, kN/m^2	ϕ°	q_u, $kN/m/m$
1-5	25°	1	0	0	0.0	0	18	0	37°	132.8
					4.0	4				372.6
					8.0	8				511.8
2-5			0.5	0.5	0.0	0				208.2
					4.0	4				623.2
					8.0	8				873.6
3-5			1	1	0.0	0				325.1
					4.0	4				981.1
					8.0	8				1266.0
4-5			0	0	0.0	0	0	5		136.1
					3.0	3				191.1
					6.0	6				255.2
5-5			1	1	0.0	0				229.0
					3.0	3				295.0
					6.0	6				341.0
1-5	25°	1	0	0	0.0	0	18	0	41°	256.7
					4.0	4				625.5
					8.0	8				1042.3
2-5			0.5	0.5	0.0	0				373.4
					4.0	4				1044.9
					8.0	8				1800.9
3-5			1	1	0.0	0				561.3
					4.0	4				1618.5
					8.0	8				2565.3
4-5			0	0	0.0	0	0	5		196.9
					2.0	2				277.0
					6.0	6				360.0
5-5			1	1	0.0	0				340.2
					2.0	2				433.0
					6.0	6				539.2

Table 4.2. Typical results deduced the numerical model. (Cont'd)

Test	α°	B	D_f	D_f/B	b	b/B	γ, kN/m^3	c, kN/m^2	ϕ°	q_u, kN/m/m
1-5	25°	1	0	0	0.0	0	18	0	45°	517.2
					4.0	4				1126.7
					8.0	8				1822.2
2-5			0.5	0.5	0.0	0				700.6
					4.0	4				1655.6
					8.0	8				2829.9
3-5			1	1	0.0	0				958.2
					4.0	4				2344.8
					8.0	8				4059.1
4-5			0	0	0.0	0	0	5		284.9
					2.0	2				399.4
					6.0	6				500.6
5-5			1	1	0.0	0				501.2
					2.0	2				627.4
					6.0	6				770.0
1-5	25°	1	0	0	0.0	0	18	0	48°	856.8
					4.0	4				1713.7
					8.0	8				2681.8
2-5			0.5	0.5	0.0	0				1159.1
					4.0	4				2450.3
					8.0	8				4014.6
3-5			1	1	0.0	0				1527.7
					4.0	4				3323.5
					8.0	8				5517.6
4-5			0	0	0.0	0	0	5		390.4
					2.0	2				507.4
					6.0	6				643.6
5-5			1	1	0.0	0				662.5
					2.0	2				825.3
					6.0	6				990.3

Table 4.2. Typical results deduced from the numerical model. (Cont'd)

Test	α°	B	D_f	D_f/B	b	b/B	γ, kN/m^3	c, kN/m^2	ϕ°	q_u, kN/m/m
1-6	30°	1	0	0	0.0	0	18	0	30°	29.7
					4.0	4				138.2
					8.0	8				148.7
2-6			0.5	0.5	0.0	0				66.0
					4.0	4				256.4
					8.0	8				270.3
3-6			1	1	0.0	0				114.7
					4.0	4				363.6
					8.0	8				390.6
4-6			0	0	0.0	0		5		79.5
					4.0	4				138.0
					8.0	8				148.3
5-6			1	1	0.0	0				136.9
					4.0	4				188.6
					8.0	8				192.7
7-3		0.5	0	0	0.0	0		0		22.2
					4.0	8				80.6
					6.0	12				78.7
8-3		1.5			0.0	0				50.7
					4.0	3				152.6
					6.0	4				205.8
9-3		1	2	2	0.0	0		10		623.4
					3.0	3				1311.6
					6.0	6				1533.5
10-3		1.5	0.5	0.33	0.0	0		25		568.4
					3.0	2				799.4
					6.0	4				1029.6

4.2 PARAMETRIC STUDY

From the values of ultimate bearing capacity and the deformation measured during testing, it can be reported that the two parameters, *b/B* ratio and angle of slope $\alpha°$, are the most significant parameters affecting the values of the bearing capacity factors. For the case where the footing is located far away from the edge of the slope, the bearing capacity factors become independent of these two parameters. Furthermore, different angles of shear resistance lead to different degree of reduction. Therefore, there is a coefficient (or a coefficient for each bearing capacity factor) which reduces the value of that factor for ground surface and is function of function of *b, B,* $\alpha°$, ϕ. Note that in the following parametric study, the value of N_q cannot be back-calculated directly from the obtained numerical result since the actual reduced value of N_γ for footing with embedded depth greater that zero is arbitrary. The assumption was made such that the N_γ for surface foundation condition had the same degree of reduction as the N_γ for foundation with embedded depth greater than zero. The value of N_q can be determined by Equation 3.1c.

4.2.1 The Ratio of the Distance from Slope to the Width of Footing *b/B*

According to Meyerhof's theory (1957) the bearing capacity factors vary with respect to the *b/B* ratio and slope angle $\alpha°$. Further investigation shows that the decrease of each of these factors does not vary in the same manner. Figure 4.1, 4.2 and 4.3 show the variation of the bearing capacity factor with respect to *b/B* for an angle of shear resistance $\phi°$=30°.

For a small angle of slope $\alpha°$ (i.e.: $\alpha° = 5°$), the bearing capacity factor N_c reduces about 8% and N_γ reduces up to about 20% when the foundation is at the edge of the slope (*b/B*=0). It increases parabolically and approaches to the bearing capacity factors for

horizontal surface with the increase of the distance *b (or b/B)*. Beyond a distance about 2 to 4 times of the footing width, the bearing capacity factors, N_c, N_q, and N_γ, become independent of the angle of slope.

For a medium values of the angle α (i.e. 20°), the reduction in the bearing capacity factors becomes more obvious. The factors N_q and N_γ were reduced for about 60% of the horizontal surface, and about 30% for the factor N_c. The factors increase linearly with the increase of the ration *b/B* when the foundation is relatively closed to the edge of the slope. Beyond a distance about 2 to 4 times of the footing width, the increment becomes exponential. When *b/B* is about 4 to 6, the bearing capacity of the foundation becomes independent of the slope.

It can be concluded that, the trend in the reduction of the bearing capacity factors due to presence of the slope has the following characteristics:

1. Its variation may have exponential characteristic;
2. It is a convergent function. The limit of this function approaches to unity when *b/B* is approaching to certain value or infinity.

Refer to Figure 4.4, it can be noted that the decrease in the factor N_c is relatively low when the foundation is at the edge of the slope. However it is considerably higher for the factors N_q and N_γ.

Refer to Figure 4.4, when the foundation is rests near the slope, the displacement of the soil underneath the footing concentrates more on the side of the slope than that on the side of the flat surface. Furthermore, the log-spiral slip-line and the equivalent free surface are slightly reduced. However, the overburden pressure and the weight of the radial and the mixed shear zone are significantly reduced. Since the pressure above the

free surface controls the values of N_q and the shear zones controls the values of N_γ, the effect of slope is obvious in these two factors. Meyerhof (1957) indicated that for slopes with inclination less than 30°, the decrease in the bearing capacity is relatively small in case of clays ($c \neq 0$) but can be considerable high in sand and gravel ($\phi° \neq 0$). This is due to the fact that the bearing capacity in cohesionless soils decreases approximately parabolically with the increase in slope angle.

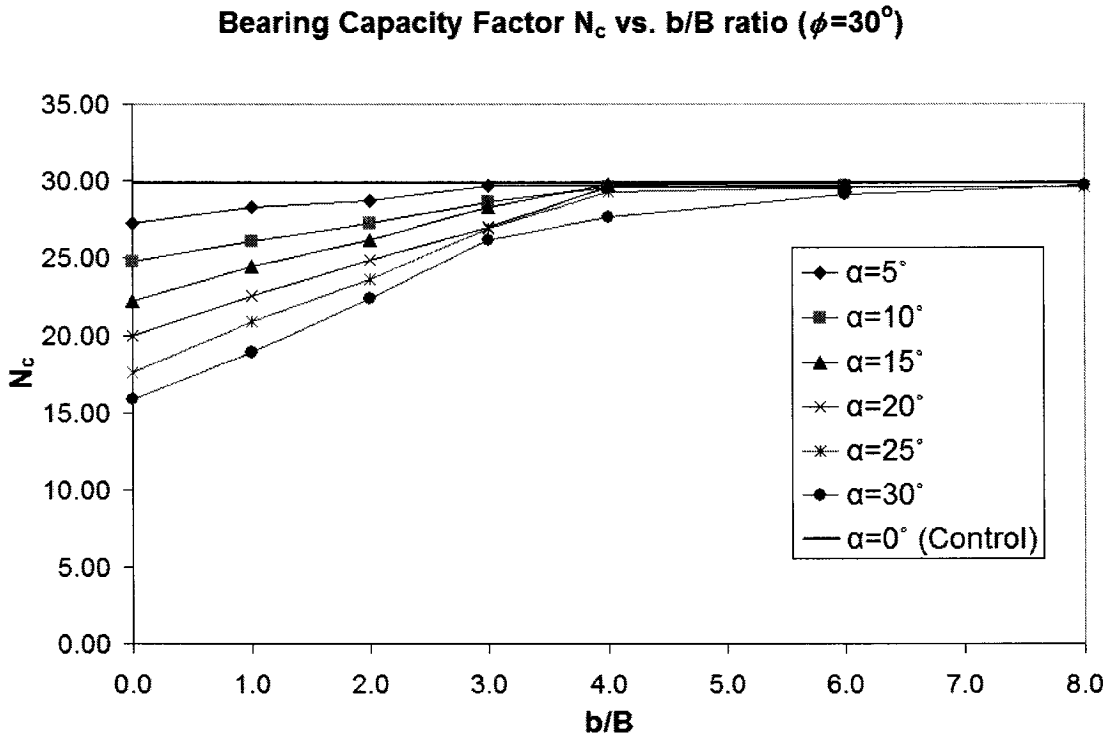

Figure 4.1. Coefficient of N_c vs. b/B ratio (ϕ=30°)

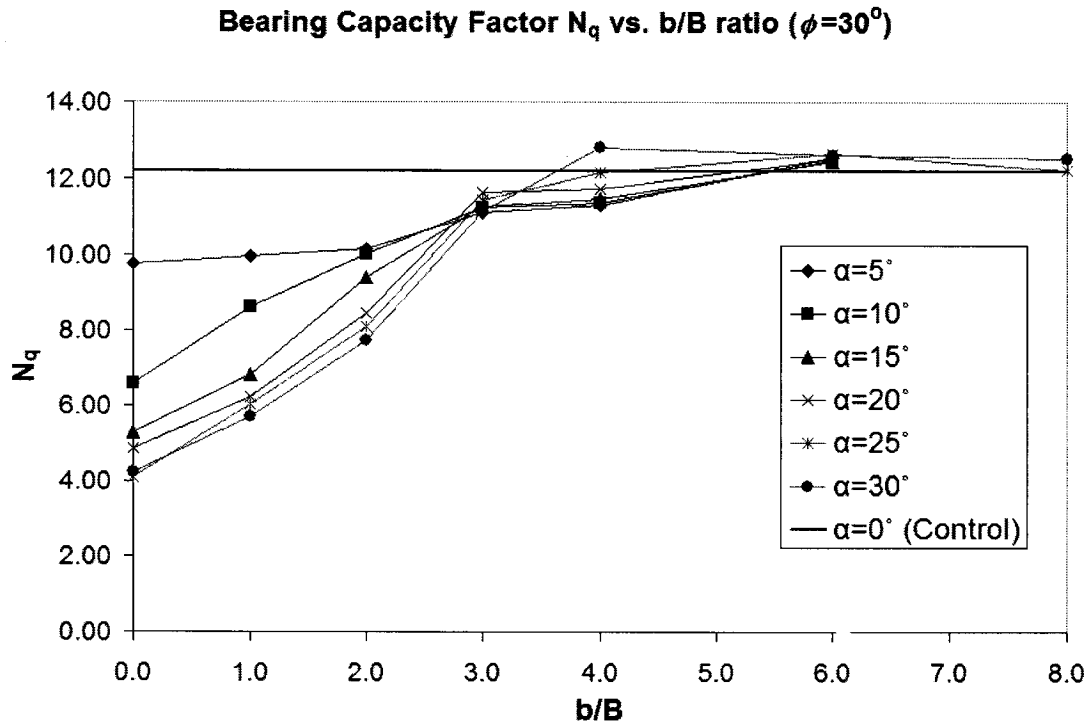

Figure 4.2. Coefficient of N_q vs b/B ratio (ϕ=30° D_f/B=1)

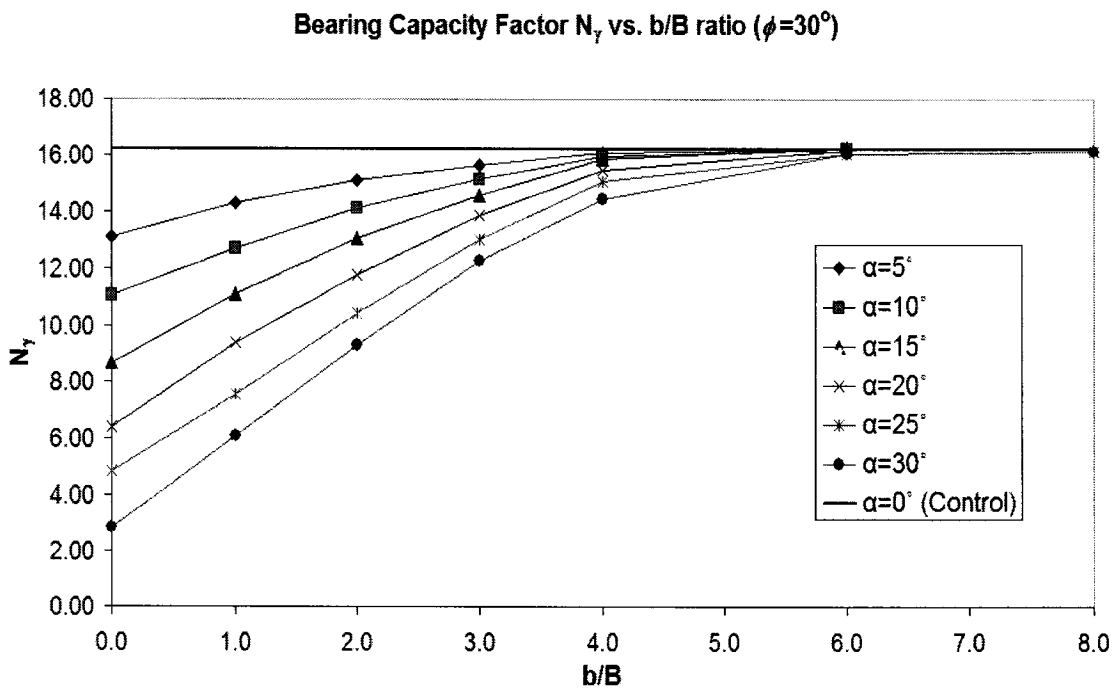

Figure 4.3. Coefficient of N_γ vs. b/B ratio (ϕ=30°)

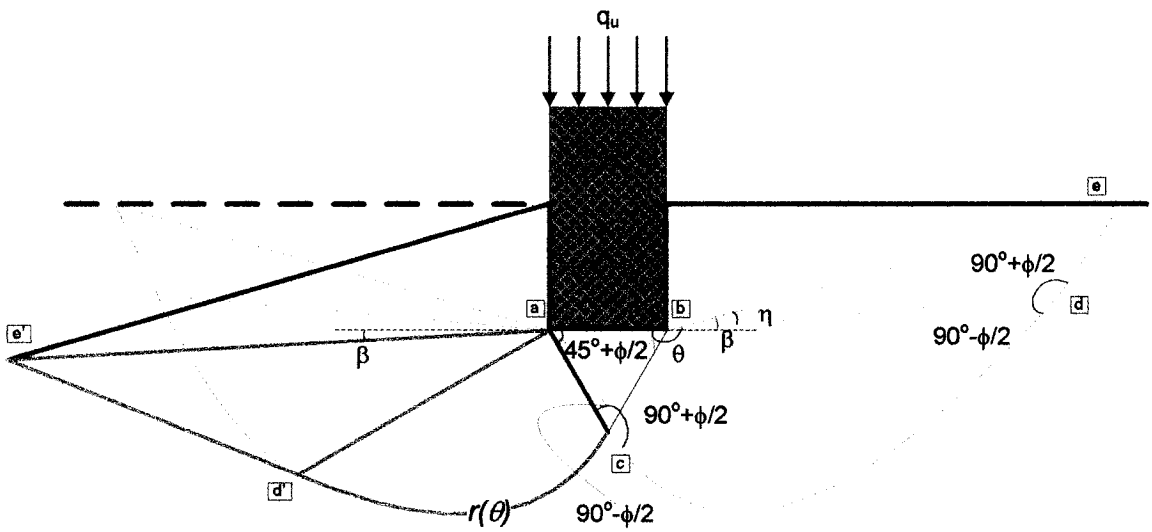

Figure 4.4 Failure planes of shallow foundation for the cases of horizontal surface (*bcde*) and near the edge of slope (*acde*).

4.2.2 The Angle of Slope $\alpha°$

Based on the results of this investigation, it can be reported that the bearing capacity factors decrease with the increase of the inclination angle for a given value of *b/B* ratio. A sample of variation of bearing capacity factors N_c, N_q, and N_γ vs. angle of slope with different *b/B* ratio are shown in Figures 4.5, 4.6, and 4.7.

For footing relatively far from the top of the slope (i.e.: $b/B \geq 6$), the bearing capacity factors are nearly unchanged when the slope has the angle no greater than 25° (for N_c and N_q) and 20° (for N_γ). Beyond these values, the bearing capacity factors decrease slightly and exponentially. If the footing is located further from the slope, the bearing capacity factors will remain unchanged.

For footing at an intermediate distance from the top of the slope (i.e.: b/B =2 to 4), the effect due to slope becomes more obvious. The magnitude of bearing capacity factors reduce slightly when $\alpha°$=5° and decreases exponentially with the increase of the angle $\alpha°$. A significant decrease was found for the case of N_q and N_γ. By comparing this variation

with different *b/B* ratio, it can be noted that by decreasing the *b/B* ratio (footing approaching to the edge of slope) the rate of change of the reduction the angle $\alpha°$ becomes more linear and much higher. When the footing is located adjacent to the top of the slope (*b/B*=0), it is found that this variation become nearly linear.

The degree of reduction was found to be not significant in the case of N_c as compare to the case of N_q and N_γ. This observation was explained in previous section.

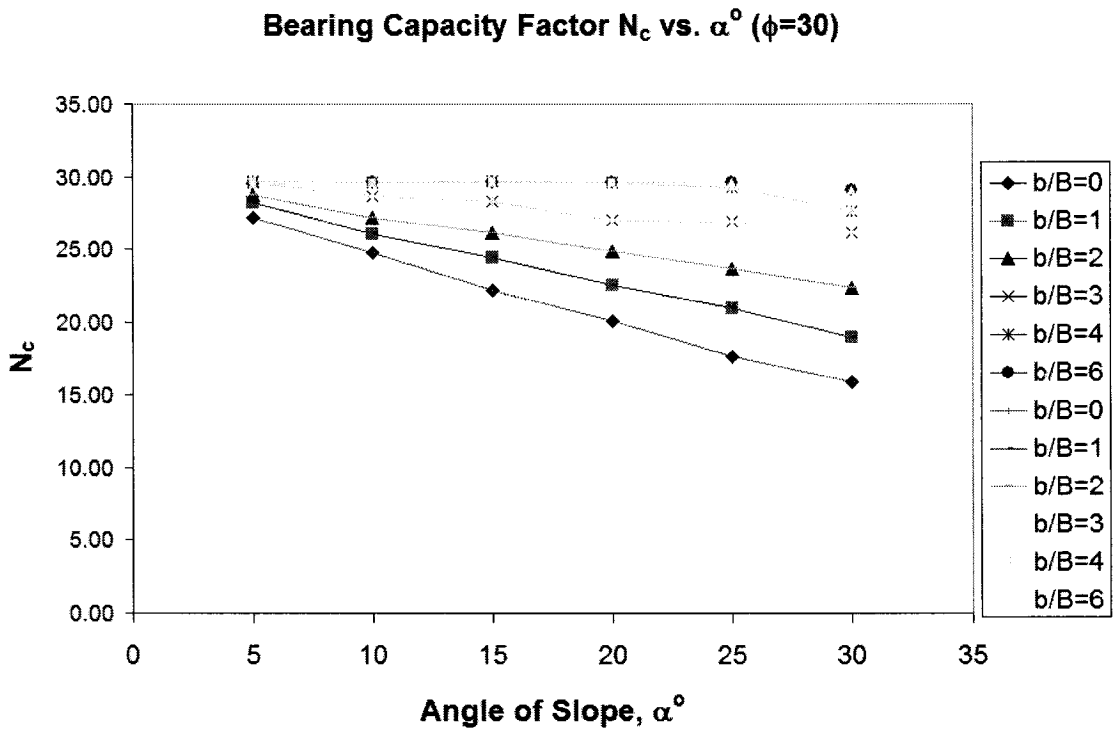

Figure 4.5. Coefficient of N_c vs. angle of the slope for the case of $\phi°$=30°

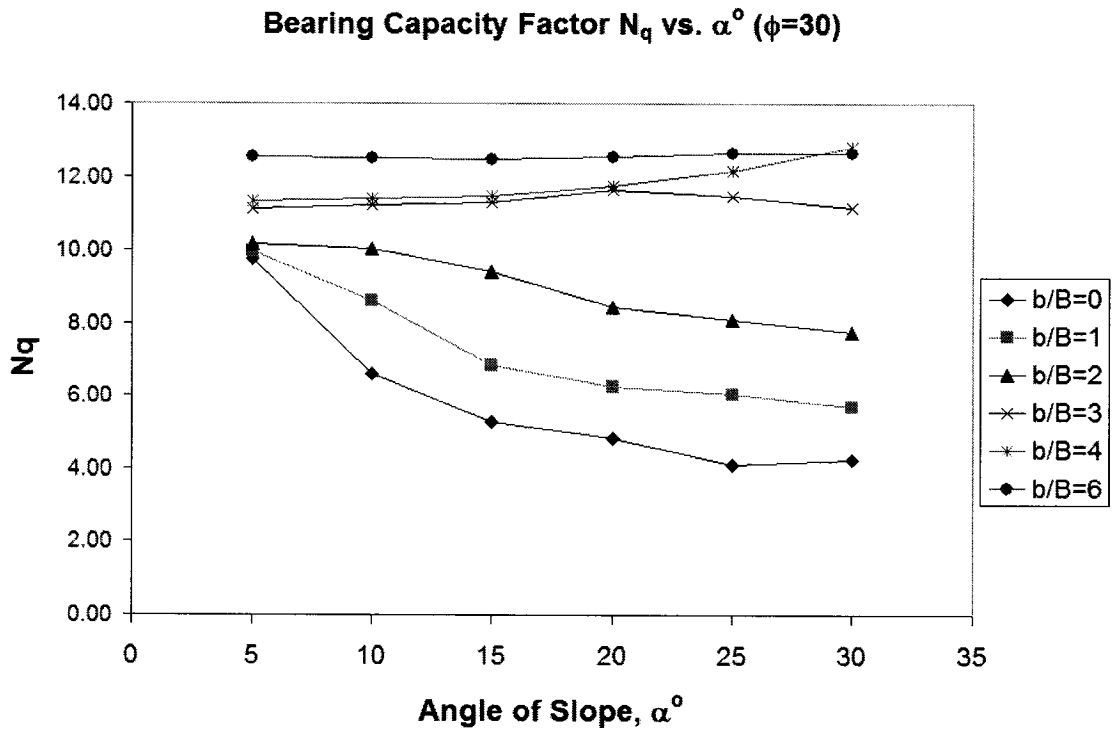

Figure 4.6. Coefficient of N_q vs. angle of the slope for the case of ϕ°=30°

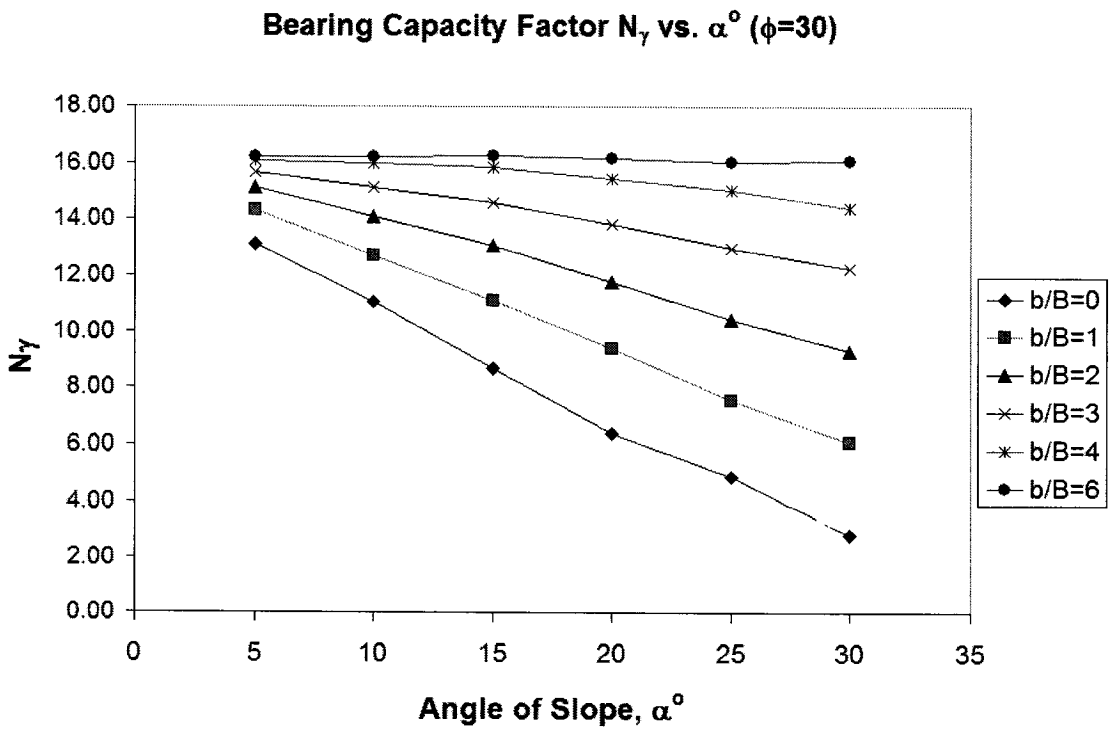

Figure 4.7. Coefficient of N_γ vs. angle of the slope for the case of ϕ°=30°

4.2.3 The Angle of Shear Resistance of the Soil ϕ°

For a given angle of the slope $\alpha°$, and a *b/B* ratio, the reduction of the bearing capacity factors does not follow the same trend at for different angle of shear resistance $\phi°$ of the soil. To demonstrate these trends, the relationships were plotted as the relative bearing capacity factor vs. *b/B*. The term "relative bearing capacity" was calculated as the ratio of $\frac{q_u(\alpha > 0°)}{q_u(\alpha = 0°)}$. These graphs were plotted in Figures 4.8, 4.9 and 4.10.

When footing is located at the edge of slope (*b/B*=0), the ratio of ultimate bearing capacity due to cohesion of the soil (Figure 4.8) decreases to about 0.6 for soil having lower value of ϕ^o (i.e.: 25°) and 0.35 for higher value of ϕ^o (i.e.: 50°). The ratio of ultimate bearing capacity due to overburden pressure (Figure 4.9) and weight of soil (Figure 4.10) were found to be much lower: less than 0.4 for lower ϕ^o and less than 0.2 for higher ϕ^o. Regardless the value of *b/B*, soil having higher angle ϕ^o always has higher ratio of ultimate bearing capacity. The required distance from the slope (or *b/B*) where the ultimate bearing capacity becomes independent of slope is about 4 time of the footing width for soil having lower angle ϕ^o. As the angle ϕ^o increases, a greater distance is required. This to confirm the founding of Meyerhof (1957), namely that the bearing capacity factors becomes the same as that of a foundation on a horizontal ground surface depends on not only D_f/B ratio and *b/B* ratio, but also the angle of shear resistance ϕ^o.

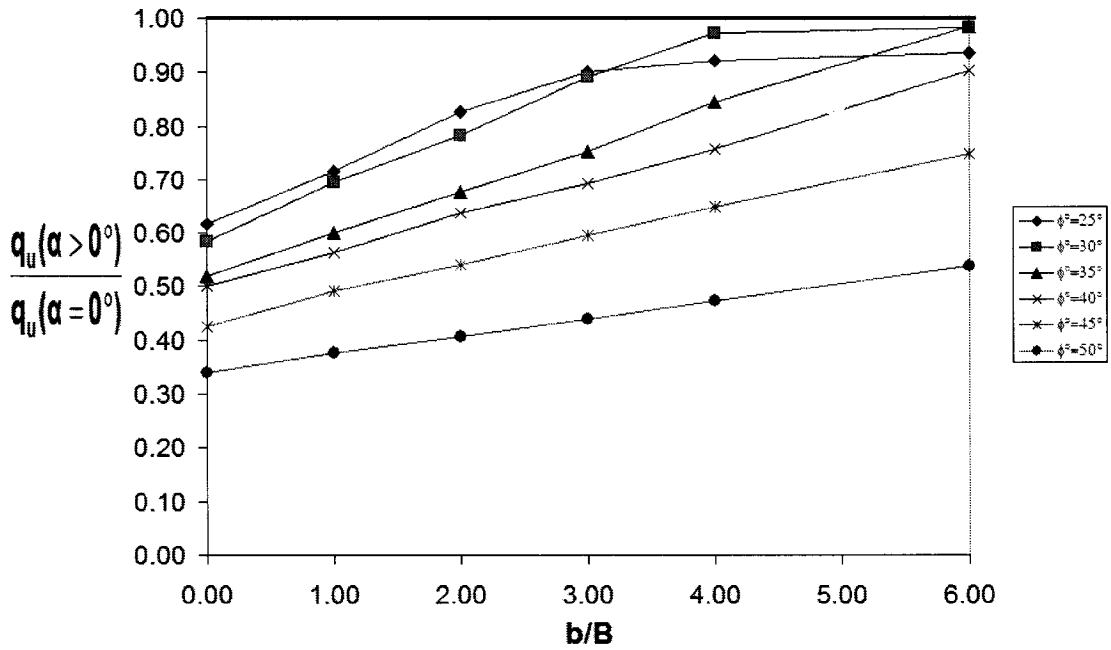

Figure 4.8. $\frac{q_u(\alpha > 0°)}{q_u(\alpha = 0°)}$ vs. *b/B* ratio (Test No. 4-5)

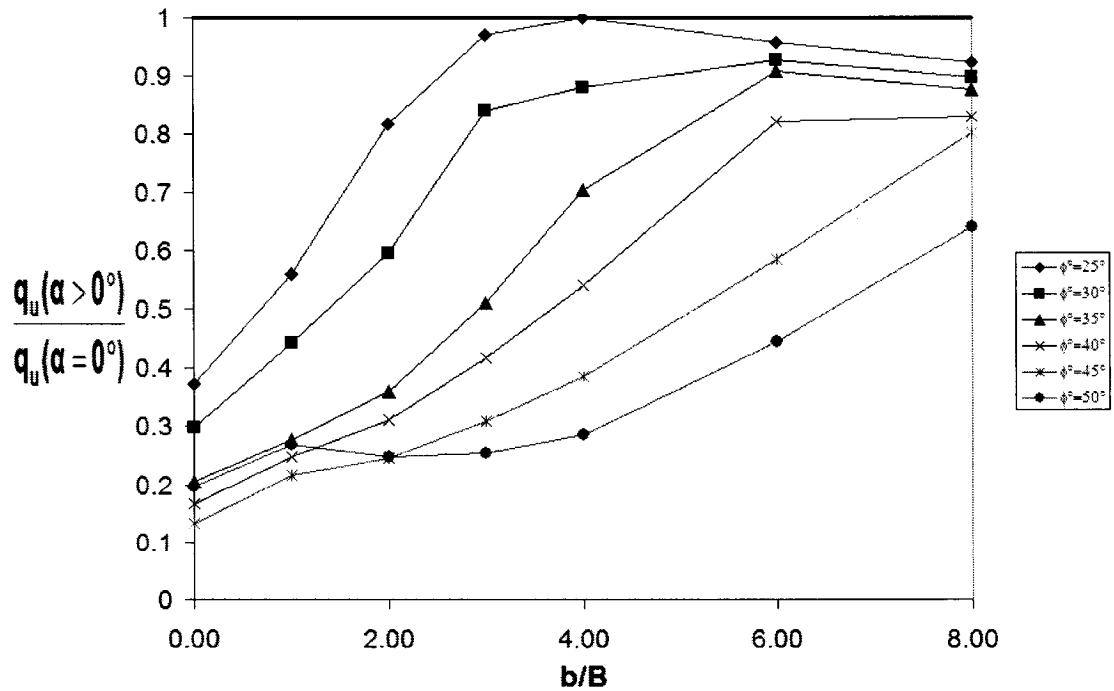

Figure 4.9. $\frac{q_u(\alpha > 0°)}{q_u(\alpha = 0°)}$ vs. *b/B* ratio (Test No. 3-5)

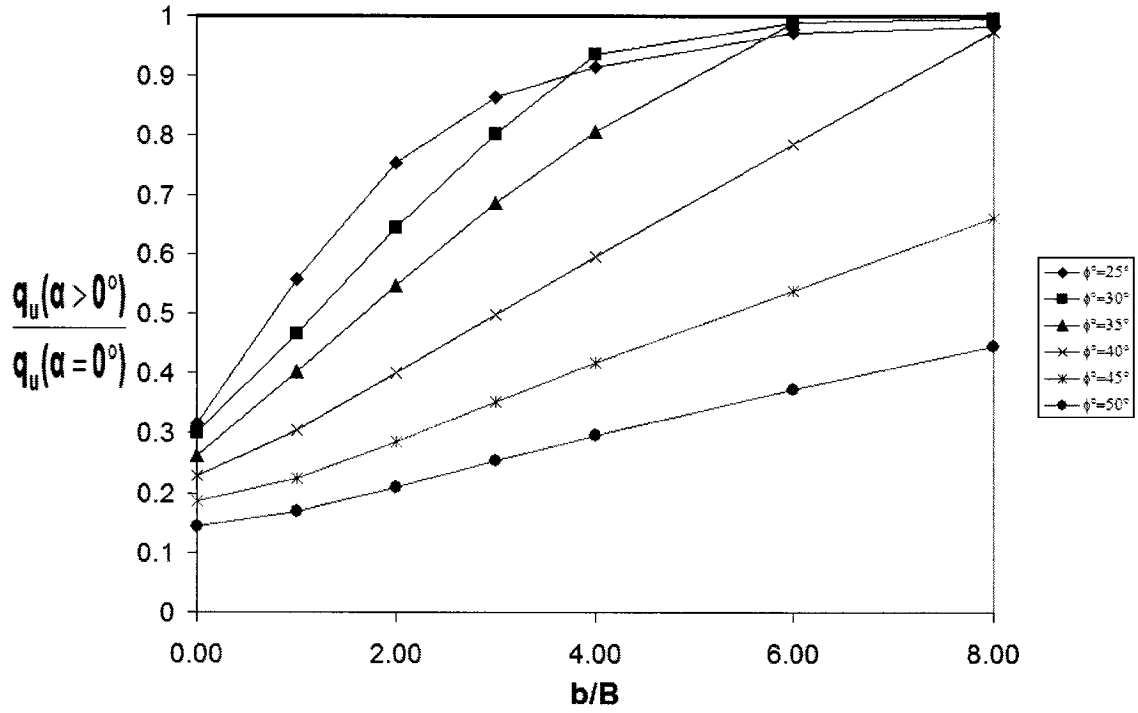

Figure 4.10. $\frac{q_u(\alpha > 0°)}{q_u(\alpha = 0°)}$ vs. *b/B* ratio (Test No. 1-5)

4.3 ANALYTICAL MODEL FOR THE CASE OF FOOTINGS NEAR SLOPE

The failure mechanism deduced from the results of the numerical model, was idealized by an elastic triangular wedge with angle of $45°+\phi°/2$ to the horizontal under the footing, and radial log-spiral shear zone extended from the elastic wedge, and a mixed shear zone extended from the radial shear zone to the ground surface. When vertical load is applied on the footing which was built on the top or near the slope, the failure plane starts below the footing base and extends to both sides of the footing. The extent of the failure plan depends on the distance from the top of slope and the angle of shear resistance of the soil, $\phi°$. Consider the case of a footing embedded at depth of D_f near a slope having an angle $\alpha°$ and distance b from the top of slope (Figure 4.11):

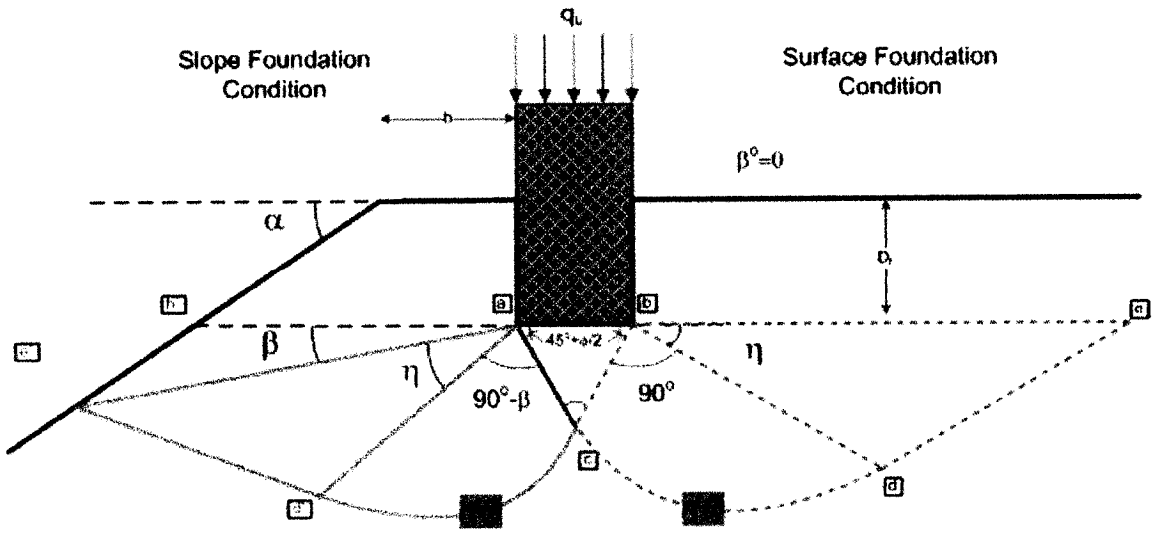

(a) Failure mechanism

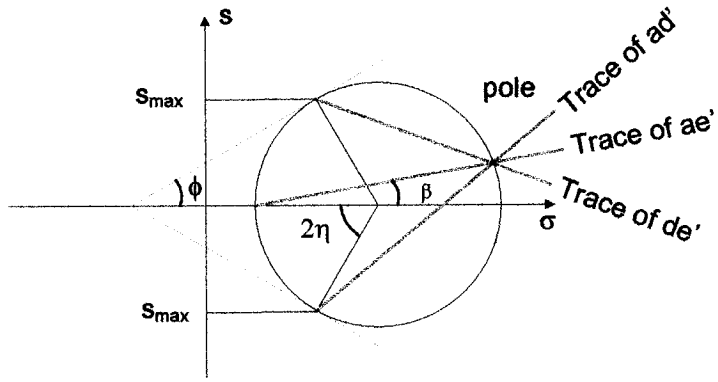

(b) Mohr-Coulomb Envelope

Figure 4.11. Proposed failure mechanism for foundation near slope and the corresponding Mohr-Coulomb Envelope.

The failure plane on the side of slope is considered as the actual failure plane at the ultimate load level. The failure plane on the other side is assumed to intersect the ground surface. The equivalent-free surface (line $\overline{ae'}$) for both slope and the horizontal surface is assumed to be not fully mobilized (m=0 but $\beta^o \neq 0°$ for slope condition). When

the vertical load is applied on the footing, soil on both sides experiences the same shear stress level; nevertheless, soil on the side of slope fails first. Soil deformation will also occur on the side of horizontal surface, but it may or may not reach to 100% of its actual shear strength depending on the distance b and angle of slope α°. Accordingly, the failure plane on the side of slope is the key element to the reduction factor.

The angle of this equivalent-free surface (line $\overline{ae'}$) to the horizontal, denote by β^{o} can be calculated trigonometrically by trial and error as following.

$$\frac{\frac{D_f}{\tan\alpha}+b}{\sin(\alpha+\beta)}=\frac{\overline{ae'}}{\sin(180^\circ-\alpha)} \qquad \ldots (4.1a)$$

$$\frac{\overline{ae'}}{\sin(90^\circ+\phi)}=\frac{r_1}{\sin(90^\circ-\phi-\eta)}=\frac{Be^{\theta\tan\phi}}{2\sin\left(45^\circ-\frac{\phi}{2}\right)\sin(90^\circ-\phi-\eta)} \qquad \ldots (4.1b)$$

Combine both equation and become:

$$\therefore \frac{D_f}{B\tan\alpha}+\frac{b}{B}=\frac{e^{\theta\tan\phi}\sin(\alpha+\beta)\cos\phi}{2\sin\left(45^\circ-\frac{\phi}{2}\right)\cos(\eta+\phi)\sin\alpha} \qquad \ldots (4.1c)$$

$$\Rightarrow \beta=\beta\left(D_f/B, b/B, \phi, \alpha\right)$$

$$where \quad \theta=90^\circ+\beta \quad (m=0), \beta\le 0^\circ$$

The above equation is dimensionless (with D_f/B and b/B ratio) and thus it is universal for various foundation characteristics (b, B and D_f). Since the surface foundation condition is considered, when the footing located relatively far away from the top of slope, the angle β^{o} remains at zero value and the foundation on the infinite horizontal surface may be considered. Figure 4.12 shows the failure planes deduced from

the present numerical model (shade) and the one produced based on Equation 4.1c (solid line).

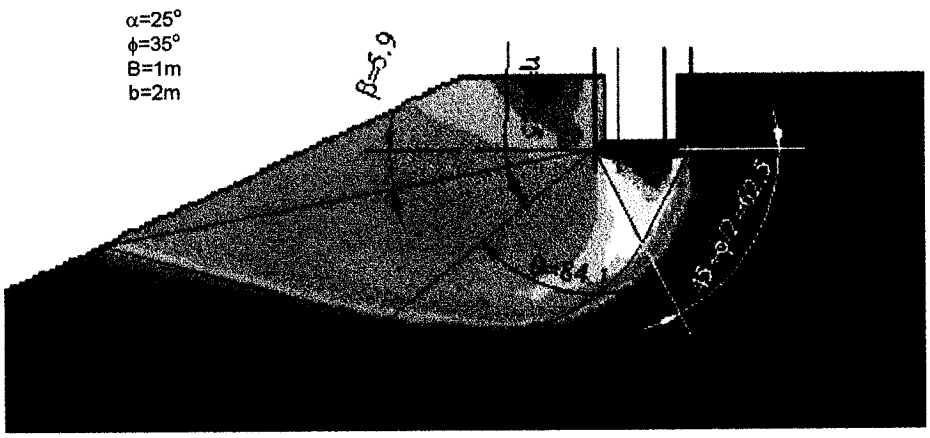

Figure 4.12. Failure planes deduced from the present numerical model (shade) and Equation 4.1c (solid line)

4.3.1 Reduction Factor for the Coefficient N_q

Consider Meyerhof's bearing capacity factor (1951) N_q for foundation on horizontal surface ground ($m=0$ and $\beta^o=0^o$), the expression is given as follows:

For $m=0$ and $\beta^o=0°$, $\eta=45^o-\phi/2$, $\theta=90^o+\beta^o=90^o$

$$N_q = \frac{(1+\sin\phi)e^{2\theta\tan\phi}}{(1-\sin\phi)\sin(2\eta+\phi)} = \frac{(1+\sin\phi)e^{\pi\tan\phi}}{(1-\sin\phi)} \qquad \ldots (4.2a)$$

In the case of surface foundation in a slope, the failure plane terminates on the surface of the slope. In this case, the angle β^o is negative and the factor N_q becomes:

For $m=0$ and $\beta^o<0$, $\eta=45^o-\phi/2$, $\theta=90^o+\beta^o$

$$N_q = \frac{(1+\sin\phi)e^{2\theta\tan\phi}}{(1-\sin\phi)\sin(2\eta+\phi)} = \frac{(1+\sin\phi)e^{2(90^o-\beta^o)\tan\phi}}{(1-\sin\phi)} \qquad \ldots (4.2b)$$

The ratio of $N_{q,\ slope}$ to $N_{q,\ horizontal,}$ denoted as R_q can be expressed as:

$$N_{q,slope} = \frac{(1+\sin\phi)e^{2(90°-\beta°)\tan\phi}}{(1-\sin\phi)} = \overbrace{\frac{(1+\sin\phi)e^{\pi\tan\phi}}{(1-\sin\phi)}}^{N_q} \times \overbrace{\frac{e^{2(90°-\beta°)\tan\phi}}{e^{\pi\tan\phi}}}^{R_q^*} = N_{q,horizontal} \times R_q \quad \ldots (4.2c)$$

$$R_q = e^{-2\beta\tan\phi} \quad \ldots (4.2d)$$

Considering that the bearing capacity factor N_q represents the bearing capacity of the footing contributed by the surcharge, the coefficient R_q is only valid for surface foundation with additional, uniformly distributed surcharge along the slope and the ground surface. For embedded footings, the overburden pressure is acting like a surcharge. This surcharge is reduced on the side of slope and continues to decrease with the decrease of the distance to the slope. In order to account for such loss, the term γD_f will be adjusted as follows (Figure 4.11):

$$q_o = \frac{W}{\text{length of Equivalent - Free Surface}} = \gamma \times D_f \quad \ldots (4.3)$$

$$\textit{where}\quad W = \gamma \times D_f \times \text{length of Equivalent - Free Surface}$$

In the case of footing built near slope, the total weight of the soil above the footing is the area of the trapezoid (Figure 4.11). The equivalent surcharge is assumed to be uniformly distributed along the equivalent free surface (line $\overline{ae'}$). The total weight of this portion is calculated as following:

$$W = \frac{(b+b_q)D_f}{2}\gamma \quad \ldots (4.4a)$$

$$\textit{where}\quad b_q > b$$

$$q_o = \frac{(b+b_q)D_f}{2}\frac{1}{b_q}\gamma = \frac{\overbrace{(b+b_q)}^{R_{D_f}}}{2b_q}D_f\gamma = R_{D_f}D_f\gamma \qquad \ldots (4.4b)$$

Where b_q is the base of the trapeze (line $\overline{ah'}$).

Using the trigonometrical relationship, the length b_q is calculated as following:

$$\frac{b_q}{\sin(\alpha-\beta)} = \frac{\overline{ae'}}{\sin(180^\circ-\alpha)} \qquad \ldots (4.5a)$$

$$\frac{\overline{ae'}}{\sin(90^\circ+\phi)} = \frac{r_1}{\sin(90^\circ-\phi-\eta)} = \frac{Be^{\theta\tan\phi}}{2\sin\left(45^\circ-\frac{\phi}{2}\right)\sin(90^\circ-\phi-\eta)} \qquad \ldots (4.5b)$$

Combine Equations 4.5a and 4.5b and yield:

$$\frac{b_q}{B} = \frac{e^{\theta\tan\phi}\sin(\alpha+\beta)\cos\phi}{2\sin\left(45^\circ-\frac{\phi}{2}\right)\cos(\eta+\phi)\sin\alpha} \qquad \ldots (4.5c)$$

Note that when $\beta^o=0^o$ or $\alpha^\circ=0^o$, $\frac{b_q}{B}$ becomes equal to the length of line $\overline{be}$ (Figure 4.11). If $\frac{b}{B}$ is greater than $\frac{b_q}{B}$ (Figure 4.13), which imply that the slope has no effect on the bearing capacity and the foundation is considered as if it is on horizontal surface. On the other hand if $\frac{b}{B}$ is smaller than $\frac{b_q}{B}$ (Figure 4.13), the effect of the slope is incorporated.

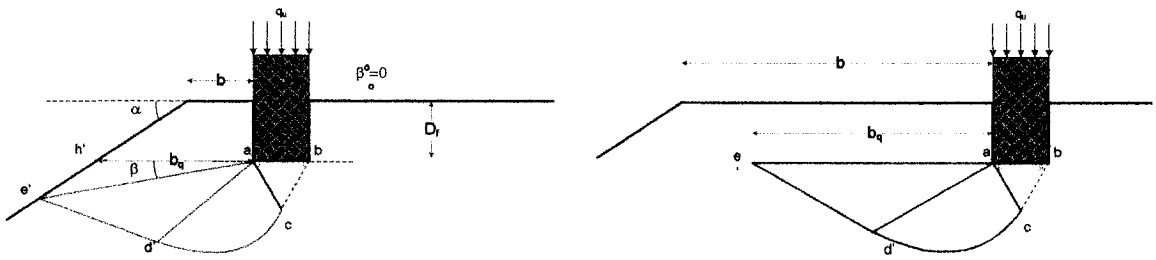

Figure 4.13. Proposed failure mechanisms for foundations near slope for different *b/B* ratio.

Thus, the weight of the soil, above the footing, on the side of the slope can be calculated as following:

$$\frac{W}{B^2} = \left[\frac{b_q}{B}\frac{D_f}{B} - \frac{\left(\frac{b_q}{B} - \frac{b}{B}\right)^2 \tan\alpha}{2} \right]\gamma \qquad \ldots (4.6)$$

where $b_q > b$

Furthermore, the equivalent surcharge normal to the equivalent free surface (line $\overline{ae'}$) is:

$$\frac{\overline{ae'}}{B} = \frac{e^{\theta \tan\phi}\cos(\phi)}{2\sin\left(45^\circ - \frac{\phi}{2}\right)\cos(\phi+\eta)} \qquad \ldots (4.7)$$

$$\frac{W}{B^2} \div \frac{\overline{ae'}}{B} = \left[\frac{b_q}{B}\frac{D_f}{B} - \frac{\left(\frac{b_q}{B} - \frac{b}{B}\right)^2 \tan\alpha}{2} \right]\cos\beta \times \left[\frac{2\sin\left(45^\circ - \frac{\phi}{2}\right)\cos(\phi+\eta)}{e^{\theta\tan\phi}\cos(\phi)} \right]\gamma = \frac{D_{f,eq}\gamma}{B} \qquad \ldots (4.8a)$$

$$\therefore \frac{D_{f,eq}\gamma}{B} = \frac{D_f}{B}\overbrace{\left[\frac{b_q}{B} - \frac{\left(\frac{b_q}{B} - \frac{b}{B}\right)^2 \tan\alpha}{2}\frac{B}{D_f}\right]}^{R_{D_f}} \times \left[\frac{2\sin\left(45^\circ - \frac{\phi}{2}\right)\cos(\phi+\eta)\cos\beta}{e^{\theta\tan\phi}\cos(\phi)}\right]\gamma \quad \ldots (4.8b)$$

where $b_q > b$

$$\Updownarrow$$

$$D_{f,eq}\gamma = R_{D_f} D_f \gamma \quad \ldots (4.8c)$$

For footing near the slope, the ultimate bearing capacity due to surcharge can be estimated as following:

$$q_{N_q} = \overbrace{R_{D_f} D_f \gamma}^{\text{Reduction of sursharge}} \times \overbrace{R_q N_q}^{\text{Reduction of bearing capacity factor}} = D_f \gamma R_q^* N_q \quad \ldots (4.9)$$

where $R_q^* = R_{D_f} \times R_q$ is the coefficient of reduction due to the surcharge and the term R_{D_f} is the coefficient, which accounts the loss of soil mass due to the present of slope

4.3.2 Reduction Factor for the Coefficient N_c

The factor N_c of the soil due to the cohesion is characterized by the size of the failure plane, which depends on the angle β^o for a given ϕ^o. Thus for a footing below or on the ground surface, the factor N_c is equal to *(*N_q *-1) cot* ϕ^o. Therefore the coefficient of reduction R_c can be calculated as following

$$R_c N_c = \left(R_q N_q - 1\right)\cot\phi \quad \ldots (4.10a)$$

$$R_c = \frac{\left(R_q N_q - 1\right)\cot\phi}{N_c} = \frac{\left(R_q N_q - 1\right)}{\left(N_q - 1\right)} \quad \ldots (4.10b)$$

4.3.3 Reduction Factor for the Coefficient N_γ

For the case of foundation on horizontal ground, the factor N_γ was given by Meyerhof (1951) as follows:

$$N_\gamma = \left[\frac{4P_{p\gamma}\sin(45°+\phi/2)}{\gamma B^2} - \frac{1}{2}\tan\left(45°+\frac{\phi}{2}\right)\right] \quad \ldots (4.11)$$

Where $P_{p\gamma}$ is the passive force acting on the elastic wedge *abc* (Figure 4.14).

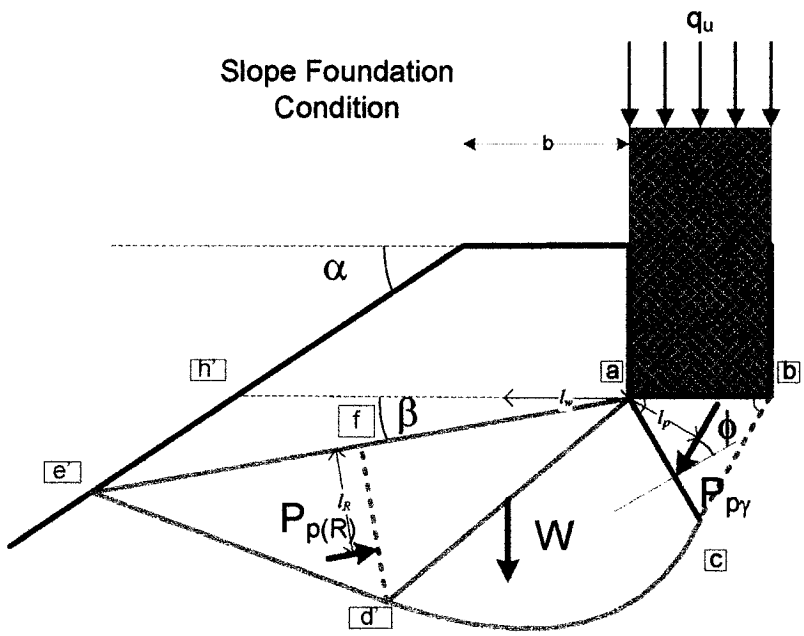

Figure 4.14. Forces acting on the failing wedge.

Taking the moment of the forces about the center of the trial log spiral line (line $\overline{cd'}$ of Figure 4.14) as following:

$$P_{p\gamma} = \frac{Wl_w + P_{p(R)}l_r}{l_p} \quad \ldots (4.12)$$

It can be noted that any change in size of the failure plane (or angle β^o) will change the weight of the wedge *acdf* and accordingly the direction of the passive

force $P_{p(R)}$. Thus the ratio of N_γ for foundation in slope to N_γ for horizontal surface can be expressed as:

$$R_\gamma = \frac{N_{\gamma,slope}}{N_{\gamma,horizontal}} = \frac{\left[\frac{4P_{p\gamma,slope}\sin(45°+\phi/2)}{\gamma B^2} - \frac{1}{2}\tan\left(45°+\frac{\phi}{2}\right)\right]}{\left[\frac{4P_{p\gamma,horizontal}\sin(45°+\phi/2)}{\gamma B^2} - \frac{1}{2}\tan\left(45°+\frac{\phi}{2}\right)\right]} \quad \ldots (4.13)$$

In this analysis, the center of the log spiral was taken at point "a". The moment of the wedge *acdf* is given as

$$Wl_w = \int_0^\theta \frac{r_o e^{\tilde{\theta}\tan\phi} r_o e^{\tilde{\theta}\tan\phi}}{2} \times \frac{2}{3} r_o e^{\tilde{\theta}\tan\phi} \cos\left(45° + \frac{\phi}{2} + \tilde{\theta}\right) d\tilde{\theta}$$
$$+ \frac{r_o e^{\theta\tan\phi}\cos\eta \times r_o e^{\theta\tan\phi}\sin\eta}{2} \times \frac{2}{3} r_o e^{\theta\tan\phi}\cos\eta\cos\beta$$

$$= \frac{1}{3} r_o^3 \left\{ \left[\frac{3\tan\phi}{9\tan^2\phi+1} e^{3\tilde{\theta}\tan\phi} \cos\left(45° + \frac{\phi}{2} + \tilde{\theta}\right) + \frac{\tan\phi}{9\tan^2\phi+1} e^{3\tilde{\theta}\tan\phi} \sin\left(45° + \frac{\phi}{2} + \tilde{\theta}\right) \right]_0^\theta \right.$$
$$\left. + e^{3\theta\tan\phi}\cos^2\eta\sin\eta\cos\beta \right\} \quad \ldots (4.14)$$

The moment of Rankine passive force (on line *df*) is given by the following Equation:

$$P_{p(R)} l_R = \frac{1}{2}\gamma H^2 K_p \times \frac{2}{3} H = \frac{1}{3} r_o^3 e^{3\theta\tan\phi}\gamma K_p \quad \ldots (4.15)$$

Note that for foundation on horizontal surface, the angle β^o is equal to zero. Thus the angle θ is equal 90° and the Rankine's passive coefficient is $tan^2(45^o+\phi/2)$. Thus for foundation in slope, the angle β^o is less than zero and angle the θ is therefore equal (90^o-β^o). The Rankine's passive force on line *df* is considered as the passive earth pressure for inclined backfill having an inclination of β^o. The coefficient K_p for the inclined backfill is taken as:

$$K_p = \cos\beta \frac{\cos\beta + \sqrt{\cos^2\beta - \cos^2\phi}}{\cos\beta - \sqrt{\cos^2\beta - \cos^2\phi}} \quad \ldots (4.16)$$

The passive force P_{py} for both horizontal and slope foundation conditions can be determined and the coefficient of reduction for N_γ, denoted as R_γ can be determined by Equation 4.12.

4.3.4 General Bearing Capacity Equation for Foundations near Slope

For strip foundation subjected to vertical loading built on horizontal ground surface, the bearing capacity can be predicted using Equation 2.5. In the case of strip foundation near slope, the general bearing capacity equation becomes:

$$q_u = cN_c R_c \lambda_{cd} + \gamma R_{D_f} D_f N_q R_q \lambda_{qd} + \frac{1}{2}\gamma B N_\gamma R_\gamma \lambda_{\gamma d} \ldots (4.17)$$

Generally there are three scenario of foundation near slope.

1 – Case of $\beta^o < 0^o$

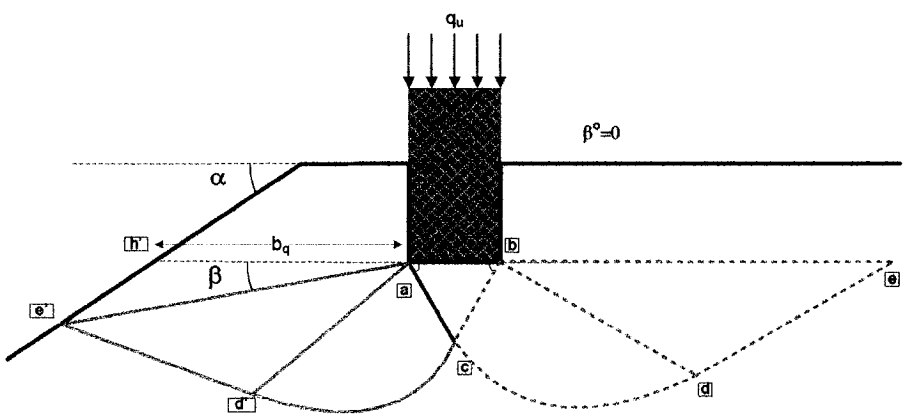

Figure 4.15. Failure mechanism, case of β^o <0°

In this case, the failure plane does not extend above the line $\overline{ah'}$ therefore it is suggested that the depth factors should not be included. Equation 4.17 becomes

$$q_u = cN_c R_c + \gamma R_{D_f} D_f N_q R_q + \frac{1}{2}\gamma B N_\gamma R_\gamma \ldots \quad (4.18a)$$

2 – Case of $\beta^o = 0^o$ and $\frac{b_q}{B} > \frac{b}{B}$

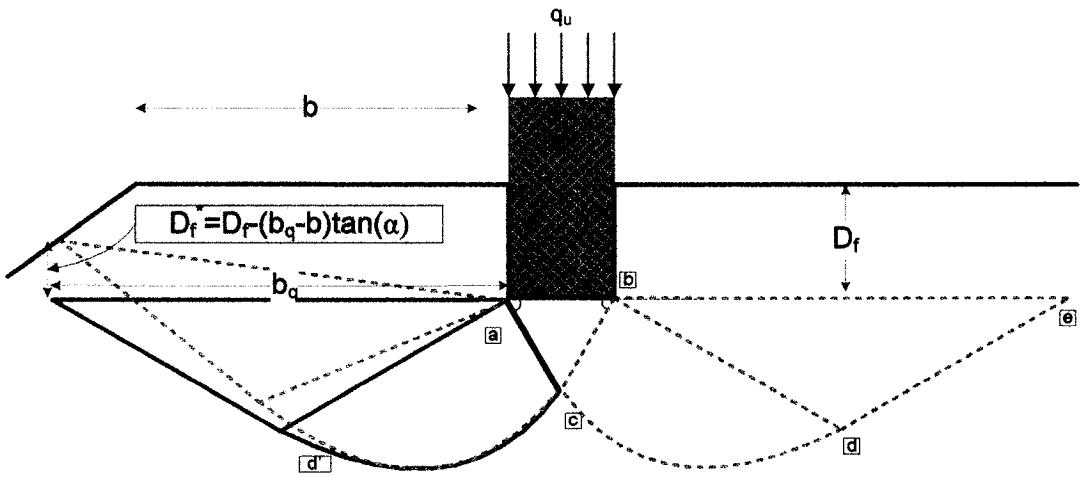

Figure 4.16. Failure mechanism, case of β^o=0° and $\frac{b_q}{B} > \frac{b}{B}$

In this case, the failure plane extends above the foundation base and therefore the depth factors of Meyerhof are applied. The D_f in the depth factors is replaced by D_f* and Equation 4.17 becomes:

$$q_u = cN_c R_c \lambda_{cd} + \gamma R_{D_f} D_f N_q R_q \lambda_{qd} + \frac{1}{2}\gamma B N_\gamma R_\gamma \lambda_{\gamma d} \quad \ldots \quad (4.18b)$$

Where

For $\phi = 0°$

$$\lambda_{cd} = 1 + 0.2\left(\frac{D_f - (b_q - b)\tan\alpha}{B}\right) \quad \ldots \quad (4.19a)$$

$$\lambda_{qd} = \lambda_{\gamma d} = 1 \quad \ldots \quad (4.19b)$$

For $\phi > 10°$

$$\lambda_{cd} = 1 + 0.2\left(\frac{D_f - (b_q - b)\tan\alpha}{B}\right)\tan\left(45° + \frac{\phi}{2}\right) \quad \ldots \quad (4.19c)$$

$$\lambda_{qd} = \lambda_{\gamma d} = 1 + 0.1\left(\frac{D_f - (b_q - b)\tan\alpha}{B}\right)\tan\left(45° + \frac{\phi}{2}\right) \quad \ldots (4.19d)$$

where $b_q > b$

3 – Case of β° = 0° and $\frac{b_q}{B} \leq \frac{b}{B}$

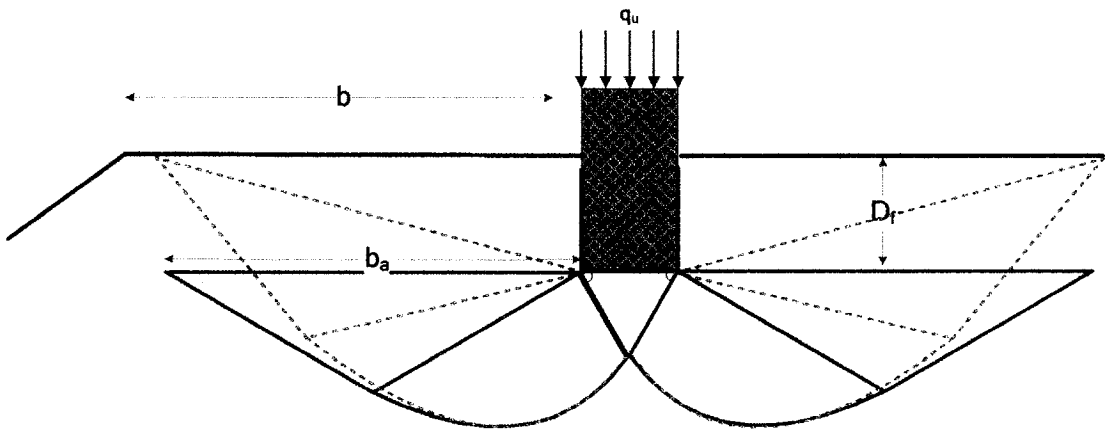

Figure 4.17. Failure mechanism, case of β°=0° and $\frac{b_q}{B} \leq \frac{b}{B}$

In this case, the failure plane extends to the horizontal surface and therefore it is considered as horizontal surface foundation. The depth factors and the equation for strip foundation on horizontal surface are used.

4.4 VALIDATION OF THE ANALYTICAL MODEL

To validate the present analytical model, the predicted values of the ultimate bearing capacity of the footings were first compared with the results given by the numerical model. The model was then validated with the experimental result of Shields et al. (1977) and the theoretical values of Meyerhof (1957).

4.4.1 Comparison between the Analytical and the Numerical Values

The reduction factors (R_c, R_q, and R_γ) deduced from the numerical model were compared with those predicted by the analytical model (Figure 4.18 to 4.22). In this analysis, the bearing capacity factors, N_c, N_q, and N_γ, determined from Test No. 6 (α°=0°) were used to back-calculate the reduction factors. The following procedure was followed to back-calculate the reduction factors.

$$R_\gamma = \frac{q_u(\text{Test No.1})}{\frac{1}{2}\gamma B N_\gamma \lambda_{\gamma d}} \quad \ldots (4.20)$$

$$R_q = \frac{q_u(\text{Test No.2 \& 3}) - \frac{1}{2}\gamma B N_\gamma \lambda_{\gamma d} R_\gamma}{\gamma R_{D_f} D_f N_q \lambda_{qd}} \quad \ldots (4.21)$$

$$R_c = \frac{q_u(\text{Test No.4 \& 5})}{c N_c \lambda_{cd}} \quad \ldots (4.22)$$

The depth factors λ_{cd}, λ_{qd} and $\lambda_{\gamma d}$ suggested by Meyerhof (1963) were employed and follow the rule stated in Section 4.3.4. The comparisons of reduction factors are produced and graphical plotted in Figure 4.18 to 4.22.

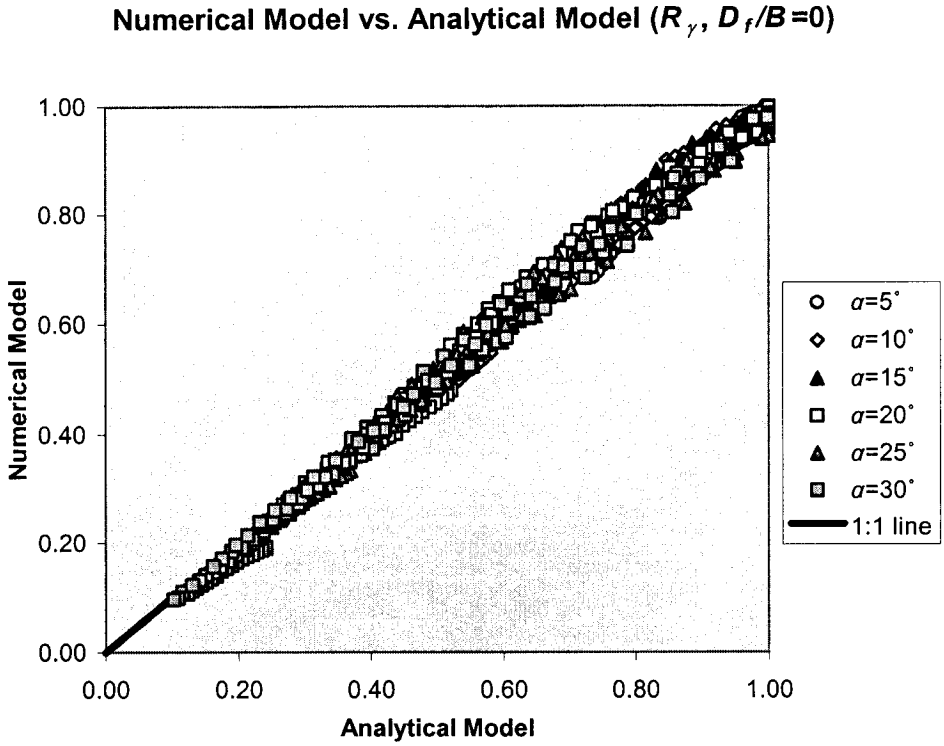

Figure 4.18. Comparison of the reduction factor R_γ deduced from the analytical and numerical models (Test No. 1).

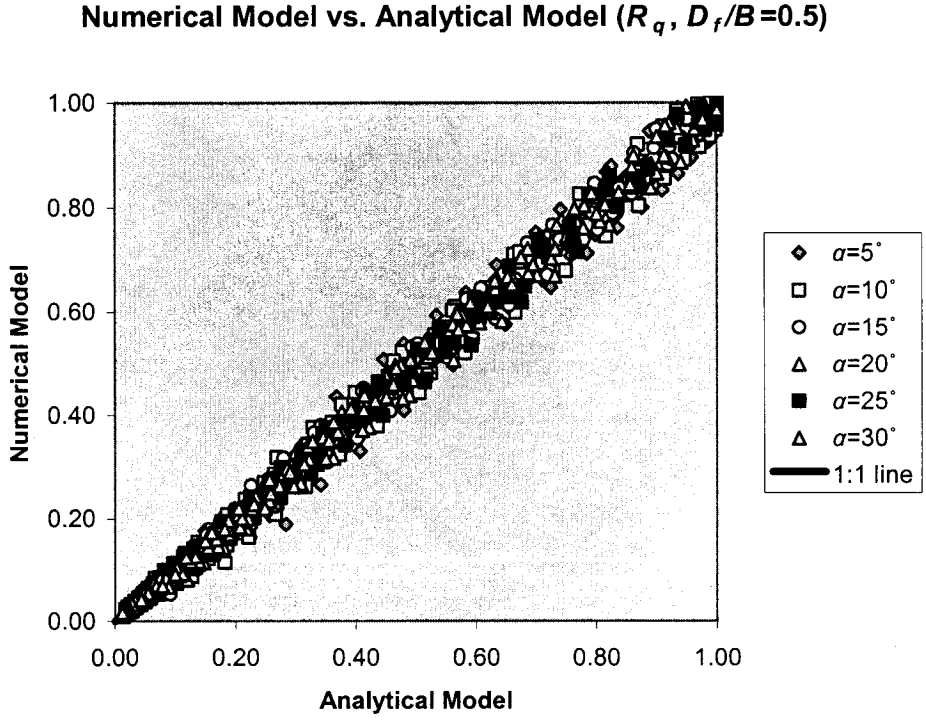

Figure 4.19. Comparison of the reduction factor R_q deduced from the analytical and numerical models (Test No. 2).

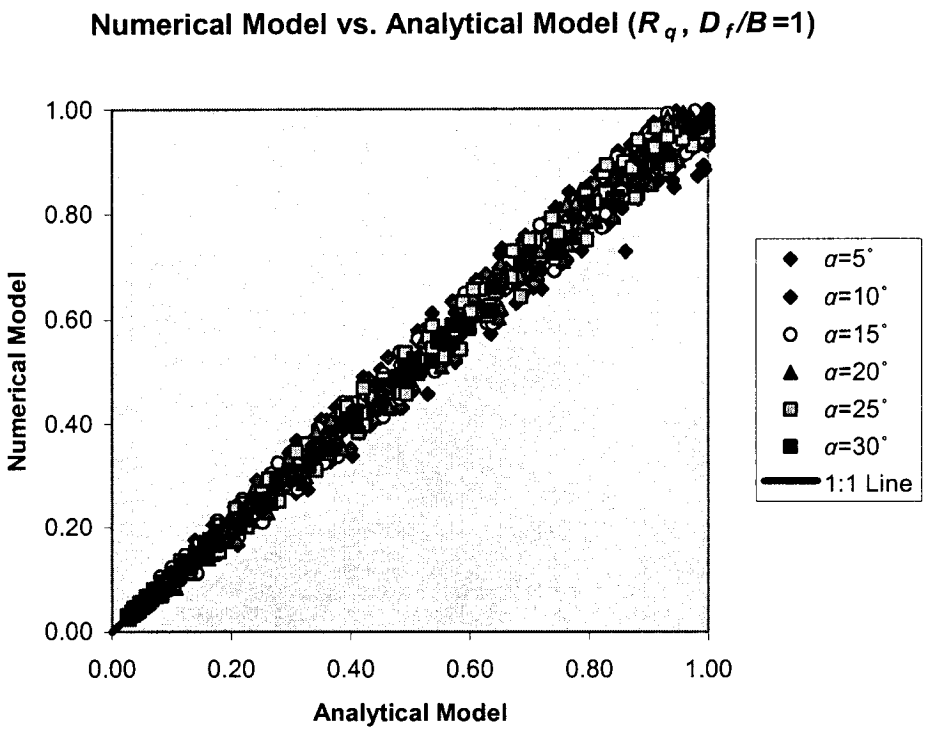

Figure 4.20. Comparison of the reduction factor R_q deduced from the analytical and numerical models (Test No. 3).

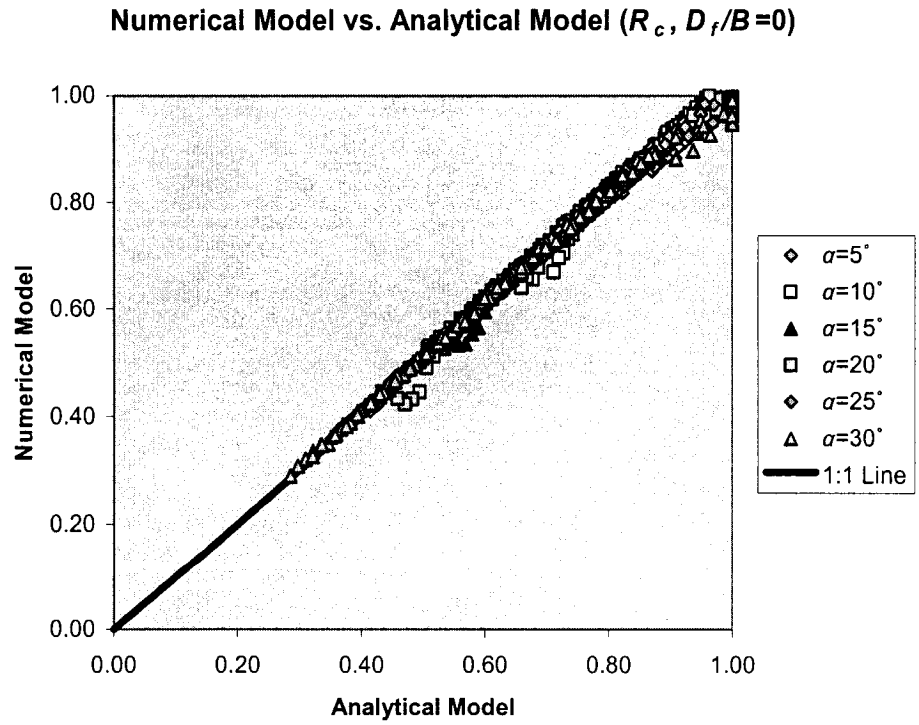

Figure 4.21. Comparison of the reduction factor R_c. deduced from the analytical and numerical model (Test No. 4).

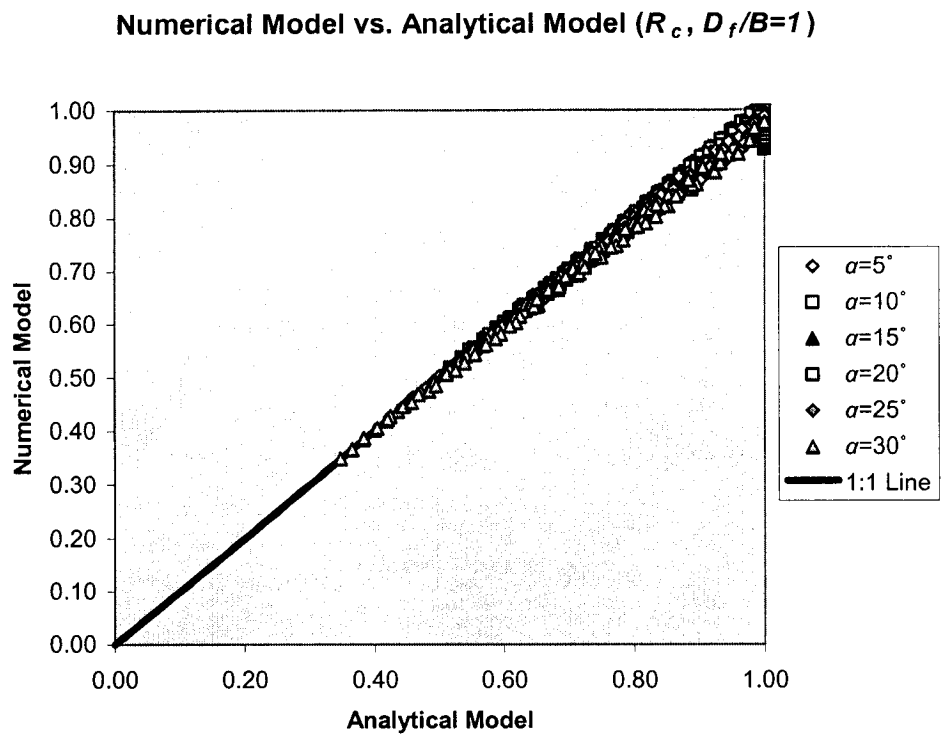

Figure 4.22. Comparison of the reduction factor R_c deduced from the analytical and numerical models (Test No. 5).

It can be noted from these figures that good agreement between the results of analytical and numerical models for the reduction factor R_c was achieved. When calculating the coefficient of reduction R_q from the result of numerical model, the superposition method cannot be used to calculate the ultimate load due to overburden pressure only. As the result, the problem became complicated and a larger error was obtained. However the overall error does not exceed more than 10%. The variation of reduction factor with respect to *b/B* ratio from the proposed analytical model give very reasonable fit to the value given by numerical model. Figure 4.23 to 4.27 show sample of the variation of the reduction factors vs. the *b/B* ratio for soil having ϕ°=30°.

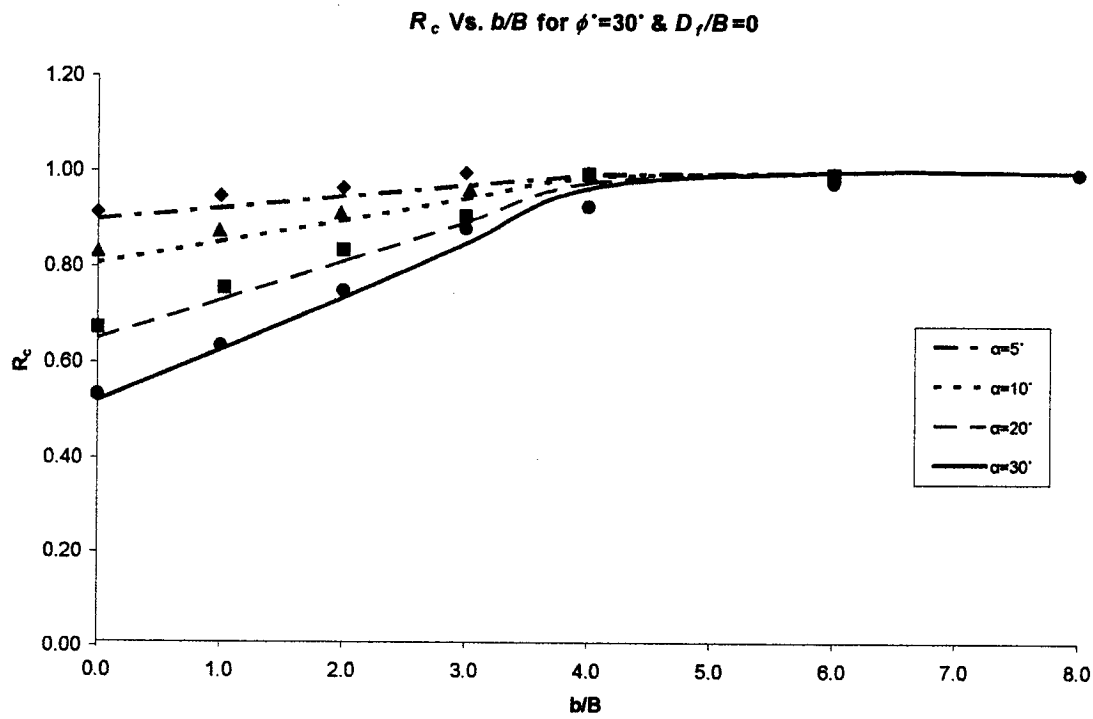

Figure 4.23. Reduction Factor R_c versus b/B ratio for ϕ°=30° (Line=Analytical model; Point = Value from Numerical Model)

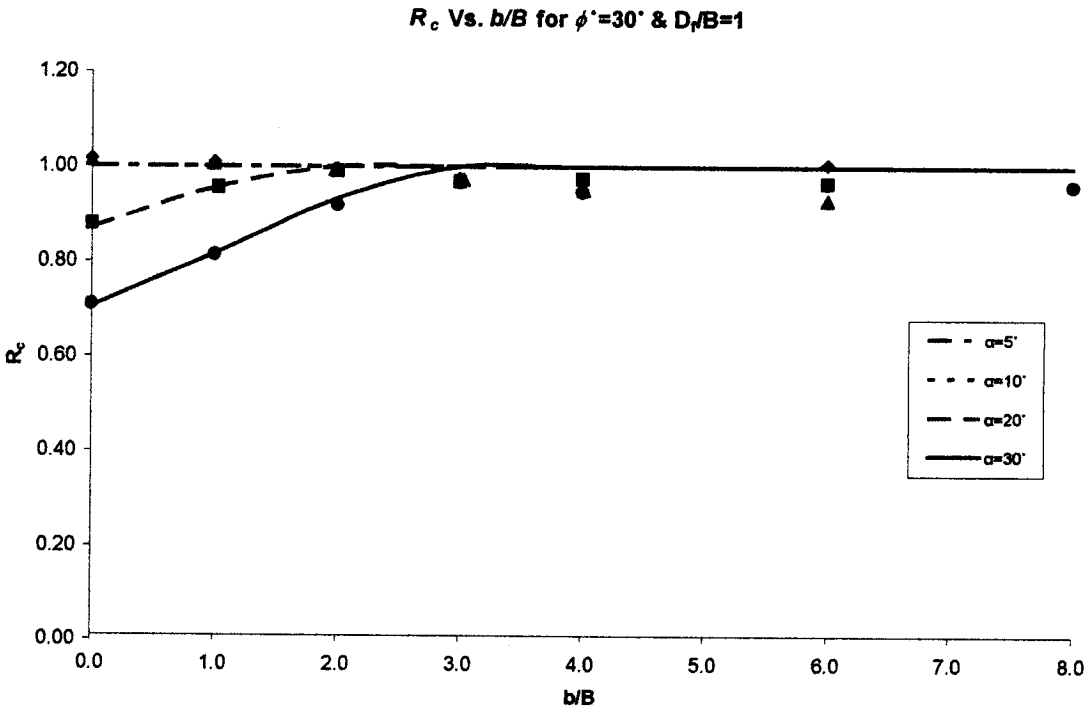

Figure 4.24. Reduction Factor R_c versus b/B ratio for ϕ°=30° (Line=Analytical model; Point = Value from Numerical Model)

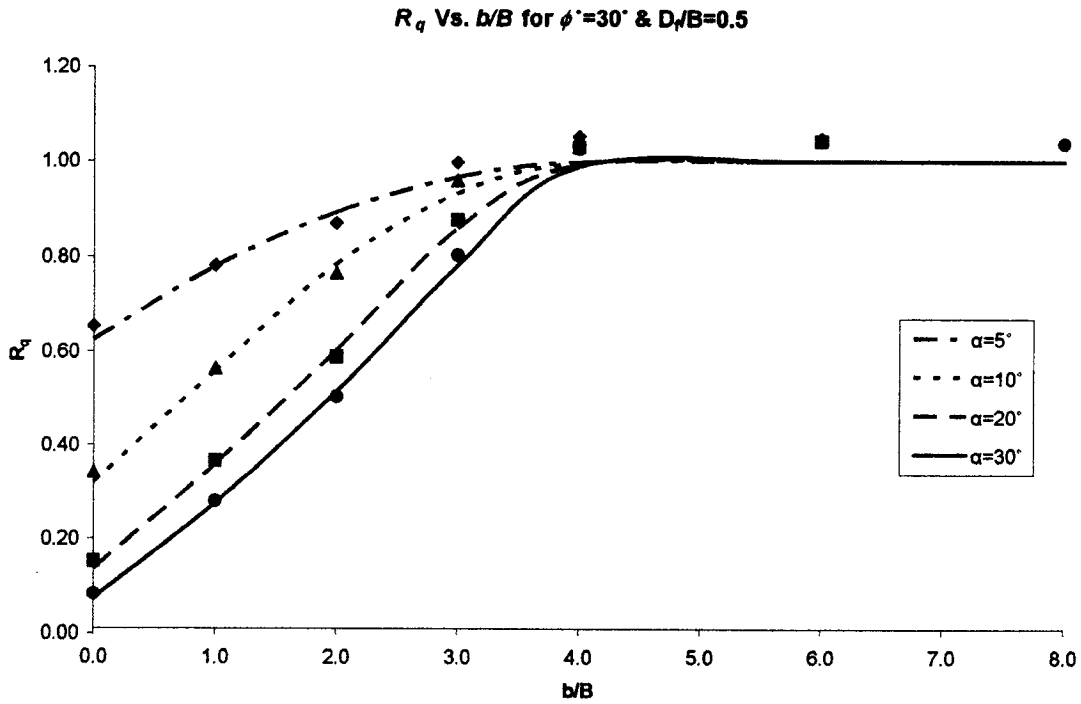

Figure 4.25. Reduction Factor R_q versus b/B ratio for ϕ^{o}=30° (Line=Analytical model; Point = Value from Numerical Model)

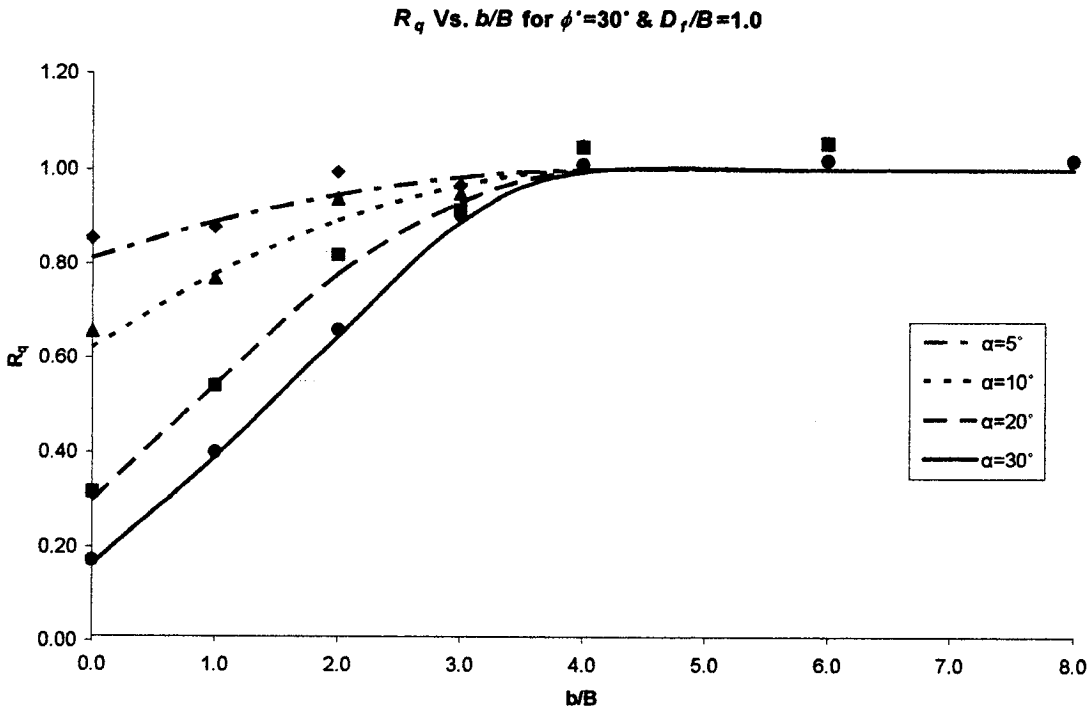

Figure 4.26. Reduction Factor R_q versus b/B ratio for ϕ^{o}=30° (Line=Analytical model; Point = Value from Numerical Model)

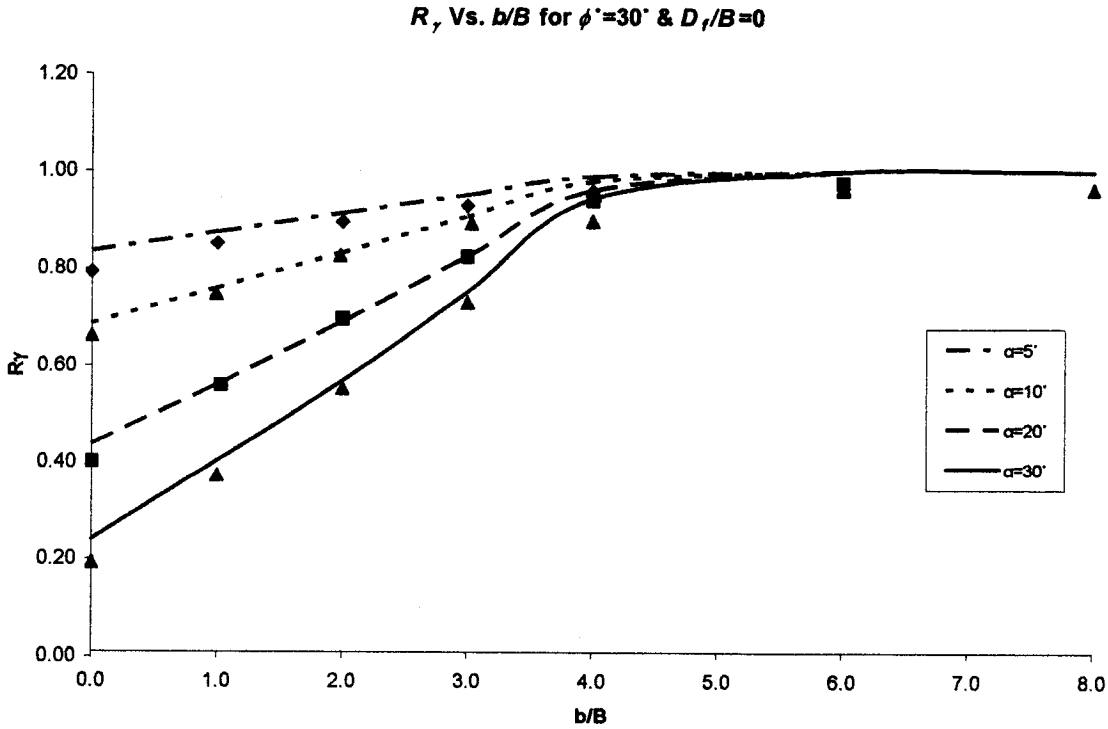

Figure 4.27. Reduction Factor R_γ versus b/B ratio for ϕ°=30° (Line=Analytical model; Point = Value from Numerical Model)

In the above mentioned comparisons the superposition method was use to determine the reduction factors for the case of a footing having a width of one meter and. To ensure that the analytical model is capable to predict these values for different foundation configurations, a series of tests (Test No. 7, 8, 9 & 10) were performed on embedded footings with different soil parameters.

The validation was performed by comparing the value of ultimate bearing capacity (in kN/m/m length of the footing) as deduced from the proposed analytical model. The bearing capacity factors are then calculated as described in Section 4.3.1 to 4.3.3 and the reduction factors and the depth factors were calculated following the procedures given in Section 4.3.4. Figures 4.28 & 4.29, 4.30 and 4.31.

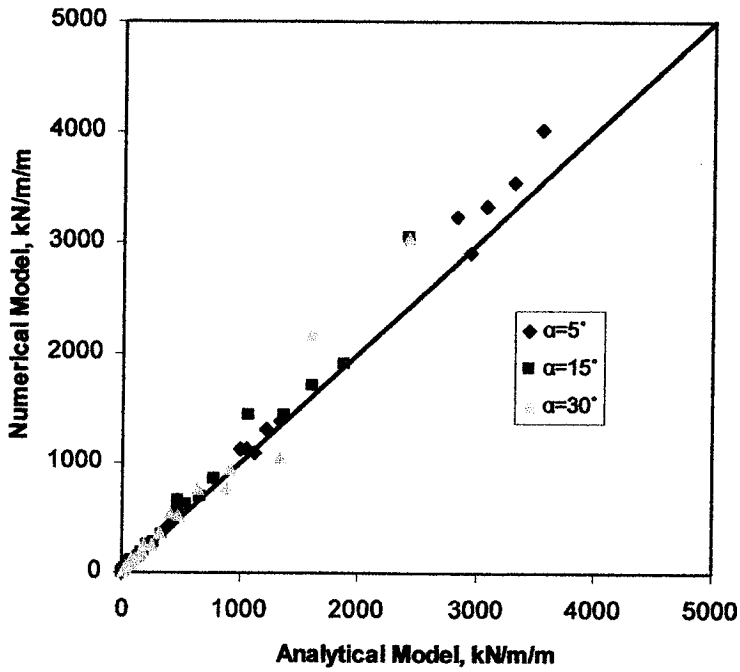

Figure 4.28. Comparison of the ultimate bearing capacities deduced from the analytical and numerical models (Test No. 7).

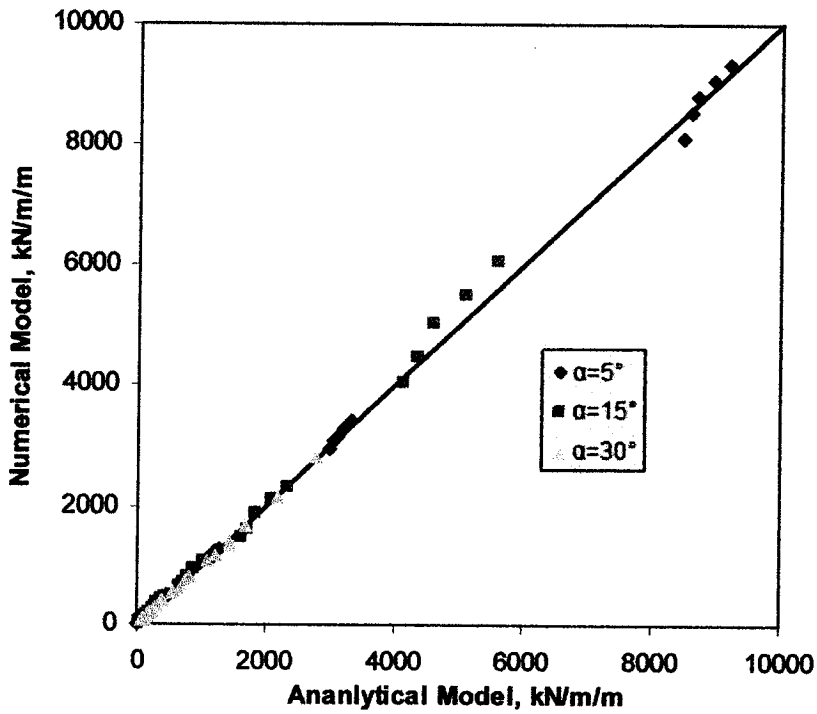

Figure 4.29. Comparison of the ultimate bearing capacities deduced from the analytical and numerical models (Test No. 8).

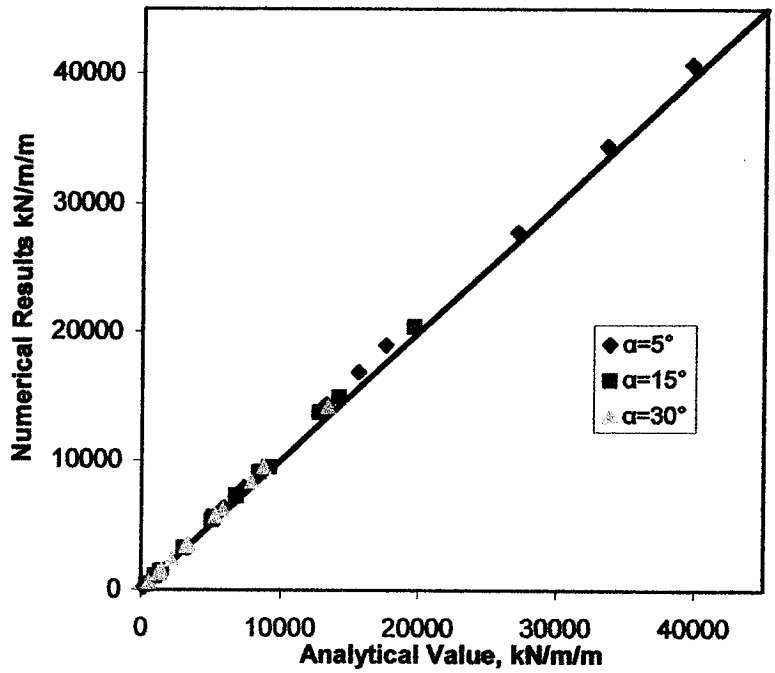

Figure 4.30. Comparison of the ultimate bearing capacities deduced from the analytical and numerical models. (Test No. 9).

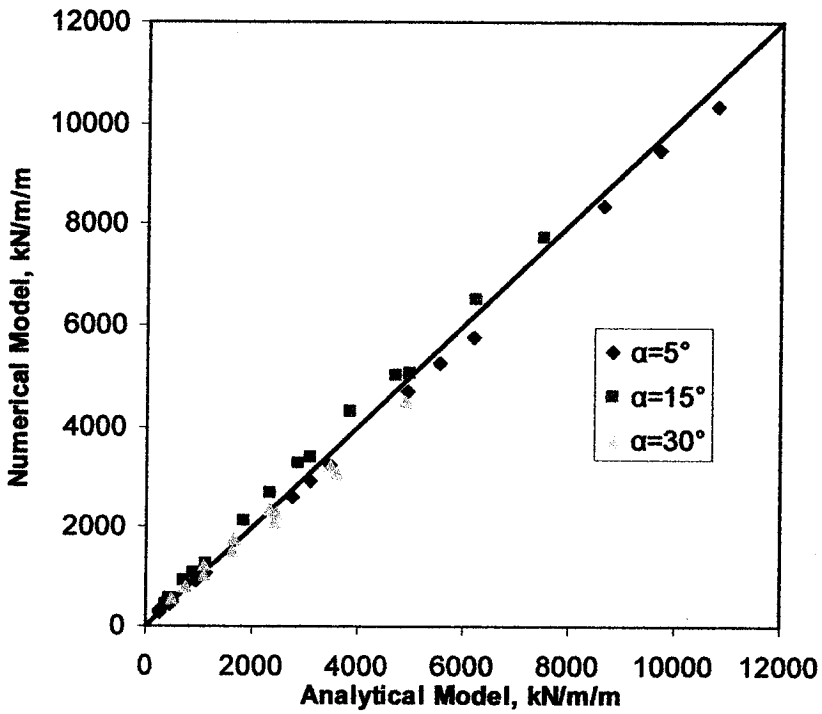

Figure 4.31. Comparison of the ultimate bearing capacities deduced from the analytical and numerical models (Test No. 10)

From Figures 4.29 & 4.30 and 4.31, the values of ultimate bearing capacity (q_u) given by analytical model agreed fairly well with those given by numerical model. The values of the ultimate bearing capacity given by the analytical model were in the vicinity of 90% of the values obtained by numerical model. While for smaller footing (Figure 4.28), the values of ultimate bearing capacity were slightly higher than those estimated from the analytical model. Although the above results produced about 10 to 35% of error, the values of percentage error are nearly constant for the same angle of ϕ° with different α° and b/B ratio. This implies that the variation given by analytical model with respect to these parameters reflects the variation of the q_u calculated by the numerical model. In the literature, theories can be found to claim that the ultimate bearing capacity decreases with the increase of size of the footing (Debeer 1965, Bauer et al 1981, Gottardi et al 1994). This is mainly due to the scale effect, as explained below:

1. For larger foundations, the rupture along the slip lines in soil is progressive. Accordingly, the average shear strength mobilized along the slip line decreases with the increase of footing width.
2. The existence of zones of weakness in the soil under the foundation.
3. The actual curvature of the Mohr-Coulumb envelope for small scale footing is different than that for large scale footing.

4.4.2 Comparison between the Analytical Results and the Experimental Data of Shields, Bauer, Deschenes and Barsvary (1977)

Shields et al. (1977) had published values for bearing capacity factor $N_{\gamma q}$ for a slope of 2 horizontal to 1 vertical ($\alpha^\circ \approx 26.57^\circ$) with compact and dense sand. Since the experimental values of bearing capacity factor $N_{\gamma q}$ consists of both the effect of surcharge and strength underneath the footing, it is assumed that the analytical value of $N_{\gamma q}$ is the resultant of the bearing capacity factor N_q and N_γ and can be calculated according to the following relationship:

$$q_u = \overbrace{\lambda_{cd} R_c c N_c + \gamma R_{D_f} D_f R_q \lambda_{qd} N_q + \frac{1}{2}\gamma B R_\gamma \lambda_{\gamma d} N_\gamma}^{\text{Analytical Model}} = \overbrace{c N_{cq} + \frac{1}{2}\gamma B N_{\gamma q}}^{\text{Meyerhof(1957)}} \quad \ldots (4.23)$$

For cohesionless material (c=0),

$$q_u = \gamma R_{D_f} D_f R_q \lambda_{qd} N_q + \frac{1}{2}\gamma B R_\gamma \lambda_{\gamma d} N_\gamma = \frac{1}{2}\gamma B N_{\gamma q} \quad \ldots (4.24)$$

For $D_f/B = 0$,

$$q_u = \overbrace{\gamma R_{D_f} D_f \lambda_{dq} R_q N_q}^{D_f=0} + \frac{1}{2}\gamma B R_\gamma N_\gamma = \frac{1}{2}\gamma B N_{\gamma q, D_f/B=0}$$

$$\frac{1}{2}\gamma R_\gamma B N_\gamma = \frac{1}{2}\gamma B N_{\gamma q, D_f/B=0}$$

or

$$\overbrace{R_\gamma N_\gamma}^{\text{Analytical Model}} = \overbrace{N_{\gamma q, D_f/B=0}}^{\text{Shields's Value}} \quad \ldots (4.25)$$

And for $D_f/B > 0$,

$$q_u = \gamma R_{D_f} D_f R_q \lambda_{qd} N_q + \frac{1}{2}\gamma B R_\gamma \lambda_{\gamma d} N_\gamma = \frac{1}{2}\gamma B N_{\gamma q, D_f/B>0}$$

then

$$R_{D_f} D_f R_q \lambda_{qd} N_q + \frac{1}{2} R_\gamma \lambda_{\gamma d} N_\gamma = \frac{1}{2} N_{\gamma q, D_f/B>0}$$

or

$$\overbrace{2R_{D_f} D_f R_q \lambda_{qd} N_q + R_\gamma \lambda_{\gamma d} N_\gamma}^{\text{Analytical Model}} = \overbrace{N_{\gamma q, D_f/B>0}}^{\text{Shield's Value}} \quad \ldots (4.26)$$

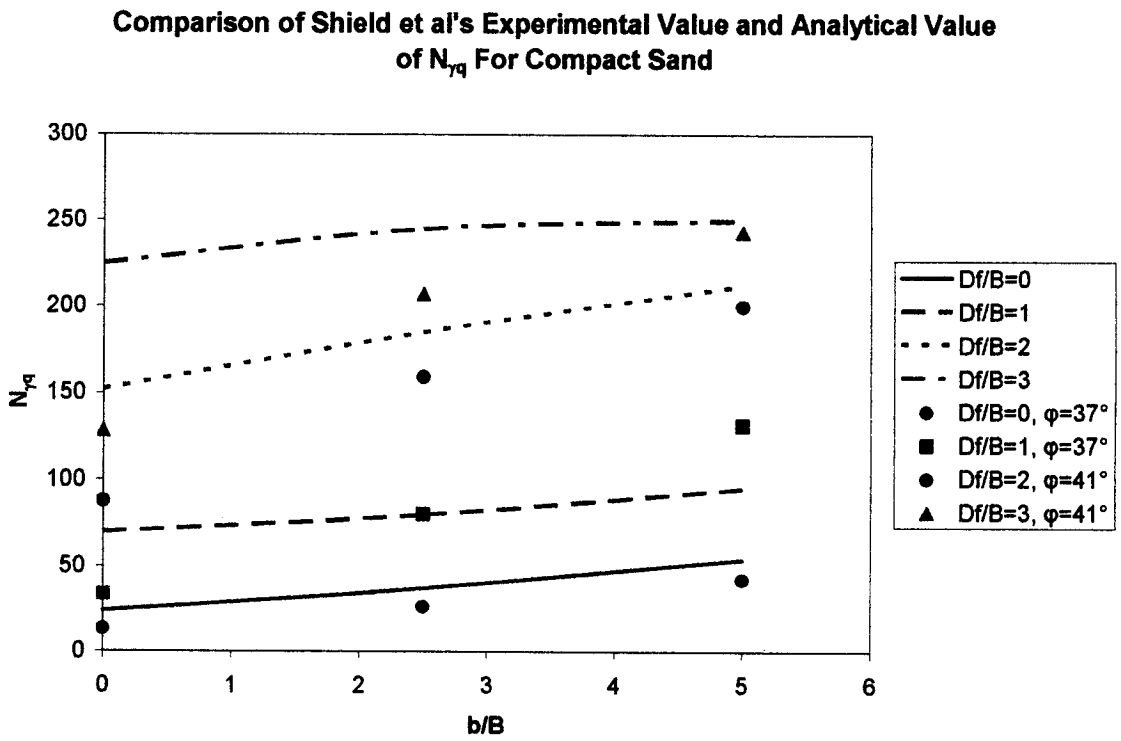

Figure 4.32. Comparison of the bearing capacity factor $N_{\gamma q}$ of Shield et al.'s and the analytical model for compact sand.

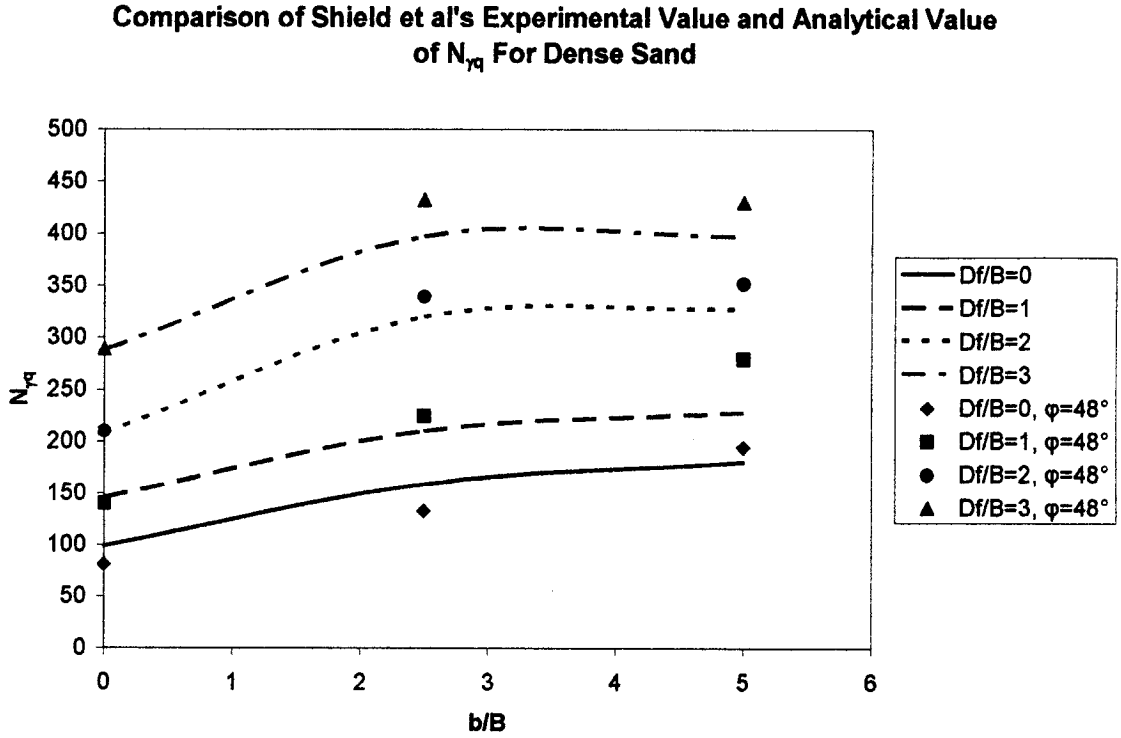

Figure 4.33. Comparison of the bearing capacity factor $N_{\gamma q}$ of Shield et al's and the analytical model for dense.

From Figure 4.32 and 4.33, it can be noted that Shields's values of $N_{\gamma q}$ are within the minimum (lowest $\phi°$) and maximum (largest $\phi°$) value of $N_{\gamma q}$ given by the analytical model. In the case of compact sand the analytical value of $N_{\gamma q}$ with $\phi°$=37° is fairly close to the values produced by Shields et al. when the footing was rested on the surface or had an embedded depth of 1. While the value of $N_{\gamma q}$ with $\phi°$=41° is close to those of Shields et al when the footing was rested deeper from the ground ($D_f/B \geq 2$) and farther from the edge of slope. In the case of dense sand, the values of $N_{\gamma q}$ with $\phi°$=48° have better agreement with the all the values of Shields et al.

Considering that Shield et al. have used the angle of shearing resistance $\phi°$, which was determined from the triaxial test results, while the comparison was made for

the case of plane-strain condition, support a reasonable fit between the theoretical and experimental bearing capacity values.

4.4.3 Comparison between the Analytical Values and the Results Produced by Meyerhof's Theory (1957)

In order to compare the bearing capacity factors derived from the analytical model to that predicted by Meyerhof's theory, superimposition of the theoretical values of bearing capacity factor $N_{\gamma q}$ to generate the value of the factors N_γ and N_q. The comparison is limited to soil having $\phi^\circ = 30°$ and 40°, as well as foundation parameter $D_f/B = 0$ and 1, and $\alpha°$=30 for $\phi^\circ = 30°$ and $\alpha°$=20 & 40° for $\phi^\circ = 40°$. The method of calculating the value of $N_{\gamma q}$ is the same as stated in Section 4.4.2.

Figure 4.34 & 4.35, shows that the increase in *b/B* ratio, increases the value of bearing capacity factors, where good agreement can be noted. Refer to the curves with $\phi°$=30° (Figure 4.34), the magnitude of $N_{\gamma q}$ calculated from analytical model is approximately equal to theoretical value when *b/B* equal to zero and *b/B* equal to infinite (horizontal surface). However, the variation with respect to *b/B* is different. Both analytical model (Figure 4.34 & 4.35) and data from numerical model (Test No. 1-4 & 3-4 for $\phi°$=40° and Test No. 1-6 & 3-6 for $\phi°$=30°) show that the actual distance/width ratio at which the bearing capacity factor becomes independent of the slope is 4.5B to 6B for surface (D_f/B = 0) and shallow (D_f/B = 1) foundation, rather that 2B and 3.5B respectively. From the results of the numerical model for the case of $\phi°$=30° and $\alpha°$=30° (Figure 3.9c and 3.10c), it shows that the shear stress concentrates on the side of slope when *b*=2B. When *b* is 4B, the failure plane becomes more symmetric and no noticeable slope effect is found. For $\phi°$=40° (Figure 4.35), the difference of variation between the

theory and the analytical model is more noticeable. When surface foundation ($D_f/B = 0$) is at the edge of the slope (b/B=0), the magnitude of $N_{\gamma q}$ from analytical has approximately the same value as theoretical one. Beyond the edge of slope, the increase of $N_{\gamma q}$ with respect to b/B ratio seems to be more linear, rather than exponential. The theory shows that, at a distance about 4.5B, the bearing capacity factor is independent of slope. However from both numerical and analytical model, this distance is greater than 6B. By using the analytical model, this distance was found to be about 8B from the edge of the slope.

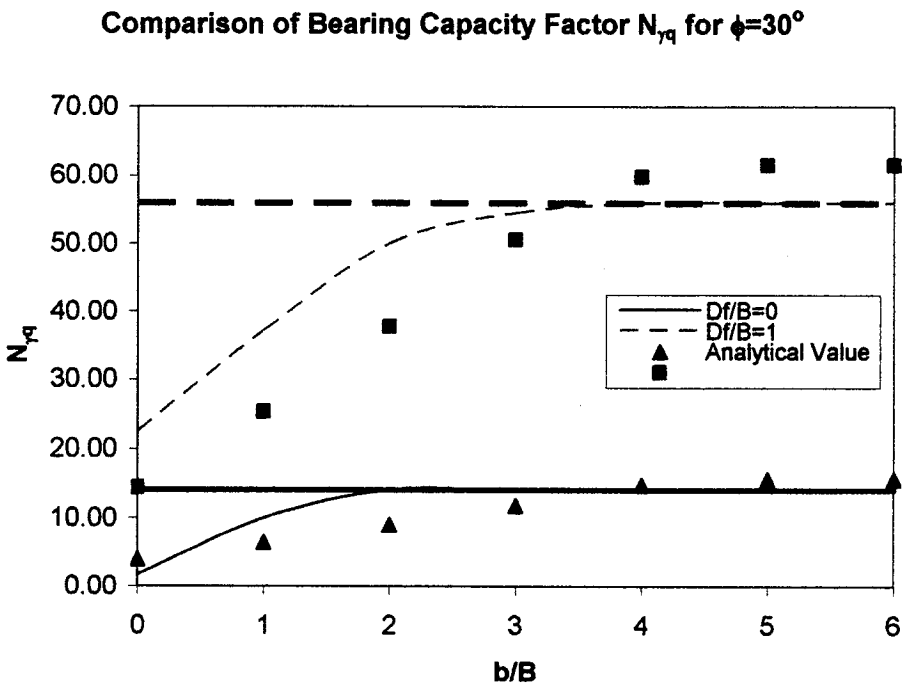

Figure 4.34. Values of bearing capacity factors $N_{\gamma q}$ predicted by the analytical model for ϕ=30°

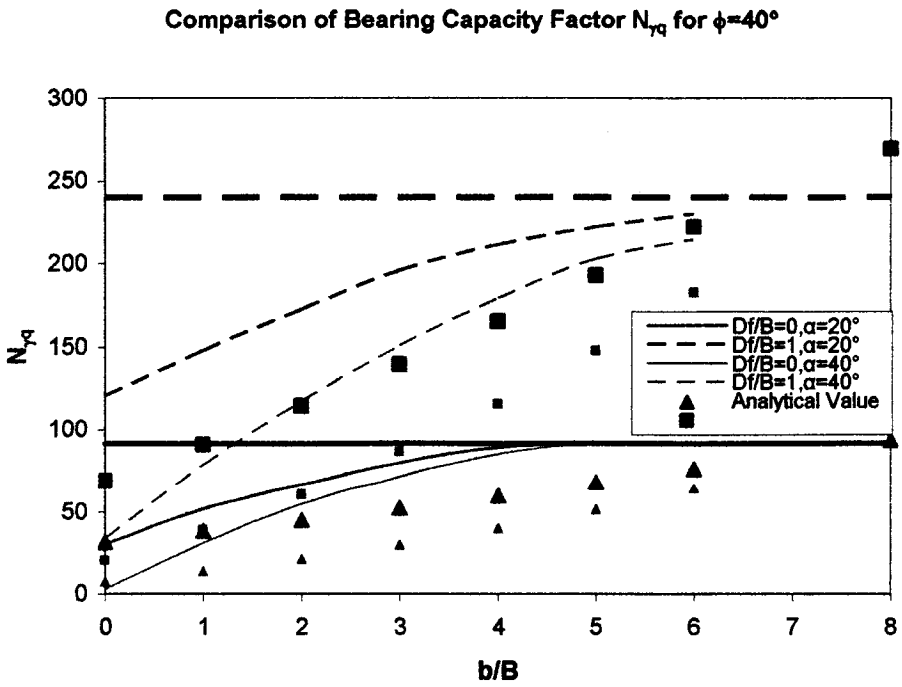

Figure 4.35. Values of bearing capacity factors $N_{\gamma q}$ predicted by the analytical model for ϕ=40°

4.5 DESIGN PROCEDURE

The proposed coefficient of reduction R_c, R_q and R_γ in Section 4.3 (Equation 4.10b, 4.2d, & 4.13 respectively) describe mathematically the percentage of the bearing capacity factors N_c, N_q and N_γ, in terms of $\beta°$, $\phi°$ and $\alpha°$. These coefficients, called slope factors, can be used in the existing general bearing capacity equation. It can be represented graphically thus designers are able to determine the foundations in a simpler way. The charts also give the comparison of the reduction of bearing capacity factor with different physical characteristics of the foundation. Thus engineers are able to determine the feasible location of the foundation, which fit to the requirement.

The following steps summarize the recommended design procedure for foundation near the slope:

1. Obtain a soil sample at the field and determine the soil parameters: angle of shear resistance "ϕ", the cohesion "c", and the unit weight of soil "γ". The angle of shear resistance and the cohesion are determined using triaxial compression test.
2. Determine the parameter of the footing and the adjacent slope.
    a. Determine the distance between the edge of slope and the edge of footing "b".
    b. Determine the angle of slope respected to horizontal, α°
    c. The size of the footing "B" and the depth of embedment, D_f.
3. Calculate the equivalent distance/width ratio $\frac{b_{eq}}{B} = \frac{D_f}{B\tan\alpha} + \frac{b}{B}$ (Equation 4.1c)
4. Use the value of $\frac{b_{eq}}{B}$ and the value of α° and ϕ° to determine the angle of β^o from Figure 4.36 to 4.41. Note that the value given by these figure are negative.
5. Using the value of β^o, determine the slope factors R_c, R_q, and R_γ using Figure 4.42, 4.43 and 4.44 respectively.
6. If β^o is found to be less than zero, $\frac{b_q}{B}$ is equal to $\frac{b_{eq}}{B}$; if β^o is equal to zero, $\frac{b_q}{B}$ is equal to $\frac{b_{eq}}{B}$ with β^o=0° from Figures 4.36 to 4.41.
7. Compare the actual $\frac{b}{B}$ with $\frac{b_q}{B}$.

a. If $\frac{b}{B} > \frac{b_q}{B}$ (β^o=0°), foundation on level ground is considered. The depth factors are calculated using equations stated in Table 2.1.

b. If $\frac{b}{B} < \frac{b_q}{B}$ ($\beta^o \leq$ 0°), foundation near slope is considered. The depth factors are calculated using Equation 4.19a to d. The coefficient R_{D_f} is calculated using Equation 4.8b

8. Using Equation 4.17 to determine the ultimate bearing capacity.

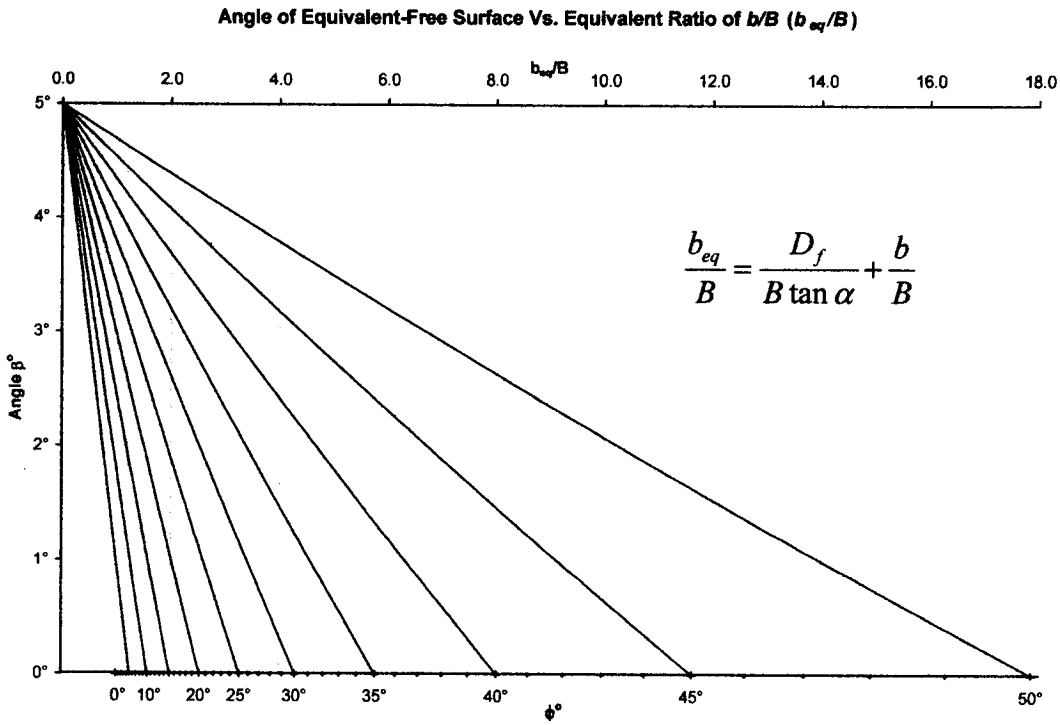

Figure 4.36. Angle of equivalent-free surface β^o vs. equivalent distance/footing width ratio (b_{eq}/B) for angle of slope α° =5°

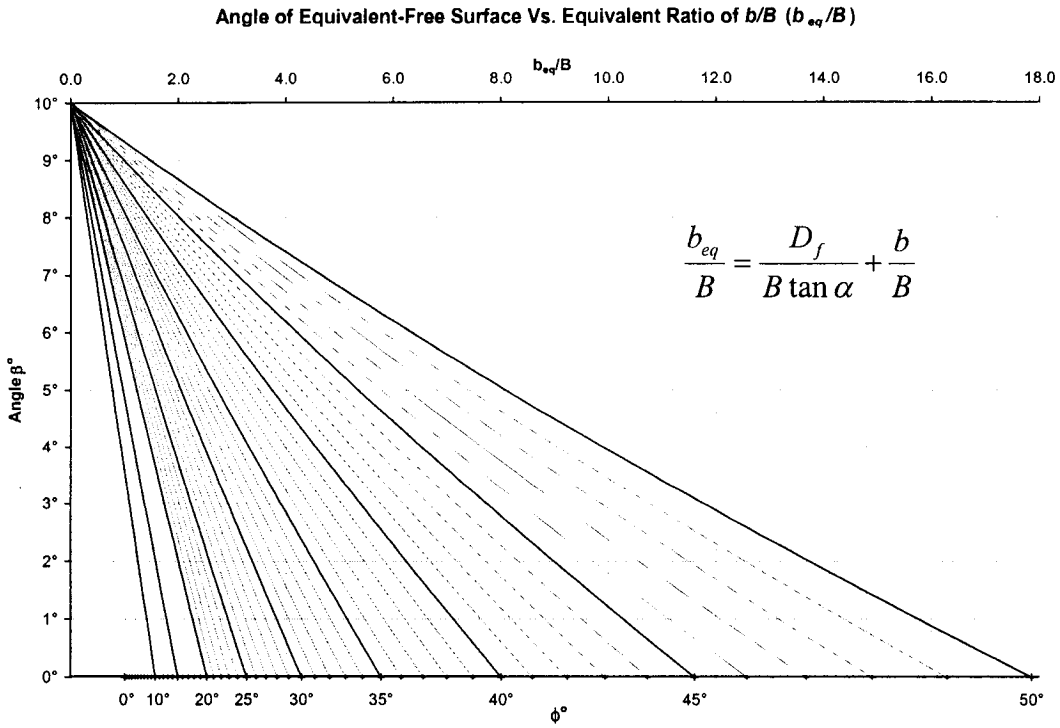

Figure 4.37. Angle of equivalent-free surface β^o vs. equivalent distance/footing width ratio (b_{eq}/B) for angle of slope $\alpha^\circ = 10^\circ$

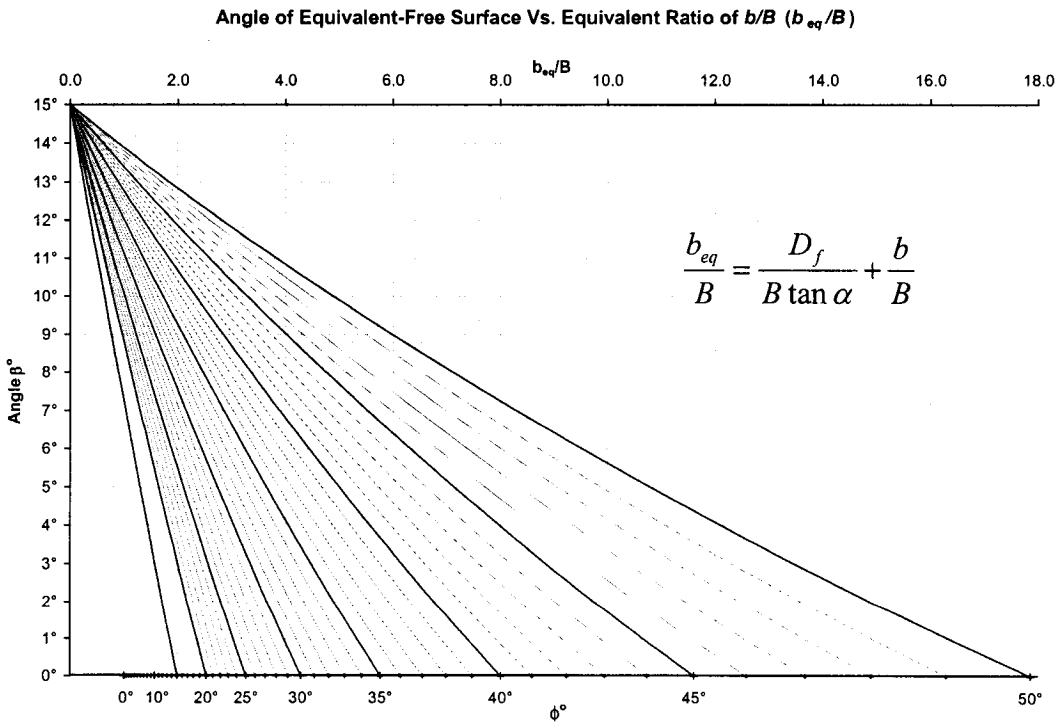

Figure 4.38. Angle of equivalent-free surface β^o vs. equivalent distance/footing width ratio (b_{eq}/B) for angle of slope $\alpha^\circ = 15^\circ$

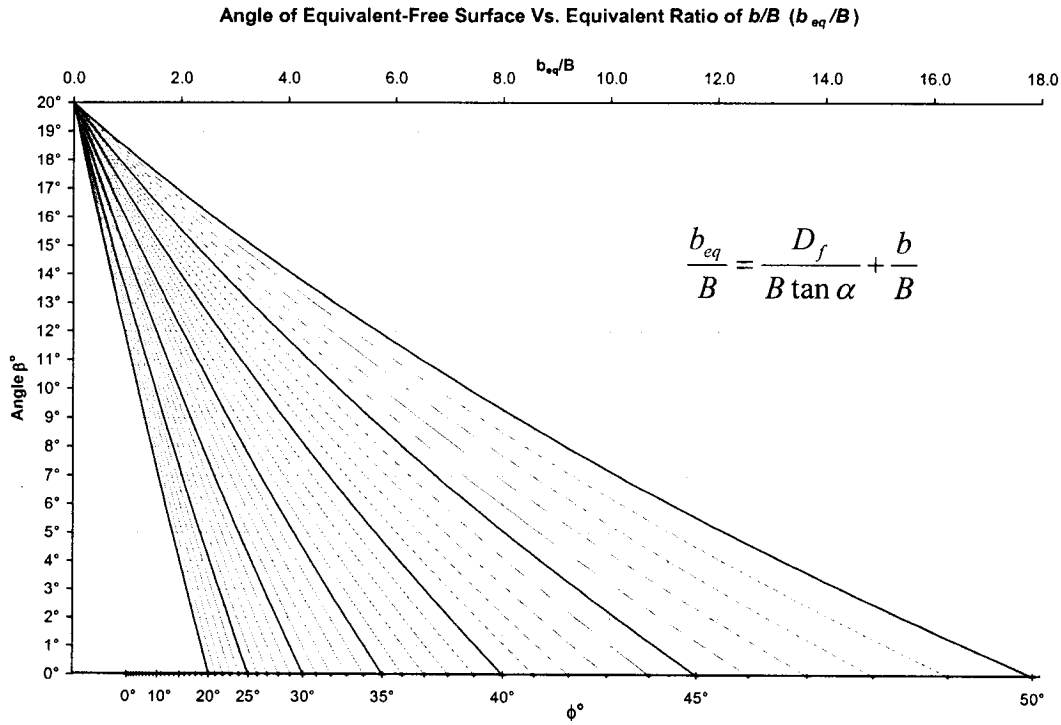

Figure 4.39. Angle of equivalent-free surface β^o vs. equivalent distance/footing width ratio (b_{eq}/B) for angle of slope $\alpha° = 20°$

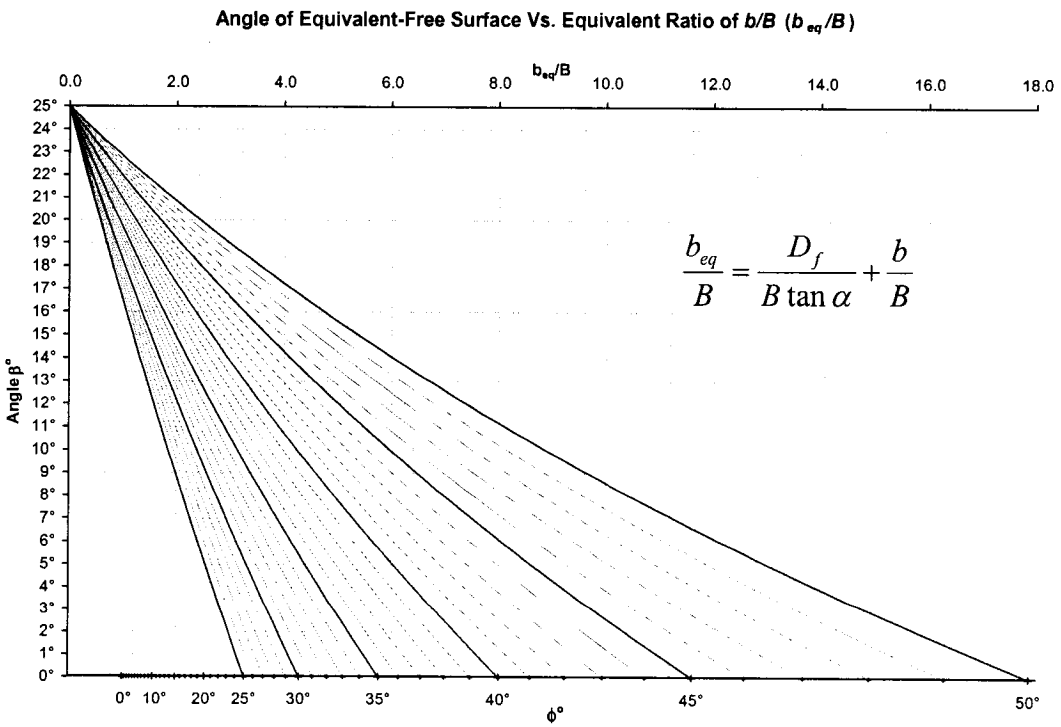

Figure 4.40. Angle of equivalent-free surface β^o vs. equivalent distance/footing width ratio (b_{eq}/B) for angle of slope $\alpha° = 25°$

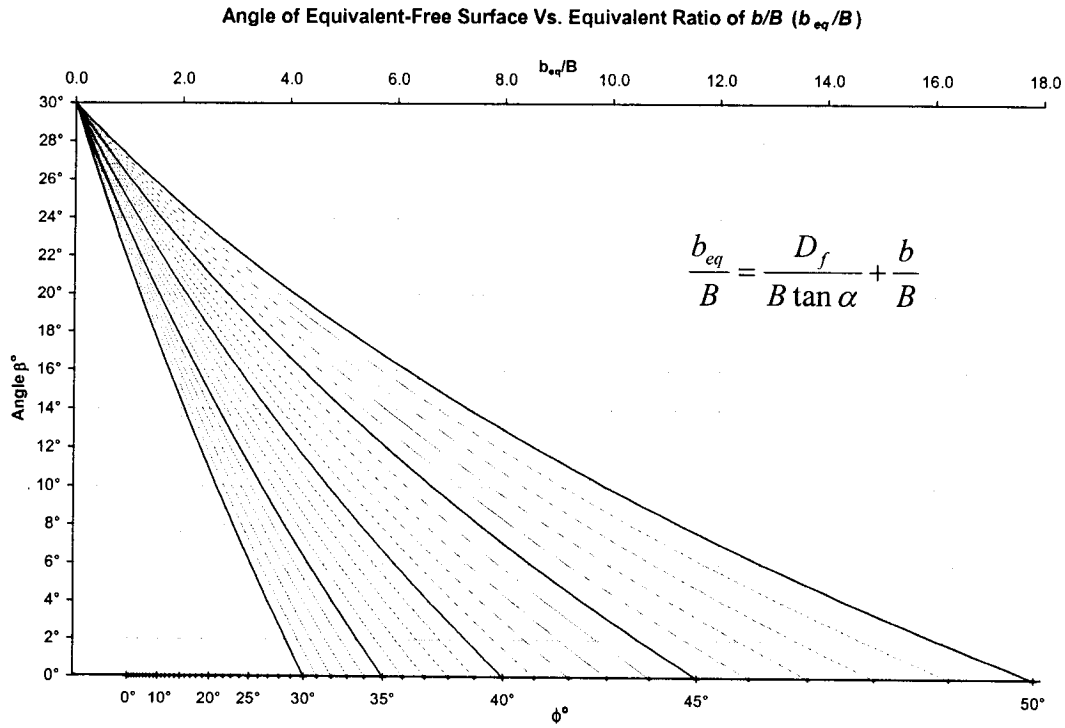

Figure 4.41. Angle of equivalent-free surface β^o vs. equivalent distance/footing width ratio (b_{eq}/B) for angle of slope $\alpha^\circ = 30^\circ$

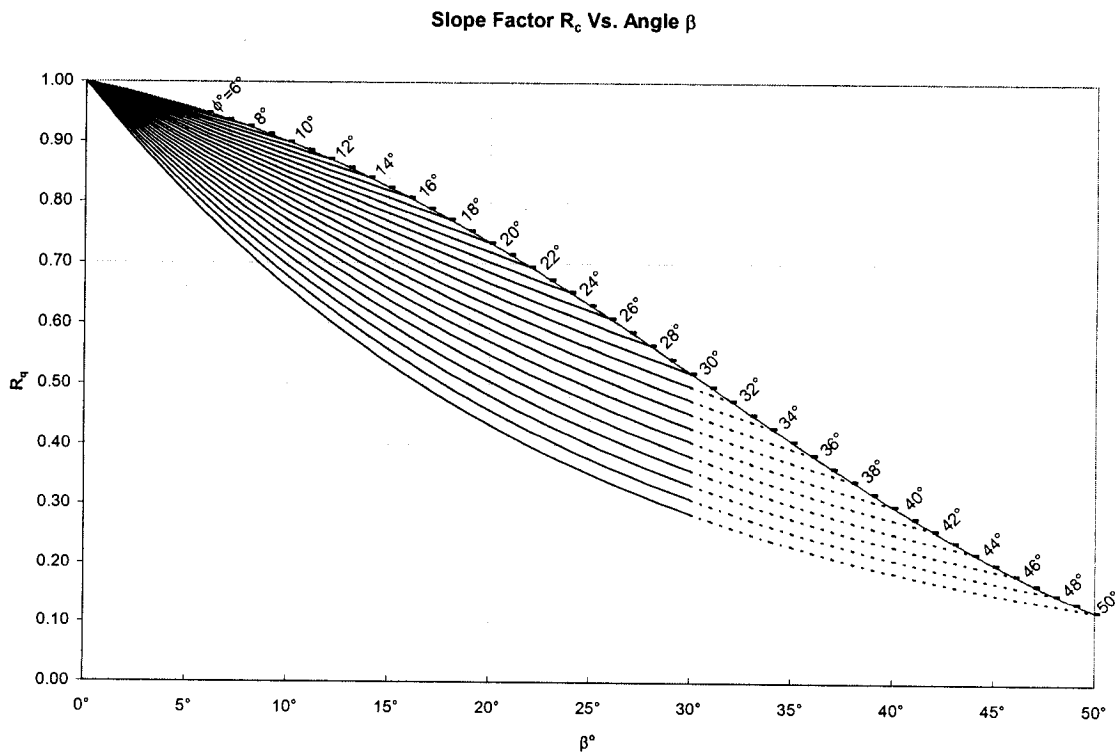

Figure 4.42. Slope Factor R_c vs. Angle of equivalent-free surface (Equation 4.10b)

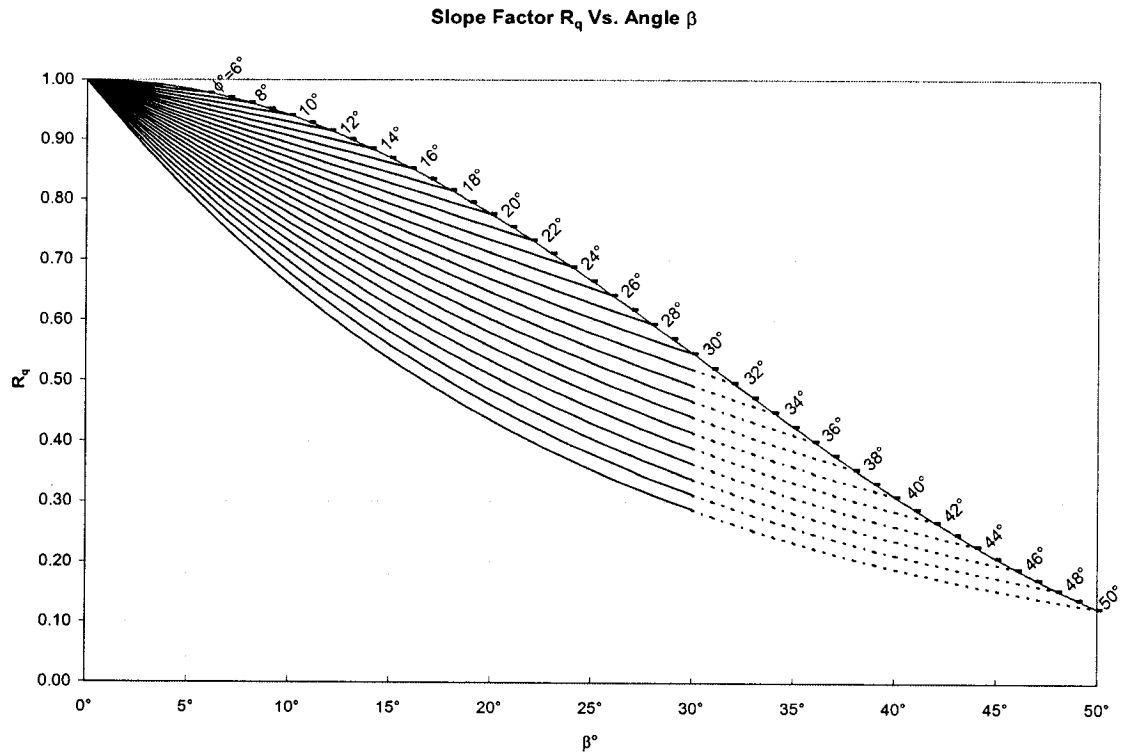

Figure 4.43. Slope Factor R_q vs. Angle of equivalent-free surface. (Equation 4.2d)

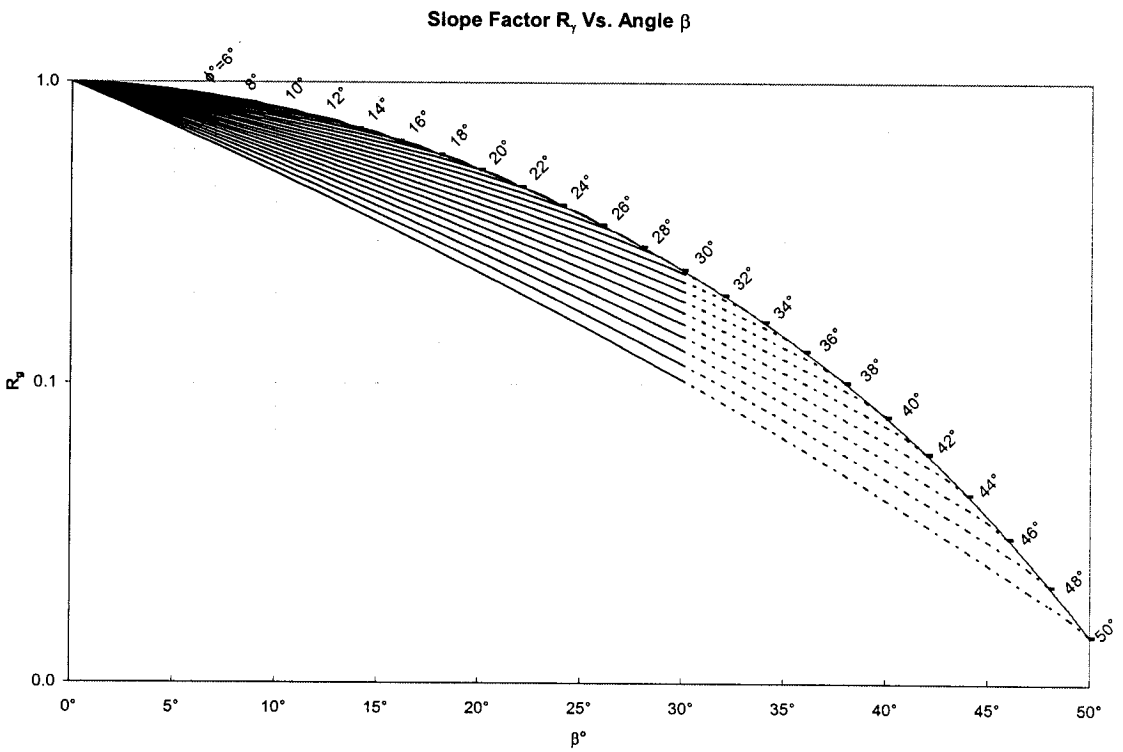

Figure 4.44. Slope Factor R_γ vs. Angle of equivalent-free surface. (Equation 4.13)

4.5.1 Design Example

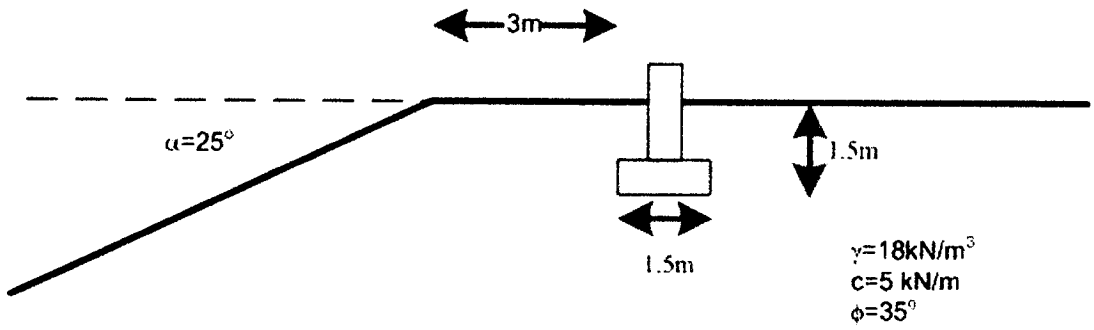

Figure 4.45. Design Example

$$\frac{b}{B} = 2; \frac{b_{eq}}{B} = 4.14$$

From Figure 4.40, $\beta^o \approx 5.95°$

So $R_{D_f} = 0.569$ (Equation 4.8b)

From Figures 4.42 to 4.44, with β^o=5.95°:

R_γ=0.776
R_q=0.865
R_c=0.860

The depth factors (Equations. 4.19a to d)

$$\lambda_{cd} = \lambda_{qd} = \lambda_{\gamma d} = 1$$

Bearing Capacity Factor for horizontal surface (Meyerhof, 1951):

N_c=46.12; N_q=33.3; N_γ=37.15

Substitute the all the value into Equation 4.17,

$$q_u = cN_cR_c\lambda_{cd} + \gamma D_f R_{D_f} N_q R_q \lambda_{qd} + \frac{1}{2}\gamma B N_\gamma R_\gamma \lambda_{\gamma d} = \underline{1030.023 kN/m^2}$$

Using numerical model, the ultimate bearing capacity is estimated as:

$$q_u = 1214.17 \text{ kN/m}^2 \text{ (\%error} \approx 18\%)$$

CHAPTER 5

CONCLUSION

A numerical model was developed using the finite element technique together with the program "PLAXIS" for the case of foundation near a slope. The model provides a realistic failure mechanism beneath the footing and a reasonable value of ultimate bearing capacity of these footing. Analytical model and design procedure are developed and compared well with the available experimental data. Design charts and an example are presented for practicing use. The following can be concluded:

1. The bearing capacity of foundation near slope decreases due to the increase of the slope angle and/or the decrease in the distance between the top of slope and footing edge.
2. The bearing capacity of foundation near slope increases due to increase of depth embedment and/or the width of the footing. However the rate of increase is much lower as compared to the case of foundation on surface ground.
3. For relatively higher angle of shearing resistance $\phi°$, the footing requires a longer distance from the edge of the slope in order not to be affected by the slope.
4. The theory of Meyerhof (1957) overestimates the magnitude of the ultimate bearing capacity and underestimates the effect of the distance to the top of the slope. The distance at which the bearing capacity is independent of the slope was found to be higher than that stated in theory.
5. The proposed analytical model presents dimensionless coefficients which depend on the soil parameter and the footing/slope geometry. These coefficients

incorporate the slope contribution, and accordingly they can be employed in the general bearing capacity equation.

6. The design charts for slope factor will assist designers to determine relative reduction for each bearing capacity factor and accordingly the bearing capacity for the given conditions of the foundation. The charts can also be used to determine the distance of a foundation from a slope to produce a required bearing capacity, or the location of the foundation where the adjacent slope does not affect the bearing capacity.

RECOMMENDATIONS

1. The presented analytical model should be extended for the case of three dimensional cases for the design of square or rectangular foundations.
2. The presented analytical model should be extended for the case of saturated or submerged soils, slopes subjected to sudden drawdown of the water level in the river, or soils subjected to steady flow.

APPENDIX A

TEST RESULTS

Table A.1 – Value of ultimate bearing capacity obtained from Test No. 1

α=	5 (Test No. 1-1)						α=	10 (Test No. 1-2)						α=	15 (Test No. 1-3)					
b/B=	0.0	1.0	2.0	3.0	4.0	6.0	b/B=	0.0	1.0	2.0	3.0	4.0	6.0	b/B=	0.0	1.0	2.0	3.0	4.0	6.0
ϕ= 5	3.89	4.09	4.21	4.27	4.29	4.29														
6	4.52	4.71	4.86	4.93	4.95	4.95														
7	5.21	5.43	5.61	5.68	5.71	5.71														
8	5.99	6.25	6.47	6.56	6.59	6.59														
9	6.88	7.20	7.47	7.57	7.61	7.61														
10	7.91	8.29	8.62	8.74	8.78	8.78	ϕ= 10	7.08	8.17	8.62	8.75	8.85	8.90							
11	9.09	9.54	9.94	10.08	10.13	10.13	11	8.18	9.37	9.94	10.10	10.21	10.27							
12	10.44	10.98	11.48	11.63	11.69	11.69	12	9.38	10.74	11.46	11.65	11.78	11.84							
13	11.99	12.64	13.24	13.43	13.49	13.49	13	10.75	12.31	13.21	13.44	13.58	13.66							
14	13.77	14.55	15.28	15.49	15.57	15.57	14	12.31	14.12	15.23	15.50	15.67	15.75							
15	15.81	16.75	17.63	17.88	17.96	17.97	15	14.10	16.18	17.56	17.88	18.07	18.17	ϕ=15	11.99	15.81	17.75	18.00	18.20	18.39
16	18.15	19.27	20.32	20.63	20.73	20.74	16	16.13	18.54	20.18	20.63	20.84	20.95	16	13.81	18.01	20.32	20.73	20.98	21.19
17	20.84	22.17	23.40	23.81	23.92	23.94	17	18.46	21.24	23.19	23.79	24.04	24.17	17	15.76	20.52	23.25	23.89	24.19	24.43
18	23.93	25.51	26.95	27.48	27.60	27.62	18	21.12	24.34	26.63	27.45	27.73	27.87	18	17.97	23.38	26.58	27.52	27.88	28.16
19	27.47	29.35	31.03	31.71	31.85	31.88	19	24.17	27.88	30.57	31.66	31.99	32.15	19	20.47	26.62	30.37	31.70	32.14	32.46
20	31.53	33.77	35.73	36.60	36.78	36.79	20	27.65	31.93	35.09	36.52	36.90	37.07	20	23.31	30.31	34.70	36.52	37.06	37.41
21	36.20	38.84	41.14	42.23	42.42	42.46	21	31.62	36.57	40.27	42.13	42.56	42.76	21	26.53	34.51	39.62	42.08	42.72	43.12
22	41.55	44.68	47.36	48.74	48.95	49.00	22	36.17	41.88	46.20	48.60	49.09	49.31	22	30.19	39.29	45.23	48.48	49.24	49.71
23	47.70	51.39	54.51	56.24	56.48	56.55	23	41.37	47.95	52.99	56.06	56.63	56.88	23	34.36	44.71	51.62	55.85	56.76	57.30
24	54.74	59.11	62.73	64.80	65.18	65.26	24	47.31	54.89	60.77	64.46	65.32	65.60	24	39.08	50.88	58.89	64.04	65.44	66.04
25	62.83	67.98	72.19	74.57	75.22	75.31	25	54.10	62.83	69.68	73.95	75.34	75.66	25	44.45	57.88	67.16	73.19	75.43	76.13
26	72.12	78.18	83.07	85.81	86.80	86.92	26	61.86	71.92	79.88	84.83	86.90	87.26	26	50.56	65.84	76.57	83.62	86.96	87.75
27	82.76	89.91	95.58	98.73	100.16	100.31	27	70.74	82.30	91.55	97.27	100.24	100.64	27	57.49	74.89	84.52	95.49	100.24	101.15
28	94.98	103.39	109.96	113.58	115.58	115.76	28	80.88	94.18	104.91	111.51	115.62	116.07	28	65.37	82.34	95.84	109.00	115.55	116.59
29	109.00	118.88	126.49	130.64	133.26	133.59	29	92.46	107.77	120.21	127.81	133.14	133.86	29	74.32	93.31	108.63	124.38	132.89	134.39
30	122.28	131.24	137.93	143.17	147.74	149.08	30	102.04	115.39	127.55	137.59	146.56	149.15	30	81.04	100.35	117.34	132.00	145.38	149.33
31	141.24	151.56	159.23	165.19	170.39	173.16	31	117.27	132.42	146.28	157.70	167.87	173.21	31	92.66	114.38	133.60	150.24	165.43	173.38
32	163.11	175.00	183.77	190.55	196.45	201.12	32	134.73	151.92	167.71	180.66	192.18	201.13	32	105.90	130.32	152.05	170.87	188.07	201.28
33	188.33	202.01	212.05	219.75	226.43	233.57	33	154.74	174.24	192.21	206.86	219.87	233.53	33	120.97	148.41	172.96	194.22	213.64	233.67
34	230.47	247.15	259.31	268.55	276.55	287.52	34	188.34	211.77	233.43	250.98	266.50	287.41	34	146.42	179.08	208.45	233.87	257.02	287.51
35	276.05	295.95	310.37	321.23	330.58	346.47	35	224.34	251.89	277.43	297.97	316.06	346.26	35	173.41	211.47	245.83	275.53	302.49	346.32
36	348.18	373.17	391.17	404.57	416.07	438.12	36	281.35	315.44	347.14	372.43	394.57	436.36	36	216.20	262.87	305.19	341.68	374.66	435.06
37	403.75	432.62	453.25	468.44	481.42	506.35	37	324.36	363.14	399.29	427.89	452.76	499.78	37	247.74	300.34	348.24	389.41	426.43	494.16
38	499.38	534.94	560.16	578.52	594.10	624.09	38	398.79	445.84	489.81	524.25	553.97	610.25	38	302.69	365.92	423.71	473.22	517.44	598.18
39	608.44	651.58	681.94	703.77	722.17	757.64	39	482.91	539.12	591.77	632.59	667.52	733.68	39	364.19	424.50	485.35	542.40	597.07	703.52
40	724.02	775.15	810.84	836.15	857.33	898.21	40	571.04	636.62	698.19	745.38	785.38	861.15	40	427.81	496.27	565.92	631.07	693.27	814.38
41	848.85	908.55	949.86	978.75	1002.74	1049.06	41	665.17	740.55	811.46	865.17	910.21	995.46	41	494.95	571.37	649.86	723.04	792.62	927.91
42	1105.47	1182.91	1236.03	1272.62	1302.72	1360.92	42	823.94	916.08	1002.93	1067.89	1121.72	1223.47	42	608.81	699.36	793.35	880.65	963.26	1123.51
43	1293.56	1383.82	1445.18	1486.77	1520.67	1586.21	43	960.27	1066.25	1166.36	1240.22	1300.65	1414.63	43	704.44	805.19	911.02	1008.91	1101.00	1279.07
44	1623.98	1736.88	1812.92	1863.60	1904.45	1983.48	44	1200.45	1331.23	1455.02	1545.05	1617.67	1754.30	44	874.09	994.09	1121.84	1239.45	1349.34	1560.96
45	1940.37	2074.79	2164.48	2223.17	2269.95	2360.46	45	1427.90	1581.48	1687.08	1788.41	1874.44	2039.95	45	1031.75	1167.41	1314.05	1448.35	1572.89	1811.49
46	2463.36	2633.47	2745.86	2818.03	2874.82	2984.70	46	1804.17	1995.82	2124.38	2248.38	2352.29	2551.66	46	1293.32	1455.82	1634.55	1797.31	1946.96	2231.88
47	2845.44	3041.35	3169.50	3250.18	3312.78	3433.88	47	2073.54	2359.51	2505.92	2647.96	2765.25	2989.64	47	1518.26	1700.08	1904.07	2088.68	2256.80	2574.57
48	3578.97	3824.75	3983.90	4082.00	4156.96	4301.96	48	2501.15	2760.59	2925.31	3086.22	3216.97	3486.19	48	1878.35	2092.11	2337.48	2558.04	2756.79	3129.25
49	4444.58	4749.14	4944.34	5062.00	5150.44	5321.43	49	3204.94	3617.90	3825.15	4029.19	4192.07	4501.24	49	2257.35	2500.69	2787.41	3043.29	3271.17	3694.05
50	5297.85	5660.25	5890.10	6025.47	6125.36	6318.42	50	3868.25	4210.06	4441.15	4670.77	4850.51	5190.02	50	2685.25	2958.41	3290.15	3583.91	3842.14	4316.00

Table A.1 – Value of ultimate bearing capacity obtained from Test No. 1 (Cont'd)

α=	20 (Test No. 1-4)						α=	25 (Test No. 1-5)							α=	30 (Test No. 1-6)						
b/B=	0.0	1.0	2.0	3.0	4.0	6.0	b/B=	0.0	1.0	2.0	3.0	4.0	6.0	8.0	b/B=	0.0	1.0	2.0	3.0	4.0	6.0	8.0
⇐ 20	17.79	27.71	32.93	35.51	36.27	36.98																
21	20.42	31.37	37.43	40.88	41.81	42.64																
22	23.22	35.49	42.52	47.06	48.20	49.17																
23	26.35	40.16	48.30	54.18	55.56	56.70																
24	29.88	45.42	54.83	61.99	64.05	65.36																
25	33.87	51.36	62.22	70.62	73.84	75.39	⇐ 25	25.22	42.35	56.98	67.56	71.42	74.02	74.53								
26	38.38	58.07	70.58	80.41	85.13	86.93	26	29.13	47.68	64.20	76.53	82.29	85.43	86.04								
27	43.47	65.64	80.03	91.50	98.13	100.23	27	33.07	53.66	72.31	86.63	94.81	98.59	99.32								
28	49.22	74.18	90.72	104.07	113.13	115.58	28	37.42	60.38	81.40	98.00	109.24	113.78	114.65								
29	55.72	83.81	102.81	118.30	130.01	133.27	29	42.27	67.92	91.81	110.78	125.39	131.32	132.35								
30	60.02	83.49	103.82	122.82	140.09	145.61	30	46.91	70.22	95.12	118.75	140.51	148.20	148.61	⇐ 30	29.71	57.66	85.37	112.56	138.22	148.30	148.69
31	68.67	94.91	117.85	139.43	159.10	169.81	31	53.07	78.98	106.63	133.19	157.85	172.13	172.63	31	33.99	64.39	94.87	125.14	154.11	172.24	172.71
32	78.49	107.84	133.69	158.13	180.45	198.01	32	59.99	88.79	119.45	149.23	177.06	199.93	200.52	32	38.45	71.86	105.33	138.95	171.49	200.04	200.61
33	89.65	122.46	151.56	179.20	204.43	230.86	33	67.77	99.75	133.71	167.03	198.32	232.19	232.90	33	43.43	80.14	116.85	154.11	190.50	232.31	233.00
34	108.46	147.31	182.01	215.08	245.22	285.29	34	81.11	118.71	158.54	197.99	235.15	285.82	286.72	34	51.92	94.65	137.29	180.96	223.94	285.96	286.83
35	128.37	173.39	213.86	252.52	287.66	345.10	35	94.97	138.21	183.90	229.56	272.64	344.43	345.53	35	60.73	109.36	157.78	207.80	257.35	344.57	345.67
36	159.70	214.57	264.18	311.68	354.66	433.66	36	117.11	169.36	224.50	280.07	332.54	430.50	438.54	36	74.76	132.95	190.82	251.05	311.04	428.43	438.70
37	182.22	243.55	299.32	352.81	400.99	489.34	37	132.83	190.71	251.84	313.97	372.59	481.87	511.80	37	84.57	148.52	212.03	278.63	345.27	472.61	511.97
38	221.61	294.70	361.53	425.72	483.15	588.15	38	160.64	228.93	301.17	375.17	444.93	574.42	637.17	38	102.01	176.83	251.12	329.58	408.38	554.66	637.37
39	263.36	334.66	405.41	476.32	544.76	679.31	39	192.35	257.33	332.50	411.95	492.79	657.66	782.84	39	122.52	196.45	274.15	358.85	448.44	636.74	782.30
40	307.12	387.40	467.63	548.07	625.42	777.35	40	223.95	295.58	379.66	468.90	559.66	744.88	938.72	40	142.50	223.68	309.80	403.97	503.76	714.01	935.90
41	352.61	441.51	531.04	620.83	708.75	875.18	41	256.75	334.20	426.79	525.31	625.48	829.68	1042.32	41	158.22	254.93	350.42	455.10	566.21	800.48	1049.05
42	430.29	534.77	640.93	747.39	848.67	1046.51	42	319.12	401.53	509.77	625.32	742.60	981.13	1230.44	42	200.72	296.40	407.08	526.52	653.41	920.78	1205.31
43	493.76	609.08	727.43	846.05	958.17	1176.12	43	363.97	453.56	572.45	699.77	828.73	1090.00	1363.62	43	228.50	333.89	452.08	582.26	720.65	1011.65	1321.60
44	607.40	743.65	885.08	1026.71	1159.58	1416.30	44	444.96	549.10	688.96	839.28	991.09	1297.03	1617.61	44	278.70	400.30	537.96	689.91	851.50	1190.13	1550.39
45	719.96	874.81	1037.60	1200.54	1352.07	1642.68	45	517.21	631.96	788.33	956.95	1126.70	1466.49	1822.20	45	323.10	456.12	608.42	776.93	956.13	1329.94	1726.37
46	876.48	1056.88	1249.37	1441.85	1619.15	1956.16	46	638.11	771.90	957.34	1158.07	1359.37	1759.00	2176.36	46	397.46	551.42	730.12	928.33	1139.10	1576.19	2037.35
47	996.10	1191.89	1404.39	1616.67	1810.14	2174.08	47	715.50	856.78	1058.54	1273.68	1490.49	1916.72	2360.20	47	444.24	605.59	796.01	1007.81	1232.97	1696.63	2182.32
48	1248.33	1482.10	1740.85	1999.07	2231.65	2663.95	48	856.76	997.06	1222.61	1468.93	1713.69	2189.37	2681.76	48	557.29	720.06	939.68	1184.73	1445.19	1977.09	2529.14
49	1557.98	1709.33	2001.69	2293.14	2552.31	3146.96	49	1033.49	1193.98	1455.97	1743.61	2027.91	2573.18	3133.89	49	627.57	825.38	1069.52	1342.93	1633.50	2221.24	2824.32
50	1818.02	2124.53	2439.51	2726.64	3025.75	3646.33	50	1165.68	1378.99	1672.46	1996.62	2315.18	2916.98	3530.79	50	745.66	942.24	1212.49	1518.48	1839.54	2486.00	3140.21

Table A.2 – Value of ultimate bearing capacity obtained from Test No. 2

α=	5 (Test No. 2-1)						α=	10 (Test No. 2-2)						α=	15 (Test No. 2-3)					
b/B=	0.0	1.0	2.0	3.0	4.0	6.0	b/B=	0.0	1.0	2.0	3.0	4.0	6.0	b/B=	0.0	1.0	2.0	3.0	4.0	6.0
ϕ= 5	15.69	17.01	17.09	17.06	17.10	17.10														
6	17.65	19.17	19.30	19.26	19.30	19.30														
7	18.74	20.36	20.52	20.48	20.52	20.52														
8	21.15	23.00	23.24	23.19	23.24	23.24														
9	22.37	24.32	24.61	24.57	24.61	24.61														
10	24.23	26.32	26.69	26.64	26.69	26.69	ϕ= 10	21.74	26.00	26.69	26.64	26.69	26.69							
11	27.00	29.04	29.76	30.48	30.77	30.67	11	24.08	28.63	29.79	30.44	30.74	30.63							
12	28.84	30.93	31.84	32.61	32.93	32.82	12	25.75	30.43	31.88	32.58	32.89	32.78							
13	32.14	34.52	35.66	36.52	36.88	36.75	13	28.53	33.85	35.70	36.48	36.83	36.71							
14	36.47	39.17	40.63	41.62	42.02	41.88	14	32.27	38.29	40.68	41.57	41.97	41.83							
15	38.46	41.21	42.95	43.99	44.41	44.26	15	34.01	40.17	43.00	43.94	44.36	44.21	ϕ= 15	29.22	38.83	43.55	43.73	44.34	44.19
16	43.80	46.89	47.73	50.29	50.77	50.60	16	38.61	45.57	47.77	50.23	50.71	50.54	16	32.86	43.89	48.23	49.99	50.69	50.51
17	45.88	48.96	49.91	52.76	53.26	53.08	17	40.50	47.46	49.93	52.70	53.20	53.02	17	34.33	45.58	50.38	52.44	53.18	52.99
18	52.45	55.91	57.12	60.53	61.12	60.91	18	46.19	54.01	57.08	60.46	61.05	60.84	18	38.82	51.68	57.53	60.17	61.02	60.81
19	58.18	62.08	63.61	67.56	68.21	67.98	19	50.89	59.70	63.48	67.48	68.13	67.90	19	42.22	56.83	63.88	67.15	68.10	67.86
20	66.73	71.10	72.96	77.77	78.52	78.25	20	58.21	68.12	72.68	77.68	78.43	78.16	20	47.91	64.57	73.01	77.31	78.39	78.12
21	73.89	78.81	81.09	86.69	87.53	87.23	21	63.96	75.10	80.58	86.59	87.42	87.13	21	52.00	70.75	80.75	86.18	87.38	87.08
22	89.23	95.49	98.61	105.73	106.75	106.39	22	76.22	90.31	97.69	105.61	106.62	106.26	22	61.01	84.36	97.57	105.10	106.57	106.20
23	98.51	105.54	109.26	117.64	118.77	118.37	23	82.85	99.15	107.87	117.50	118.63	118.23	23	66.00	91.34	107.34	116.94	118.58	118.17
24	113.06	120.88	125.23	130.42	136.87	136.41	24	94.08	113.04	123.21	130.26	136.71	136.25	24	75.09	102.40	122.16	129.61	136.65	136.18
25	124.59	133.35	138.48	144.73	152.13	151.62	25	101.89	123.74	135.63	144.43	151.96	151.44	25	81.09	110.00	133.81	143.60	151.88	151.36
26	137.28	145.82	151.00	157.99	167.03	166.47	26	112.62	135.39	147.51	157.46	166.83	166.27	26	90.34	119.03	145.14	156.34	166.75	166.18
27	151.18	160.74	166.78	175.02	185.58	184.96	27	122.01	148.01	162.05	174.06	185.37	184.74	27	97.51	127.82	158.51	172.45	185.28	184.64
28	174.70	185.29	192.20	202.04	215.29	214.57	28	139.85	169.79	185.91	200.43	215.04	214.31	28	111.75	144.50	180.94	198.05	214.94	214.20
29	192.04	203.86	211.84	223.28	227.71	238.17	29	151.36	182.89	203.56	220.73	227.44	237.89	29	120.47	154.93	193.88	217.32	227.32	237.76
30	216.19	229.93	239.50	253.17	259.12	271.41	30	167.53	201.77	228.31	249.17	258.64	271.09	30	132.67	170.00	212.32	244.16	258.31	270.95
31	239.10	254.42	265.40	281.21	288.76	303.35	31	182.79	218.87	250.95	275.35	287.74	302.99	31	144.19	183.51	228.25	268.33	286.88	302.83
32	278.71	295.59	307.99	326.54	336.05	354.90	32	211.95	250.73	289.49	318.16	334.03	354.47	32	167.00	209.53	258.16	308.42	332.19	354.29
33	318.05	339.53	355.72	378.95	391.71	414.95	33	236.17	280.37	325.00	365.88	387.73	414.46	33	184.48	232.43	287.29	345.49	383.91	414.24
34	396.87	423.29	443.62	473.27	490.40	522.97	34	292.24	344.02	396.31	453.43	483.10	522.35	34	227.51	283.80	348.44	417.08	475.93	522.08
35	460.12	493.26	518.76	555.39	577.61	620.22	35	334.18	392.61	451.65	526.10	565.13	619.48	35	258.49	321.66	394.33	471.59	552.68	619.16
36	577.62	622.39	653.42	699.44	728.31	744.95	36	422.21	490.13	558.72	648.24	707.95	743.98	36	325.83	399.68	485.11	575.96	675.73	743.50
37	634.13	688.24	723.07	775.13	808.88	832.81	37	463.60	534.39	605.85	699.92	779.51	830.49	37	356.08	433.07	522.46	617.57	722.17	828.70
38	784.41	848.63	896.12	960.43	1003.15	1037.87	38	575.38	656.51	738.39	847.58	951.88	1031.84	38	440.27	528.92	632.45	742.60	863.93	1026.36
39	918.92	993.72	1063.84	1145.32	1201.33	1253.17	39	668.85	762.51	857.05	983.30	1103.88	1239.16	39	507.84	609.32	727.95	854.23	993.44	1225.61
40	1095.32	1177.23	1260.84	1366.67	1435.26	1504.19	40	797.64	901.71	1006.70	1148.66	1283.64	1477.26	40	602.58	715.58	848.39	989.74	1145.76	1438.82
41	1255.99	1352.39	1450.72	1598.51	1689.37	1789.84	41	904.16	1024.27	1145.46	1308.81	1464.38	1737.26	41	676.76	805.44	956.51	1117.36	1294.96	1629.26
42	1594.44	1695.31	1798.73	1967.96	2093.09	2212.56	42	1158.10	1289.91	1422.74	1607.07	1780.74	2100.08	42	864.61	1008.03	1178.47	1359.83	1560.47	1934.48
43	1791.66	1898.13	2007.48	2190.10	2348.11	2507.34	43	1295.60	1435.67	1576.74	1774.61	1960.34	2300.47	43	960.32	1112.30	1293.77	1486.80	1700.56	2097.76
44	2232.18	2346.56	2464.59	2672.08	2848.77	3079.62	44	1615.41	1771.38	1928.30	2153.94	2363.88	2744.54	44	1190.53	1361.09	1566.89	1785.71	2028.44	2475.82
45	2562.60	2682.18	2805.99	3031.33	3221.21	3528.92	45	1846.56	2012.45	2179.24	2423.19	2648.84	3055.20	45	1350.59	1531.98	1752.46	1986.81	2247.08	2724.13
46	3244.40	3375.68	3512.42	3775.71	3993.95	4348.42	46	2331.44	2520.24	2709.87	2994.63	3255.68	3720.88	46	1692.79	1900.29	2155.40	2426.42	2727.98	3275.98
47	3635.73	3773.55	3917.54	4202.40	4436.71	4813.70	47	2592.66	2792.09	2992.29	3297.10	3575.24	4068.14	47	1865.41	2083.42	2353.11	2639.54	2958.55	3535.50
48	4652.14	4796.30	4948.55	5277.90	5542.37	5955.30	48	3307.97	3529.92	3752.47	4104.95	4422.50	4976.53	48	2361.28	2606.45	2914.96	3242.46	3608.21	4261.46
49	5674.47	5821.90	5979.38	6350.11	6641.54	7084.00	49	4011.93	4251.76	4492.00	4886.64	5238.13	5842.69	49	2837.90	3104.36	3445.08	3806.66	4211.48	4926.28
50	6719.33	6870.45	7033.64	7447.06	7766.45	8239.91	50	4712.74	4969.24	5225.95	5661.34	6045.37	6697.75	50	3300.23	3585.37	3955.27	4347.70	4788.05	5557.77

Table A.2 – Value of ultimate bearing capacity obtained from Test No. 2 (Cont'd)

α=	20 (Test No. 2-4)						α=	25 (Test No. 2-5)							α=	30 (Test No. 2-6)						
b/B=	0.0	1.0	2.0	3.0	4.0	6.0	b/B=	0.0	1.0	2.0	3.0	4.0	6.0	8.0	b/B=	0.0	1.0	2.0	3.0	4.0	6.0	8.0
ϕ= 20	39.88	60.85	71.97	77.33	77.98	78.09																
21	43.10	65.50	79.39	86.20	86.93	87.05																
22	50.26	76.67	95.59	105.13	106.01	106.17																
23	54.14	82.16	104.74	116.97	117.98	118.13																
24	61.49	91.81	118.73	129.63	135.93	136.13																
25	66.10	98.16	129.35	143.49	151.09	151.31	ϕ= 25	53.79	87.65	123.13	143.37	151.13	151.27	149.57								
26	73.71	105.97	138.88	156.00	165.88	166.13	26	59.87	94.16	130.12	155.63	165.92	166.08	164.22								
27	79.16	113.19	148.04	171.69	184.31	184.58	27	63.94	99.98	137.96	170.86	184.35	184.53	182.48								
28	90.43	127.35	165.23	196.63	213.82	214.13	28	72.71	111.81	153.14	195.09	213.87	214.07	211.67								
29	96.97	135.74	175.65	214.91	226.13	237.68	29	77.52	118.42	161.82	212.33	226.17	237.62	234.95								
30	106.17	148.03	191.23	240.23	256.76	270.85	30	84.35	128.30	175.09	230.31	256.61	270.78	267.74	ϕ= 30	65.99	110.90	160.69	220.38	256.42	270.73	270.35
31	114.78	158.82	204.34	258.38	284.64	302.73	31	90.67	136.74	185.90	244.18	283.92	302.65	299.25	31	70.52	117.38	169.48	232.25	283.11	302.58	302.16
32	132.40	180.27	229.74	288.76	328.71	354.17	32	104.04	154.12	207.56	271.21	326.92	354.08	350.10	32	80.47	131.29	187.83	256.27	324.96	354.00	353.51
33	145.12	198.54	253.89	320.05	378.11	414.10	33	113.22	168.60	227.88	296.68	372.71	413.99	409.35	33	86.98	142.71	204.92	280.48	359.32	413.90	413.33
34	178.04	240.81	305.84	383.88	464.08	521.90	34	138.07	202.99	272.50	355.79	443.07	521.77	515.91	34	105.43	170.50	243.19	331.76	424.45	521.65	520.93
35	200.92	270.99	343.65	431.04	521.02	618.95	35	154.76	226.79	304.00	398.73	494.16	618.79	611.84	35	117.39	189.14	269.38	367.40	470.31	618.65	617.79
36	252.02	334.35	419.60	522.60	628.61	743.15	36	192.97	277.58	368.10	477.22	591.93	742.86	778.74	36	145.44	229.48	323.35	438.34	559.20	742.59	786.31
37	273.74	359.57	448.36	556.02	666.84	826.99	37	208.20	296.10	390.10	503.68	623.18	825.25	873.58	37	155.87	242.78	339.81	458.93	584.27	823.42	882.05
38	336.50	435.74	538.21	663.03	791.39	1020.84	38	254.26	355.74	464.05	595.35	733.45	1015.06	1095.37	38	189.04	289.03	400.47	537.61	681.92	994.99	1106.02
39	385.18	497.94	614.39	756.41	902.59	1202.25	39	288.85	403.32	525.50	673.77	829.89	1157.64	1329.49	39	213.18	325.19	450.00	603.73	765.68	1118.13	1342.42
40	454.05	579.88	709.58	868.39	1031.67	1366.26	40	338.07	465.45	601.14	766.23	939.96	1304.88	1508.32	40	247.67	371.78	509.79	680.10	859.40	1250.25	1522.98
41	505.62	647.26	793.31	972.10	1156.09	1533.84	41	373.44	515.49	666.84	850.97	1044.93	1453.16	1800.94	41	271.47	408.77	561.39	749.71	948.18	1381.68	1815.13
42	642.24	802.40	966.76	1169.77	1377.82	1803.44	42	470.97	631.99	802.76	1011.58	1230.87	1691.43	2171.19	42	339.69	495.10	667.13	880.04	1103.72	1592.12	2136.83
43	707.72	877.18	1050.78	1265.90	1486.08	1936.10	43	514.77	684.30	863.71	1083.52	1314.11	1798.24	2303.03	43	368.27	530.93	710.59	933.16	1166.71	1676.79	2246.73
44	870.83	1062.54	1258.16	1502.42	1751.55	2259.16	44	628.26	819.80	1021.74	1270.18	1530.11	2074.66	2642.11	44	445.65	628.74	830.20	1080.35	1342.10	1913.23	2552.08
45	979.65	1183.79	1391.51	1652.25	1917.54	2456.89	45	700.64	903.71	1117.19	1380.56	1655.56	2230.77	2829.89	45	492.64	685.66	897.40	1160.69	1435.55	2034.78	2705.47
46	1217.44	1452.48	1690.73	1992.10	2297.63	2916.62	46	862.94	1096.10	1340.28	1642.80	1957.74	2614.73	3297.98	46	601.22	821.74	1062.76	1363.09	1675.58	2355.76	3117.05
47	1329.04	1575.35	1824.43	2140.85	2460.95	3108.08	47	933.19	1175.96	1429.54	1744.38	2071.53	2752.77	3460.48	47	644.08	872.10	1120.61	1430.54	1752.26	2451.58	3234.06
48	1666.90	1947.18	2229.17	2591.48	2956.16	3689.52	48	1159.08	1434.87	1721.55	2079.71	2450.30	3218.77	4014.64	48	792.05	1049.85	1329.51	1679.47	2041.02	2824.72	3700.69
49	1983.60	2290.77	2598.40	2997.83	3398.00	4198.79	49	1365.29	1666.49	1978.19	2369.85	2773.52	3607.19	4467.85	49	923.36	1203.26	1505.59	1885.05	2275.29	3118.78	4060.19
50	2282.58	2612.77	2942.10	3373.74	3804.39	4662.34	50	1554.39	1876.45	2208.41	2627.65	3058.18	3943.96	4855.51	50	1040.07	1337.29	1657.07	2059.44	2471.49	3359.50	4348.93

Table A.3 – Value of ultimate bearing capacity obtained from Test No. 3

α=	5 (Test No. 3-1)						α=	10 (Test No. 3-2)						α=	15 (Test No. 3-3)					
b/B=	0.0	1.0	2.0	3.0	4.0	6.0	b/B=	0.0	1.0	2.0	3.0	4.0	6.0	b/B=	0.0	1.0	2.0	3.0	4.0	6.0
ϕ= 5	27.06	29.01	29.66	30.16	30.24	30.26														
6	29.24	33.28	32.11	32.32	34.66	34.68														
7	31.28	33.27	34.09	34.31	34.40	34.42														
8	36.20	35.87	39.36	39.60	39.70	37.42														
9	37.79	37.95	41.59	41.86	41.97	39.62														
10	40.63	40.49	44.30	45.05	45.16	45.18	ϕ= 10	34.70	39.81	43.38	41.97	42.41	42.63							
11	47.49	48.21	51.75	49.75	51.78	51.78	11	44.41	47.85	51.71	49.76	51.78	51.78							
12	49.62	50.34	54.30	52.21	54.34	54.34	12	46.35	49.90	54.27	52.22	54.34	54.34							
13	55.23	56.09	60.67	58.33	60.70	60.70	13	51.44	55.48	60.63	58.33	60.70	60.70							
14	62.21	63.19	68.60	65.96	68.65	68.65	14	57.79	62.39	68.56	65.97	68.65	68.65							
15	64.41	65.39	71.34	68.60	71.39	71.39	15	59.74	64.44	71.30	68.60	71.39	71.39	ϕ= 15	54.95	63.45	71.25	68.61	71.39	71.39
16	72.71	73.82	78.04	77.78	80.94	80.94	16	67.27	72.58	77.98	77.79	80.94	80.94	16	61.70	71.30	77.92	77.79	80.94	80.94
17	74.41	75.47	79.90	79.99	83.24	83.24	17	68.78	74.07	79.81	79.99	83.24	83.24	17	63.01	72.61	79.72	80.00	83.24	83.24
18	84.24	85.41	90.57	90.97	94.67	94.67	18	77.69	83.62	90.41	90.98	94.67	94.67	18	70.97	81.77	90.24	90.98	94.67	94.67
19	93.35	94.72	100.63	101.26	105.38	105.38	19	85.73	92.46	100.36	101.27	105.38	105.38	19	77.91	90.11	100.07	101.28	105.38	105.38
20	105.99	107.50	114.36	115.55	120.26	120.26	20	97.10	104.65	113.91	115.56	120.26	120.26	20	87.99	101.71	113.44	115.57	120.26	120.26
21	117.26	119.02	126.83	128.47	133.70	133.70	21	106.91	115.45	126.13	128.48	133.70	133.70	21	96.30	111.77	125.41	128.49	133.70	133.70
22	143.55	145.91	155.81	158.08	164.52	164.52	22	130.00	140.93	154.65	158.10	164.52	164.52	22	116.12	135.76	153.44	158.11	164.52	164.52
23	158.38	161.10	172.32	175.38	182.52	182.52	23	142.60	154.93	170.63	175.40	182.52	182.52	23	126.45	148.53	168.90	175.42	182.52	182.52
24	179.77	182.73	195.61	190.19	208.42	208.42	24	161.41	175.13	193.24	190.19	208.42	208.42	24	142.60	167.27	190.80	190.19	208.42	208.42
25	197.92	201.34	215.88	210.40	230.90	230.90	25	176.55	192.00	212.61	210.29	230.90	230.90	25	154.65	182.34	209.24	210.17	230.90	230.90
26	210.32	213.25	228.43	222.89	246.82	246.82	26	188.12	203.10	224.48	222.57	246.82	246.82	26	165.36	192.59	220.42	222.24	246.82	246.82
27	231.19	234.58	251.64	246.06	273.15	273.15	27	205.30	222.17	246.37	245.35	273.15	273.15	27	178.77	209.32	240.95	244.61	273.15	273.15
28	264.31	267.87	287.39	281.40	314.35	314.35	28	234.11	252.76	280.45	280.08	314.35	314.35	28	201.57	237.12	273.29	278.72	314.35	314.35
29	289.71	293.84	315.67	309.69	324.59	347.18	29	254.50	275.46	306.62	307.48	324.59	347.18	29	213.62	256.44	297.29	305.19	324.58	347.18
30	329.80	334.74	360.09	353.93	371.88	398.45	30	287.14	311.58	347.94	350.32	371.68	398.45	30	235.08	287.61	335.44	346.61	371.49	398.45
31	362.75	368.42	396.79	390.70	411.48	442.06	31	312.87	340.31	381.20	385.30	410.78	442.06	31	250.10	311.21	365.14	379.74	410.06	442.06
32	418.07	423.88	456.31	449.59	474.30	513.34	32	359.69	389.86	436.42	441.80	472.66	513.34	32	283.11	352.70	415.94	433.76	470.97	513.34
33	487.21	495.69	535.30	528.99	559.71	605.55	33	410.52	449.39	507.00	516.66	556.15	605.55	33	313.28	392.64	477.84	503.95	552.48	605.55
34	608.61	618.77	668.35	661.11	700.70	763.67	34	508.93	556.74	628.75	642.28	693.91	763.67	34	381.97	474.39	587.97	622.86	686.90	763.67
35	710.92	724.35	784.13	777.48	826.14	903.90	35	580.28	642.14	729.62	749.50	814.22	903.90	35	427.46	531.08	671.96	720.64	801.92	903.90
36	892.00	906.99	980.97	972.73	1034.64	1053.95	36	714.78	799.27	906.87	932.13	1014.95	1053.86	36	528.65	647.84	812.07	890.25	994.64	1053.77
37	973.78	990.69	1072.56	1065.05	1134.91	1161.85	37	758.61	861.41	980.66	1011.72	1106.21	1160.51	37	559.47	681.87	851.58	956.72	1076.62	1159.13
38	1207.56	1226.15	1326.24	1316.85	1404.20	1442.71	38	924.96	1045.19	1203.26	1241.81	1360.23	1437.86	38	683.62	822.57	1018.07	1148.18	1314.89	1432.85
39	1434.24	1461.18	1585.35	1578.80	1688.41	1744.92	39	1057.86	1196.99	1410.87	1487.40	1618.36	1732.24	39	774.88	934.11	1157.76	1307.22	1546.12	1719.17
40	1721.95	1751.93	1899.76	1892.17	2025.07	2099.65	40	1248.58	1400.41	1651.66	1740.61	1923.88	2074.20	40	914.63	1090.22	1340.35	1504.24	1794.98	2047.96
41	2021.75	2068.15	2253.39	2254.02	2421.84	2529.19	41	1404.27	1581.95	1872.18	2026.20	2261.77	2478.11	41	1016.43	1218.53	1504.35	1693.71	2026.27	2425.43
42	2480.23	2521.39	2734.89	2727.25	2924.89	3052.82	42	1731.28	1915.59	2234.97	2397.19	2714.58	2972.42	42	1261.71	1478.13	1794.19	1994.05	2361.40	2889.50
43	2747.50	2797.88	3040.26	3037.58	3264.34	3422.58	43	1871.88	2064.37	2402.16	2570.86	2951.21	3295.94	43	1355.80	1581.71	1913.85	2121.82	2507.83	3135.69
44	3381.94	3430.60	3717.45	3707.28	3979.85	4172.69	44	2296.29	2501.56	2681.79	3058.47	3486.18	3981.16	44	1663.82	1911.08	2284.99	2509.58	2943.71	3638.86
45	3771.33	3840.00	4164.63	4157.75	4469.28	4701.18	45	2526.09	2737.86	3140.60	3321.14	3773.92	4420.68	45	1819.81	2076.64	2470.25	2701.92	3158.70	3884.71
46	4672.79	4799.12	5206.47	5189.52	5572.92	5860.35	46	3159.81	3390.46	3856.35	4048.60	4571.85	5309.98	46	2270.08	2557.61	3011.72	3267.20	3793.65	4616.63
47	5081.07	5209.81	5728.73	5746.24	6185.62	6535.97	47	3414.75	3654.16	4146.69	4344.69	4897.60	5671.71	47	2432.45	2730.83	3206.42	3470.08	4021.14	4877.99
48	6313.22	6420.87	7009.07	7070.72	7644.16	8049.56	48	4290.82	4537.86	5097.38	5293.61	5920.91	6767.66	48	3047.28	3370.23	3909.06	4187.68	4811.19	5757.12
49	7346.22	7432.07	8073.49	8107.97	8800.74	9370.03	49	5003.94	5251.40	5859.08	6048.23	6728.84	7621.22	49	3530.80	3886.48	4447.69	4731.38	5403.23	6402.67
50	8623.67	8688.50	9398.05	9402.67	10170.19	10949.00	50	5866.79	6117.75	6787.02	6970.55	7719.48	8674.15	50	4106.74	4460.00	5094.38	5386.59	6119.21	7188.50

Table A.3 – Value of ultimate bearing capacity obtained from Test No. 3 (Cont'd)

α=	20 (Test No. 3-4)						α=	25 (Test No. 3-5)							α=	30 (Test No. 3-6)						
b/B=	0.0	1.0	2.0	3.0	4.0	6.0	b/B=	0.0	1.0	2.0	3.0	4.0	6.0	8.0	b/B=	0.0	1.0	2.0	3.0	4.0	6.0	8.0
ϕ= 20	78.54	98.60	112.98	115.59	120.26	120.26																
21	85.30	107.89	124.66	126.51	133.70	133.70																
22	101.24	130.33	152.19	158.13	164.52	164.52																
23	107.80	141.81	167.06	175.43	182.52	182.52																
24	119.50	158.99	188.24	190.20	208.42	208.42																
25	126.82	172.17	205.72	210.05	230.90	230.90	ϕ= 25	102.05	159.23	201.97	209.92	230.90	230.90	230.90								
26	134.33	181.54	216.18	221.89	246.82	246.82	26	108.33	164.44	211.83	221.52	246.82	246.82	246.82								
27	142.25	195.81	235.27	243.84	273.15	273.15	27	114.15	172.95	229.22	243.02	273.15	273.15	273.15								
28	159.18	218.86	265.80	277.29	314.35	314.35	28	127.45	190.48	257.83	275.76	314.35	314.35	314.35								
29	167.96	230.34	287.53	302.80	324.57	347.18	29	133.79	199.42	277.15	300.25	324.57	347.18	347.18								
30	184.04	251.60	322.34	342.72	371.28	398.45	30	145.83	216.66	303.89	338.56	371.06	398.45	398.45	ϕ= 30	114.68	189.41	272.31	340.65	363.55	390.63	390.63
31	194.96	265.48	348.33	373.91	409.31	442.06	31	153.71	227.38	318.47	367.69	408.50	442.06	442.06	31	120.20	197.63	283.82	368.08	399.64	433.40	433.40
32	220.65	298.07	392.30	425.34	469.19	513.34	32	173.45	252.39	350.52	416.36	467.30	513.34	513.34	32	135.05	218.08	310.59	410.73	456.12	503.26	503.26
33	241.94	327.08	435.62	490.63	548.63	605.55	33	188.66	276.96	386.62	476.42	544.53	605.55	605.55	33	145.83	237.85	340.80	452.73	529.49	593.68	593.68
34	294.28	393.61	520.96	602.49	679.56	763.67	34	228.51	331.45	460.04	566.65	671.73	763.67	763.67	34	175.72	282.83	402.80	533.57	650.24	748.69	748.69
35	327.09	437.80	579.86	689.23	789.04	903.90	35	252.28	368.31	508.94	627.61	775.30	903.90	903.90	35	192.73	310.63	442.94	587.56	742.63	886.18	886.18
36	404.06	532.08	697.71	823.80	973.35	1053.68	36	310.48	442.57	608.58	745.81	950.66	1053.57	1144.62	36	235.98	372.62	525.90	693.66	873.95	1032.81	1122.18
37	425.51	556.78	727.27	856.60	1045.60	1157.68	37	325.06	460.07	630.18	770.57	981.09	1156.14	1266.05	37	245.51	384.68	540.84	711.99	896.35	1131.83	1241.23
38	518.63	668.43	864.64	1011.61	1246.61	1427.61	38	394.33	548.58	743.87	903.76	1145.82	1422.01	1586.04	38	296.06	455.06	633.34	828.81	1039.66	1388.18	1554.94
39	583.07	753.26	975.98	1143.39	1410.64	1705.47	39	439.94	613.81	833.66	1014.54	1287.91	1690.87	1921.67	39	327.95	505.62	705.35	924.41	1161.12	1642.18	1883.99
40	685.59	873.96	1122.44	1306.89	1605.15	2020.45	40	514.39	706.83	951.43	1150.66	1454.73	1991.13	2124.71	40	380.94	577.62	797.97	1039.87	1301.46	1877.19	2083.05
41	754.51	968.56	1249.75	1460.08	1798.07	2370.23	41	561.30	777.71	1052.10	1278.82	1618.47	2246.62	2565.34	41	412.53	631.61	877.14	1146.90	1438.96	2083.24	2511.74
42	935.63	1168.52	1479.90	1705.91	2079.79	2728.19	42	692.78	929.90	1233.41	1477.03	1854.57	2543.05	3070.20	42	505.72	746.92	1016.42	1312.09	1632.07	2338.56	2995.57
43	998.12	1240.39	1565.45	1799.94	2190.26	2865.91	43	733.41	978.90	1293.64	1545.24	1936.76	2650.13	3385.24	43	531.24	779.76	1057.10	1361.25	1690.48	2418.13	3229.34
44	1219.30	1487.33	1852.41	2108.98	2546.90	3296.82	44	889.87	1162.35	1514.42	1791.04	2228.54	3019.86	3885.29	44	639.46	915.72	1223.15	1559.79	1923.94	2728.98	3627.88
45	1323.67	1602.02	1983.81	2248.72	2706.43	3486.27	45	958.19	1240.25	1605.90	1890.77	2344.83	3183.33	4059.14	45	682.78	987.72	1284.21	1630.41	2004.74	2832.39	3757.57
46	1640.51	1955.20	2393.70	2689.62	3214.66	4098.95	46	1177.99	1497.49	1915.04	2234.46	2752.23	3678.02	4691.24	46	831.95	1154.87	1512.46	1902.92	2324.68	3256.75	4299.22
47	1741.97	2067.13	2522.29	2826.62	3371.22	4284.95	47	1239.42	1567.63	1997.37	2324.05	2856.40	3805.81	4844.57	47	867.40	1197.27	1561.88	1959.53	2388.76	3336.95	4397.87
48	2166.60	2524.61	3037.73	3366.86	3979.83	4990.69	48	1527.68	1890.84	2372.18	2728.38	3323.47	4371.53	5517.57	48	1058.49	1424.46	1827.45	2265.83	2738.25	3780.49	4945.93
49	2488.15	2864.19	3413.38	3753.94	4409.09	5474.68	49	1737.18	2118.98	2629.86	2999.81	3630.30	4729.58	5930.38	49	1191.25	1575.85	1997.95	2456.09	2949.02	4034.99	5248.42
50	2865.82	3265.10	3859.00	4215.21	4822.78	6058.17	50	1979.97	2385.27	2932.58	3320.54	3994.77	5158.67	6428.40	50	1343.18	1750.86	2196.85	2679.81	3198.58	4339.64	5613.18

Table A.4 – Value of ultimate bearing capacity obtained from Test No. 4

α=	5 (Test No. 4-1)						α=	10 (Test No. 4-2)						α=	15 (Test No. 4-3)					
b/B=	0.0	1.0	2.0	3.0	4.0	6.0	b/B=	0.0	1.0	2.0	3.0	4.0	6.0	b/B=	0.0	1.0	2.0	3.0	4.0	6.0
ϕ= 5	29.84	30.25	30.95	30.94	31.01	31.04														
6	31.37	31.78	32.35	32.68	32.57	32.57														
7	32.90	33.43	34.00	34.20	34.27	34.33														
8	34.59	34.98	35.74	36.02	36.06	36.02														
9	36.34	36.87	37.61	37.81	37.85	37.91														
10	38.10	38.84	39.52	39.86	39.98	39.93	ϕ=10	37.25	38.39	39.45	39.92	40.06	40.01							
11	40.20	40.86	41.69	42.07	42.10	42.12	11	39.17	40.59	41.61	42.17	42.09	42.21							
12	42.31	43.35	43.92	44.19	44.22	44.12	12	41.27	42.66	43.89	44.11	44.17	44.15							
13	44.67	45.32	45.94	46.07	46.00	45.88	13	42.11	44.83	45.80	45.93	46.10	45.95							
14	47.06	48.14	48.20	48.26	48.27	48.30	14	44.23	47.35	48.18	48.42	48.45	48.33							
15	49.87	50.81	51.25	51.13	51.22	51.33	15	46.77	49.40	50.70	51.12	51.09	51.22	ϕ=15	44.31	48.42	50.30	51.03	51.30	51.15
16	52.57	54.38	54.68	54.73	54.70	54.49	16	49.38	52.92	54.61	54.77	54.81	54.54	16	46.70	51.27	53.18	54.66	54.79	54.58
17	56.01	57.90	58.26	58.36	58.25	58.14	17	52.42	56.25	57.77	58.16	58.12	58.15	17	49.48	54.63	56.85	58.18	58.10	58.23
18	59.02	60.84	61.40	61.55	61.66	61.26	18	55.13	59.22	60.74	61.46	61.43	61.44	18	50.68	56.15	59.86	61.43	61.54	61.52
19	62.65	64.97	65.77	65.73	65.70	65.55	19	58.49	62.79	65.32	65.74	65.41	65.61	19	55.07	60.49	63.21	65.24	66.01	65.62
20	66.64	69.53	69.89	70.21	70.11	69.89	20	62.04	66.01	69.90	69.98	70.28	69.99	20	58.23	63.39	68.41	70.09	70.10	70.10
21	70.95	74.23	74.80	74.89	74.75	75.00	21	66.01	70.26	74.48	74.75	74.68	74.82	21	61.94	67.66	74.12	74.71	74.73	74.94
22	75.57	79.07	79.88	79.97	79.90	79.45	22	69.86	74.45	79.55	79.77	79.53	79.19	22	63.70	71.02	76.56	79.92	79.36	79.65
23	80.51	82.28	85.20	85.42	85.18	84.79	23	74.09	78.58	84.45	85.01	84.96	84.53	23	67.41	75.31	80.92	84.96	84.93	84.79
24	84.31	88.20	91.08	91.20	90.88	91.02	24	79.08	84.51	88.19	90.61	90.79	90.82	24	71.68	78.59	86.81	91.13	91.03	91.17
25	92.87	93.97	97.00	97.04	96.91	97.25	25	84.63	88.27	93.82	97.10	96.62	97.42	25	76.70	83.70	92.11	97.01	97.21	97.05
26	97.88	101.62	106.22	105.89	105.69	105.54	26	90.38	95.49	101.84	105.99	105.10	105.00	26	81.70	90.13	97.21	105.55	105.52	104.98
27	102.28	111.11	113.76	114.33	113.89	114.80	27	98.39	102.58	109.59	114.24	113.80	114.41	27	89.34	96.24	104.27	113.52	113.52	114.44
28	115.21	120.47	124.96	125.81	125.61	125.85	28	106.35	112.15	120.00	125.18	125.16	125.63	28	95.80	105.16	113.34	121.92	125.18	125.63
29	126.75	132.33	138.16	138.69	138.60	138.80	29	118.16	122.89	131.54	137.96	138.62	139.04	29	105.27	115.09	123.76	133.60	138.50	139.03
30	136.08	141.23	143.58	148.24	148.46	147.51	30	123.87	130.34	135.95	143.20	148.00	148.24	30	110.87	121.94	130.71	141.38	148.60	148.18
31	145.29	152.95	159.14	160.48	160.45	161.22	31	133.13	141.13	147.12	155.23	158.81	160.43	31	118.68	130.61	140.61	152.21	159.71	161.03
32	155.47	164.52	167.44	172.44	173.42	173.97	32	143.70	149.98	157.22	166.07	172.86	173.53	32	126.72	138.95	149.96	158.73	172.74	172.73
33	167.92	174.04	177.40	182.50	183.25	184.87	33	151.53	158.92	166.05	175.70	184.13	185.48	33	134.22	146.66	157.90	166.85	178.40	184.86
34	184.24	187.01	190.22	198.73	200.96	199.79	34	163.51	171.45	178.21	188.88	197.19	199.15	34	143.35	153.42	164.79	179.86	188.70	208.17
35	199.47	208.92	213.72	216.89	218.95	221.35	35	177.15	188.85	197.04	203.83	215.73	214.55	35	156.12	167.61	179.81	195.90	205.60	221.97
36	216.09	222.03	225.42	228.32	235.83	235.31	36	188.97	198.09	207.25	214.74	226.39	234.76	36	165.12	175.95	188.87	202.07	216.49	238.76
37	228.49	235.04	244.46	247.03	254.60	253.99	37	204.29	215.02	223.56	230.71	243.40	260.65	37	176.64	188.83	202.20	216.30	232.59	253.46
38	250.47	268.02	272.38	275.08	284.97	283.41	38	225.42	237.79	244.82	255.44	271.32	288.11	38	198.99	213.01	224.41	239.41	257.83	284.13
39	251.34	302.75	305.87	317.92	324.48	321.03	39	252.57	266.03	280.62	291.82	300.82	323.28	39	223.97	236.84	250.56	267.33	285.05	317.93
40	276.81	351.70	357.74	361.07	370.87	370.31	40	286.62	304.70	323.19	333.16	342.31	368.41	40	252.47	272.77	286.18	304.45	326.18	364.43
41	278.51	378.95	388.03	392.12	401.46	401.37	41	309.86	330.15	348.56	359.93	370.29	402.00	41	271.78	291.99	307.60	326.62	351.50	386.59
42	308.71	415.54	424.82	429.89	445.14	439.47	42	330.16	359.89	381.07	393.12	404.21	435.72	42	295.35	319.14	334.34	354.64	371.86	410.63
43	345.07	488.50	488.91	494.26	508.82	506.94	43	379.18	416.21	437.56	450.90	461.92	492.16	43	337.63	365.97	383.50	404.16	423.00	466.88
44	375.81	552.64	567.56	576.28	573.09	582.20	44	423.10	483.09	498.35	508.16	527.36	560.37	44	376.42	414.12	433.91	457.96	489.74	526.94
45	399.53	603.89	614.90	631.17	635.11	634.87	45	410.92	525.06	544.34	558.46	573.06	609.74	45	393.73	443.49	467.54	493.72	516.66	569.11
46	482.53	683.59	696.03	719.37	720.75	718.44	46	472.86	579.72	599.10	631.84	644.92	690.93	46	439.94	496.45	522.17	553.14	576.83	637.02
47	641.74	773.17	784.01	812.77	812.89	808.03	47	612.50	653.34	671.65	706.23	722.71	771.91	47	483.03	562.11	584.07	614.94	640.30	705.63
48	694.15	870.86	872.02	878.89	885.49	892.34	48	661.76	719.68	740.00	759.71	796.58	830.65	48	537.34	599.95	638.69	669.10	697.36	749.33
49	774.69	961.22	975.33	999.68	1000.45	1000.32	49	753.13	813.37	822.80	864.63	882.71	916.77	49	613.23	665.07	708.42	740.73	769.09	825.35
50	769.17	1038.53	1088.24	1094.49	1091.28	1099.86	50	813.09	886.26	899.43	942.76	964.06	1000.94	50	669.59	722.30	767.84	802.25	831.77	890.03

Table A.4 – Value of ultimate bearing capacity obtained from Test No. 4 (Cont'd)

α=	20 (Test No. 4-4)						α=	25 (Test No. 4-5)						α=	30 (Test No. 4-6)						
b/B=	0.0	1.0	2.0	3.0	4.0	6.0	b/B=	0.0	1.0	2.0	3.0	4.0	6.0	b/B=	0.0	1.0	2.0	3.0	4.0	6.0	8.0
ϕ=20	53.82	61.18	65.57	68.75	70.16	69.87															
21	57.17	64.05	71.59	73.59	74.72	74.90															
22	58.62	66.88	74.64	78.06	79.51	79.39															
23	61.88	70.99	79.56	83.26	84.98	85.13															
24	65.63	75.46	83.35	89.85	90.86	91.09															
25	70.11	79.10	89.29	95.52	96.60	97.01	ϕ=25	63.94	74.20	85.78	93.24	95.51	96.90								
26	74.88	84.44	93.72	105.98	105.11	104.91	26	68.22	79.17	92.02	102.95	104.63	105.20								
27	80.06	90.02	102.24	111.83	113.43	113.89	27	72.90	84.29	97.43	107.18	110.74	114.53								
28	87.05	98.06	108.35	119.62	124.48	125.81	28	77.59	91.70	103.74	118.79	121.56	126.16								
29	95.29	107.33	118.57	131.79	138.37	138.97	29	84.23	99.96	113.10	128.71	137.54	138.97								
30	100.18	112.52	124.34	134.95	148.06	148.10	30	88.06	104.59	118.08	134.49	146.39	148.07	ϕ=30	79.54	94.75	111.73	130.90	137.98	145.52	148.33
31	106.98	120.56	132.83	147.53	156.44	159.89	31	94.47	111.37	125.36	141.61	152.03	160.20	31	84.81	101.00	118.80	138.96	146.09	155.51	160.22
32	113.45	127.92	141.61	153.93	166.82	172.68	32	102.12	115.67	132.92	151.08	166.82	172.21	32	89.26	108.80	125.25	142.78	154.70	167.51	172.20
33	119.50	134.19	148.21	161.06	176.40	184.23	33	104.34	120.68	139.14	153.78	172.35	184.06	33	92.84	110.23	130.11	150.14	165.31	177.27	184.52
34	128.10	140.04	154.26	168.51	185.23	206.64	34	111.00	128.33	144.29	164.61	180.68	207.79	34	98.39	116.67	134.95	155.74	176.09	198.00	207.73
35	138.52	151.67	167.71	185.91	200.81	226.09	35	120.07	138.26	156.14	173.80	195.01	226.81	35	105.80	125.38	148.14	166.93	188.43	211.57	222.27
36	146.30	159.08	175.10	190.55	209.55	242.05	36	128.03	144.57	162.51	180.65	202.79	239.60	36	110.45	130.55	150.64	174.62	193.73	230.21	246.05
37	155.64	169.40	186.23	202.57	218.98	259.38	37	136.10	153.38	172.37	191.13	213.62	255.25	37	116.97	137.98	158.74	184.24	204.86	247.12	264.87
38	170.09	190.28	204.65	223.47	240.24	280.77	38	148.13	167.39	188.03	209.19	234.12	274.24	38	127.30	150.44	172.76	199.31	221.30	271.24	297.89
39	193.56	211.28	232.85	248.01	267.24	308.74	39	166.07	187.92	212.50	230.88	258.33	302.65	39	142.77	169.05	193.92	217.58	242.18	295.98	329.86
40	215.73	239.50	259.77	281.85	303.65	351.48	40	188.75	212.18	240.23	260.86	285.66	340.30	40	162.87	190.39	218.36	244.51	276.98	331.39	372.51
41	231.17	257.87	277.67	301.36	323.72	389.70	41	196.88	226.67	250.38	277.01	303.19	360.05	41	189.45	202.08	230.74	259.32	287.05	347.58	399.45
42	245.83	278.50	300.46	325.60	348.17	396.91	42	209.22	244.04	268.77	297.84	325.19	383.97	42	183.37	215.76	240.60	270.95	307.40	366.48	431.23
43	278.19	315.49	341.38	369.04	394.20	449.80	43	238.21	275.57	303.81	335.43	366.78	433.20	43	209.38	242.50	269.62	304.12	337.49	412.92	483.23
44	309.37	356.09	383.87	414.73	442.67	507.40	44	266.31	308.06	339.54	374.84	409.04	471.36	44	231.58	269.75	300.97	338.38	374.63	458.11	536.67
45	308.86	381.00	410.45	444.27	474.74	529.24	45	284.85	328.91	361.44	399.37	434.94	500.63	45	242.45	285.75	318.53	356.62	395.65	471.38	557.81
46	342.82	427.21	458.53	495.04	526.41	585.32	46	322.51	366.98	400.25	441.84	469.49	551.55	46	275.07	308.53	350.48	391.87	433.50	514.79	597.09
47	381.24	476.34	509.09	533.96	580.88	643.17	47	361.11	396.27	441.53	473.87	512.85	601.29	47	302.03	339.36	384.99	429.28	462.44	560.19	645.16
48	436.21	504.51	551.25	576.22	612.45	691.87	48	390.42	426.86	476.51	507.40	549.08	643.62	48	322.70	364.22	410.86	446.97	492.31	580.67	683.84
49	511.70	557.77	606.34	631.64	668.95	755.65	49	428.07	468.43	507.03	551.72	595.20	678.65	49	350.96	395.83	435.15	483.73	530.57	623.39	732.03
50	564.69	600.99	636.39	678.18	717.37	809.70	50	453.77	501.98	541.12	586.91	631.46	719.19	50	367.21	413.48	461.82	510.72	559.11	654.37	750.64

Table A.5 – Value of ultimate bearing capacity obtained from Test No. 5

α=	5 (Test No. 5-1)						α=	10 (Test No. 5-2)						α=	15 (Test No. 5-3)					
b/B=	0.0	1.0	2.0	3.0	4.0	6.0	b/B=	0.0	1.0	2.0	3.0	4.0	6.0	b/B=	0.0	1.0	2.0	3.0	4.0	6.0
ϕ= 5	37.91	38.27	38.15	37.04	36.65	38.35														
6	39.92	40.37	40.08	39.24	38.35	40.42														
7	42.22	42.50	42.30	40.93	41.47	42.79														
8	44.44	44.83	44.47	43.40	43.57	45.11														
9	46.92	47.13	46.90	45.25	45.93	47.69														
10	49.55	49.90	49.51	48.22	48.47	50.45	ϕ=10	49.38	49.74	49.36	48.08	48.41	47.76							
11	52.40	52.57	52.37	50.43	51.26	53.45	11	52.22	52.39	52.21	50.28	51.19	50.47							
12	55.02	55.35	55.00	53.47	53.81	56.24	12	54.82	55.16	54.82	53.31	53.74	52.96							
13	57.36	57.47	57.35	56.13	56.10	58.75	13	57.14	57.27	57.15	54.95	56.02	55.17							
14	60.51	60.83	60.57	58.82	59.25	62.12	14	60.28	60.61	60.36	58.62	59.16	58.24							
15	64.41	64.54	64.61	62.07	63.19	66.27	15	64.16	64.31	64.38	61.86	63.10	62.11	ϕ=15	63.96	64.11	64.20	61.69	63.03	62.06
16	68.47	68.85	68.72	66.83	67.32	70.61	16	68.20	68.60	68.49	66.60	67.23	66.17	16	67.98	68.39	68.29	66.41	67.15	66.11
17	73.15	73.34	73.49	70.87	72.13	75.61	17	72.86	73.08	73.23	70.63	72.03	70.91	17	72.63	72.85	73.02	70.43	71.95	70.85
18	77.16	77.65	77.56	75.74	76.29	79.98	18	76.86	77.36	77.29	75.49	76.18	75.00	18	76.62	77.13	77.06	75.28	76.10	74.93
19	82.63	82.93	83.17	80.60	82.01	85.89	19	82.31	82.63	82.88	80.33	81.90	80.65	19	82.05	82.38	82.65	80.11	81.81	80.58
20	88.15	88.82	88.84	87.26	87.84	91.90	20	87.82	88.51	88.54	86.98	87.72	86.41	20	87.54	88.25	88.29	86.74	87.63	86.33
21	94.62	95.11	95.53	93.17	94.74	98.97	21	94.27	94.78	95.21	92.87	94.61	93.23	21	93.99	94.51	94.95	92.63	94.51	93.15
22	100.27	101.19	101.36	100.23	100.84	105.25	22	99.91	100.84	101.03	99.92	100.71	99.26	22	99.60	100.56	100.76	99.66	100.60	99.17
23	106.99	107.70	108.33	106.43	108.15	112.73	23	106.61	107.34	107.99	106.10	108.02	106.51	23	106.29	107.04	107.70	105.83	107.90	106.42
24	114.80	116.07	116.47	115.88	116.73	121.47	24	114.40	115.69	116.11	115.54	116.59	115.02	24	114.08	115.37	115.82	115.26	116.47	114.92
25	122.58	123.63	124.60	122.79	125.40	130.30	25	122.17	123.24	124.22	122.44	125.25	123.62	25	121.83	122.92	123.91	122.15	125.12	123.51
26	132.86	134.62	135.39	134.99	136.89	141.93	26	132.43	134.21	135.00	134.63	136.74	135.05	26	132.08	133.87	134.68	134.32	136.61	134.94
27	144.27	145.89	147.40	145.65	149.80	154.97	27	143.83	145.47	147.00	145.27	149.64	147.90	27	143.46	145.11	146.67	144.95	149.50	147.79
28	157.82	160.36	161.71	161.68	165.26	170.56	28	157.36	159.91	161.29	161.29	165.09	163.31	28	156.23	159.55	160.94	160.96	164.95	163.19
29	173.60	176.07	178.42	176.82	178.60	188.88	29	173.12	175.62	177.99	176.42	178.22	174.28	29	170.30	175.24	177.63	176.08	182.92	181.35
30	184.03	187.45	189.49	189.92	190.02	201.69	30	183.53	186.98	189.04	189.50	189.63	186.68	30	178.90	186.58	188.67	189.14	194.49	193.95
31	200.40	203.74	206.93	205.55	208.07	221.44	31	199.89	203.25	206.46	205.11	207.66	206.10	31	193.13	202.84	206.08	204.75	207.32	213.53
32	215.39	219.97	222.94	224.00	224.69	240.13	32	214.86	219.47	222.46	223.55	224.27	224.44	32	205.82	218.38	222.06	223.18	223.91	232.05
33	227.83	232.14	236.29	235.22	238.61	256.50	33	227.29	231.62	235.80	234.75	238.17	240.43	33	215.95	228.16	235.39	234.37	237.81	248.23
34	244.82	250.61	254.55	256.33	257.68	278.66	34	244.26	250.07	254.05	255.85	257.23	262.27	34	230.30	243.98	253.63	255.46	256.85	270.23
35	269.36	275.25	280.96	280.47	285.28	294.16	35	268.48	274.70	280.44	279.98	284.82	293.76	35	251.63	265.60	279.68	279.57	284.43	301.82
36	284.98	292.52	297.93	300.81	303.17	315.09	36	283.13	291.96	297.40	300.30	302.69	314.68	36	264.57	279.94	293.53	299.88	302.30	314.33
37	307.13	314.68	322.02	322.26	328.57	342.34	37	304.50	314.10	321.47	321.74	328.08	341.91	37	283.66	298.93	314.28	321.31	327.67	341.56
38	341.60	351.83	359.48	364.09	368.06	384.70	38	338.42	350.59	358.92	363.55	367.55	384.27	38	314.26	332.18	347.94	360.91	367.14	383.90
39	385.01	396.02	406.79	408.59	418.04	438.44	39	381.75	394.20	406.20	408.04	417.53	437.99	39	353.32	372.13	390.98	401.30	417.10	437.61
40	440.95	456.10	467.93	475.79	482.81	508.22	40	438.47	454.37	467.04	475.23	482.29	507.76	40	404.42	427.28	447.33	463.73	479.42	507.37
41	473.61	489.09	504.29	508.38	521.94	550.95	41	473.38	488.68	503.76	507.80	521.40	550.48	41	435.02	457.68	480.34	492.50	513.97	550.08
42	512.28	531.83	547.55	558.61	568.68	602.16	42	516.21	534.45	548.87	558.70	568.13	601.67	42	472.57	498.42	520.93	539.17	556.54	601.27
43	581.36	603.07	624.45	632.07	651.42	692.49	43	592.83	611.67	630.21	634.95	651.61	692.00	43	540.55	567.95	595.29	609.60	635.37	690.04
44	653.84	682.35	705.96	723.57	739.87	789.75	44	677.79	701.52	720.20	732.85	744.32	789.24	44	615.45	648.39	676.91	699.83	721.62	782.77
45	697.98	724.15	753.56	766.36	793.33	850.18	45	735.96	758.71	781.04	786.30	806.26	849.66	45	665.34	697.85	730.23	746.62	776.98	841.31
46	787.04	801.05	829.37	854.49	878.01	945.52	46	829.07	857.17	879.06	893.59	906.67	954.20	46	746.08	784.44	817.39	843.55	868.31	938.76
47	882.06	894.76	906.72	920.37	958.27	1037.71	47	928.19	955.92	983.07	988.76	1012.91	1064.93	47	831.25	870.19	908.89	927.68	963.77	1040.20
48	970.74	987.86	997.58	998.95	1016.46	1107.91	48	1020.33	1053.59	1079.18	1095.72	1110.51	1166.10	48	909.14	953.78	991.75	1021.47	1049.46	1130.52
49	1084.38	1099.72	1114.12	1104.32	1115.27	1187.13	49	1138.38	1170.79	1202.44	1207.86	1235.81	1296.13	49	1008.93	1053.71	1098.10	1118.46	1159.63	1246.82
50	1188.20	1208.74	1220.20	1221.46	1220.92	1248.18	50	1245.68	1284.40	1313.71	1332.02	1348.20	1412.02	50	1097.84	1148.88	1191.81	1224.79	1255.70	1347.28

Table A.5 – Value of ultimate bearing capacity obtained from Test No. 5 (Cont'd)

α=	20 (Test No. 5-4)						α=	25 (Test No. 5-5)						α=	30 (Test No. 5-6)						
b/B=	0.0	1.0	2.0	3.0	4.0	6.0	b/B=	0.0	1.0	2.0	3.0	4.0	6.0	b/B=	0.0	1.0	2.0	3.0	4.0	6.0	8.0
ϕ=20	87.32	88.03	88.09	86.55	87.55	86.27															
21	93.75	94.28	94.74	92.42	94.42	93.08															
22	98.95	100.32	100.53	99.45	100.51	99.10															
23	104.37	106.79	107.47	105.61	107.81	106.34															
24	110.70	115.12	115.57	115.03	116.37	114.84															
25	116.82	122.65	123.68	121.91	125.02	123.43	ϕ=25	108.12	120.95	123.44	121.70	124.93	123.36								
26	125.14	133.59	134.41	134.07	136.50	134.85	26	115.54	129.54	134.19	133.86	136.41	134.78								
27	134.31	144.82	146.39	144.69	149.39	147.69	27	123.68	138.06	146.16	144.47	149.29	147.61								
28	145.21	158.28	160.66	160.69	164.83	163.09	28	133.37	149.24	160.42	160.46	164.74	163.01								
29	157.87	171.42	177.33	175.79	182.79	181.25	29	144.60	161.14	177.08	175.56	182.69	181.16								
30	165.39	179.98	188.36	188.85	194.36	193.84	30	151.06	168.64	185.85	188.61	194.25	193.75	ϕ=30	136.91	157.04	177.24	188.40	188.59	193.67	192.74
31	178.04	192.96	205.76	204.44	207.03	205.55	31	162.14	180.22	199.05	204.19	206.79	205.33	31	146.52	167.28	189.16	203.98	206.59	213.24	212.36
32	189.19	205.53	220.89	222.87	223.62	223.87	32	171.76	191.32	210.31	222.60	223.37	223.85	32	154.74	177.00	199.14	220.68	223.16	231.75	230.91
33	197.89	214.00	230.49	234.05	237.50	239.85	33	179.10	198.51	218.61	233.77	237.24	239.62	33	160.84	183.01	206.21	225.70	237.02	247.92	247.10
34	210.37	228.04	244.54	255.13	256.54	261.67	34	189.78	210.79	231.04	249.95	256.27	261.43	34	169.87	193.63	217.10	239.68	256.05	269.90	269.15
35	229.12	247.36	265.96	278.92	284.11	293.13	35	205.99	227.81	250.29	267.70	283.84	292.89	35	183.76	208.52	234.27	255.62	282.73	301.49	300.87
36	240.07	259.73	277.98	294.19	301.96	314.03	36	215.08	238.29	260.52	281.10	301.68	313.78	36	191.20	217.27	242.84	267.24	291.99	322.56	323.21
37	256.49	276.28	296.38	310.15	327.33	341.25	37	228.95	252.47	276.56	294.99	319.45	341.00	37	202.78	229.30	256.74	279.18	307.70	340.77	344.60
38	283.12	305.79	326.72	345.18	363.27	383.59	38	251.77	278.31	303.58	326.81	349.91	383.32	38	222.15	251.75	280.60	307.91	335.43	383.09	392.94
39	317.11	341.15	365.51	381.99	405.88	437.30	39	280.90	309.20	338.11	359.94	389.00	437.02	39	246.88	278.54	311.16	337.55	371.07	436.79	455.17
40	361.53	390.06	416.28	439.28	461.73	507.04	40	318.95	351.99	383.31	411.93	440.26	506.76	40	279.17	315.73	351.17	384.49	417.87	498.34	537.09
41	387.28	415.91	444.82	464.11	492.29	549.75	41	340.20	373.59	407.60	432.96	466.86	539.16	41	296.50	333.57	371.61	402.06	440.78	523.99	583.81
42	418.88	450.81	479.99	505.38	530.06	593.28	42	366.33	403.01	437.58	468.95	499.86	575.80	42	317.86	358.13	396.96	433.22	469.37	556.30	639.97
43	476.99	511.20	545.66	568.26	601.65	672.34	43	415.22	454.75	494.88	524.43	564.16	648.50	43	358.60	402.14	446.66	481.90	526.83	622.81	731.66
44	540.53	580.65	617.13	648.67	679.23	757.69	44	468.25	513.88	556.66	595.26	633.14	726.18	44	402.45	452.11	499.75	543.97	587.86	693.13	812.11
45	581.46	621.60	661.94	687.84	726.71	808.78	45	501.15	547.12	593.64	627.39	673.15	769.95	45	428.54	478.75	529.93	569.95	621.21	730.17	853.02
46	648.65	694.84	736.56	772.31	806.83	896.09	46	556.10	608.13	656.64	700.07	742.55	847.21	46	473.01	529.16	582.73	632.14	680.97	798.14	929.89
47	718.79	766.30	813.93	843.78	889.42	985.62	47	612.82	666.69	721.09	759.86	813.04	925.20	47	518.35	576.70	636.00	681.76	740.75	865.62	1005.72
48	781.68	834.76	882.35	922.72	961.56	1062.96	48	662.55	721.73	776.57	825.28	872.76	990.32	48	557.15	620.45	680.51	735.52	789.69	919.88	1065.69
49	862.30	916.30	970.31	1003.09	1054.57	1162.94	49	726.42	787.05	848.13	880.74	950.11	1075.02	49	607.13	672.22	738.19	788.31	853.52	991.10	1144.91
50	932.41	992.32	1045.57	1090.20	1132.97	1246.09	50	780.44	846.50	907.30	960.82	1012.80	1142.43	50	648.08	718.05	784.06	844.07	902.95	1044.96	1203.53

Table A.6 – Value of ultimate bearing capacity obtained from Test No. 6 (Reference tests)

	q_u, kN/m/m			Bearing Capacity Factor (eq. 3.1a, b & c)			Meyerhof's Bearing Capacity Factor (eq. 2.4a, b & c)				q_u, kN/m/m			Bearing Capacity Factor (eq. 3.1a, b & c)			Meyerhof's Bearing Capacity Factor (eq. 2.4a, b & c)		
ϕ^o	Test No. 6-1	Test No. 6-2	Test No. 6-3	N_c	N_γ	N_q	N_c	N_γ	N_q	ϕ^o	Test No. 6-1	Test No. 6-2	Test No. 6-3	N_c	N_γ	N_q	N_c	N_γ	N_q
5	31.35	4.29	29.91	6.27	0.48	1.42	6.49	0.07	1.57	28	127	116	333	25.42	12.86	9.45	25.80	11.19	14.72
6	32.90	4.95	33.56	6.58	0.55	1.59	6.81	0.11	1.72	29	140	134	376	28.04	14.84	10.43	27.86	13.24	16.44
7	34.67	5.71	35.37	6.93	0.63	1.65	7.16	0.15	1.88	30	149	146	424	29.80	16.20	11.97	30.14	15.67	18.40
8	36.38	6.59	39.74	7.28	0.73	1.84	7.53	0.21	2.06	31	163	170	480	32.57	18.90	13.24	32.67	18.56	20.63
9	38.29	7.61	41.69	7.66	0.85	1.89	7.92	0.28	2.25	32	176	198	545	35.14	22.04	14.62	35.49	22.02	23.18
10	40.32	8.78	44.40	8.06	0.98	1.98	8.34	0.37	2.47	33	187	231	661	37.34	25.70	18.15	38.64	26.17	26.09
11	42.54	10.13	55.67	8.51	1.13	2.20	8.80	0.47	2.71	34	202	286	815	40.36	31.77	22.23	42.16	31.15	29.44
12	44.56	11.69	58.07	8.91	1.30	2.22	9.28	0.60	2.97	35	224	346	990	44.71	38.44	26.92	46.12	37.15	33.30
13	46.34	13.49	65.29	9.27	1.50	2.47	9.81	0.74	3.26	36	238	441	1222	47.67	48.99	32.27	50.59	44.43	37.75
14	48.79	15.57	73.41	9.76	1.73	2.75	10.37	0.92	3.59	37	259	517	1385	51.86	57.39	35.42	55.63	53.27	42.92
15	51.85	17.97	76.78	10.37	2.00	2.78	10.98	1.13	3.94	38	292	645	1690	58.33	71.72	42.03	61.35	64.07	48.93
16	55.03	20.74	86.38	11.01	2.30	3.08	11.63	1.37	4.34	39	333	789	2109	66.62	87.65	53.04	67.87	77.33	55.96
17	58.72	23.94	89.44	11.74	2.66	3.05	12.34	1.66	4.77	40	388	947	2500	77.50	105.2	61.75	75.31	93.69	64.20
18	61.87	27.62	100.68	12.37	3.07	3.38	13.10	2.00	5.26	41	424	1120	3119	84.74	124.4	79.87	83.86	114.0	73.90
19	66.21	31.88	113.41	13.24	3.54	3.75	13.93	2.40	5.80	42	468	1472	3715	93.61	163.5	86.78	93.71	139.3	85.37
20	70.59	36.79	127.88	14.12	4.09	4.17	14.83	2.87	6.40	43	545	1738	4329	109.0	193.1	99.00	105.1	171.1	99.01
21	75.75	42.46	144.11	15.15	4.72	4.63	15.81	3.42	7.07	44	632	2202	5220	126.3	244.7	112.3	118.4	211.4	115.3
22	80.25	49.00	175.61	16.05	5.44	5.77	16.88	4.07	7.82	45	696	2657	6131	139.1	295.2	126.8	133.9	262.7	134.9
23	85.63	56.55	197.64	17.13	6.28	6.40	18.05	4.82	8.66	46	795	3407	7582	159.0	378.5	148.4	152.1	328.7	158.5
24	91.93	65.26	222.39	18.39	7.25	7.08	19.32	5.72	9.60	47	903	3975	8863	180.7	441.7	171.9	173.6	414.3	187.2
25	98.23	75.31	250.39	19.65	8.37	7.84	20.72	6.77	10.66	48	1008	5177	10833	201.6	575.2	189.9	199.3	526.5	222.3
26	106.60	86.917	261.99	21.32	9.66	7.72	22.25	8.00	11.85	49	1142.3	6613.5	13135.6	228.5	734.8	208.3	229.9	674.9	265.5
27	115.95	100.31	295.54	23.19	11.15	8.54	23.94	9.46	13.20	50	1269.9	7905.5	15463.6	254.0	878.4	234.7	266.9	873.9	319.1

Table A.7 – Value of ultimate bearing capacity obtained from Test No. 7 & 8 (B≠1)

Test No. 7 (B=0.5) Ultimate Bearing Capacity, kN/m/m						Test No. 8 (B=1.5) Ultimate Bearing Capacity, kN/m/m					
α=	5 (Test No. 7-1)					α=	5 (Test No. 8-1)				
b=	0.0	1.0	2.0	4.0	6.0	*b*=	0.0	1.0	2.0	4.0	6.0
b/B=	0.0	2.0	4.0	8.0	12.0	*b/B*=	0.0	0.7	1.3	2.7	4.0
ϕ= 5	2.47	2.30	2.30	2.38	2.33	ϕ= 5	6.01	6.21	6.41	6.43	6.53
10	4.89	5.18	4.96	4.51	5.01	10	12.22	12.61	13.14	13.23	13.21
15	9.24	9.80	9.66	9.92	9.90	15	24.34	24.91	26.41	26.94	27.55
20	18.04	19.13	19.98	19.32	19.11	20	48.85	49.90	53.32	55.06	55.16
25	39.36	37.33	39.79	38.26	37.67	25	95.36	101.19	106.70	111.10	114.01
30	72.81	66.55	77.06	78.92	78.97	30	182.21	189.66	199.33	211.18	221.36
35	152.53	150.33	168.94	186.65	181.32	35	416.80	433.69	457.61	480.72	495.54
40	397.37	424.86	449.94	577.55	574.88	40	1087.56	1151.57	1200.96	1241.73	1286.43
45	1129.53	1115.11	1085.93	1309.55	1376.93	45	2934.48	3067.34	3150.68	3278.39	3403.26
50	3243.19	2920.05	3333.14	3548.32	4026.45	50	8098.77	8558.57	8822.69	9085.44	9332.49
α=	15 (Test No. 7-2)					α=	15 (Test No. 8-2)				
b=	0.0	1.0	2.0	4.0	6.0	*b*=	0.0	1.0	2.0	4.0	6.0
b/B=	0.0	2.0	4.0	8.0	12.0	*b/B*=	0.0	0.7	1.3	2.7	4.0
15	7.55	9.42	9.25	9.40	9.19	15	18.31	22.43	26.39	27.01	28.18
20	14.60	19.05	20.29	18.10	20.09	20	35.38	43.93	52.76	54.92	55.94
25	25.55	30.53	40.16	40.54	40.45	25	67.63	82.21	102.76	109.49	118.20
30	43.76	54.25	75.65	81.96	81.03	30	122.87	139.26	173.47	192.27	214.12
35	100.56	109.61	142.14	175.79	185.32	35	260.56	312.05	373.27	416.46	474.07
40	250.16	266.01	345.03	630.14	643.74	40	649.68	719.57	838.70	963.65	1097.48
45	616.89	691.41	845.02	1436.50	2331.20	45	1495.37	1627.86	1890.08	2130.12	2332.10
50	1429.16	1701.40	1894.07	3058.78	4960.56	50	4047.67	4482.23	5030.94	5497.80	6055.43
α=	30 (Test No. 7-3)					α=	30 (Test No. 8-3)				
b=	0.0	1.0	2.0	4.0	6.0	*b*=	0.0	1.0	2.0	4.0	6.0
b/B=	0.0	2.0	4.0	8.0	12.0	*b/B*=	0.0	0.7	1.3	2.7	4.0
30	22.24	42.89	75.23	80.60	78.75	30	50.66	73.82	107.96	152.61	205.77
35	45.95	81.22	130.88	178.06	197.60	35	104.51	144.30	205.81	287.66	384.23
40	118.71	168.77	256.73	530.87	531.94	40	235.96	298.31	408.75	560.03	767.14
45	246.75	366.14	528.21	759.07	1055.99	45	524.75	620.07	813.54	1078.61	1418.91
50	539.40	754.81	945.43	2171.17	3046.81	50	1185.34	1364.06	1676.17	2158.79	2809.73

Table A.8 – Value of ultimate bearing capacity obtained from Test No. 9 & 10 (Cases considered)

Test No. 9 (B=1) Ultimate Bearing Capacity, kN/m/m				Test No. 10 (B=1.5) Ultimate Bearing Capacity, kN/m/m			
α=	5 (Test No. 9-1)			α=	5 (Test No. 10-1)		
b=	0.0	3.0	6.0	*b*=	0.0	3.0	6.0
b/B=	0.0	3.0	6.0	*b/B*=	0.0	2.0	4.0
10	192.5	197.6	197.4	10	293.1	299.81	297.94
20	464.2	488.0	486.9	20	453.80	460.55	497.50
30	1368.9	1496.0	1533.5	30	911.93	1007.8	1072.9
40	6335.2	7182.9	7873.3	40	2616.2	2924.3	3235.1
45	14355.4	16853.7	18981.0	45	4689.8	5233.2	5780.2
50	27837.6	34433.9	40710.2	50	8370.0	9470.0	10350.0
α=	15 (Test No. 9-2)			α=	15 (Test No. 10-2)		
b=	0.0	3.0	6.0	*b*=	0.0	3.0	6.0
b/B=	0.0	3.0	6.0	*b/B*=	0.0	2.0	4.0
20	412.0	491.6	490.4	20	424.61	538.87	554.20
30	1076.8	1430.3	1528.0	30	904.67	1057.25	1281.8
40	3249.9	5395.6	7265.0	40	2135.5	2692.2	3281.9
45	5616.7	9105.2	13738.4	45	3380.0	4290.0	5030.0
50	9468.0	14924.2	20447.3	50	5045.8	6500.0	7755.6
α=	30 (Test No. 9-3)			α=	30 (Test No. 10-3)		
b=	0.0	3.0	6.0	*b*=	0.0	3.0	6.0
b/B=	0.0	3.0	6.0	*b/B*=	0.0	2.0	4.0
30	623.4	1311.6	1533.5	30	568.36	799.4	1029.6
40	1504.0	3419.4	6274.1	40	1234.2	1777.7	2381.0
45	2360.1	5723.9	9502.9	45	1543.1	2308.2	3243.0
50	3568.0	8351.4	14207.3	50	2099.3	3091.7	4509.2

References

Andrew, M. (1986), Computation of bearing capacity coefficients for shallow footings on cohesionless slopes using stress characteristics, M.Sc. thesis, University of Manitoba, Winnipeg, Manitoba.

Bauer, G.E., Shields, D.H., Scott, J.D. and Gruspier, J.E. (1981), "Bearing Capacity of Footings in Granular Slopes." *Proceedings of the 10th International Conference on Soil Mechanics and Foundation Engineering*, Vol. 2, pp. 33-36.

Das, Braja M, "Foundation Engineering", Fourth Edition, PWS Publishing, New York 1998

DeBeer, E.E. (1965), "Bearing Capacity and settlement of shallow foundation on sand.", *Proceedings of the Symposium on Bearing capacity and Settlement of Foundation*, Duke University, pp.15-33.

Garnier, J., Canepa, Y., Corte, J.F., and Bakir, N.E. (1994), "Etude dela Portance de Foundations en Bord deTalus." *Proceedings of the 13th International Conference on Soil Mechanics and Foundation Engineering*, Vol. 2, pp. 705-708.

Gemperline, M. C. (1988). "Centrifuge modeling of shallow foundation." Proc., ASCE Spring Convention, ASCE

Giroud, J. P., and Tran, V.-N. 1971. "Force portante d'une foundation sur une pente.", Annales de l'Institut Technique du Batiment et des Travaux Publics, Supplement 283-284

Gottardi, G., Ricceri, G., and Simonini, P. (1994), "On the Scale Effect of Footing on Sand under General Loads.", *Proceedings of the 13th International Conference on Soil Mechanics and Foundation Engineering*, Vol. 2, pp. 709-712.

Graham, J. Andrews, M. and Sheilds, D.H., (1987). "Stress Characteristics for Shallow Footings in Cohesionless Slopes." *Canadian Geotechnical Journal*, Vol. 25, No. 2, pp. 238-249.

Kimura, T., Kasakabe, O., and Saitoh, K. 1985. Geotechnical model tests of bearing capacity problems in a centrifuge. Geotechnique, 35: 33-45

Meyerhof, G. G. (1951), "The Ultimate Bearing Capacity of Foundation", *Geotechnique*, Vol. 2, pp.. 301-332

Meyerhof, G. G. (1957), "The Ultimate Bearing Capacity of Foundation on Slopes", *Proceedings of the 4th International Conference on Soil Mechanics and Foundation Engineering*, Vol.3, pp. 384-386

Meyerhof, G. G. (1963), "Some Recent Research on the Bearing Capacity of Foundations", *Canadian Geotechnical Journal*, Vol. 1, No. 1, pp. 16-26.

Peynircioglu, H. (1948), "Tests on Bearing Capacity of Shallow Foundations Horizontal Top Surfaces of Sand Fills and the Behavior of Soils Under Such Foundations." *Proceedings of the 2nd InternationalConference on Soil Mechanics and Foundation Engineering*, Vol. 3, pp. 144-205.
Saran, S., Sud, V.K. and Handa, S.C., (1989). "Bearing Capacity of Footings Adjacent to Slopes." *Journal of Geotechnical Engineering*, ASCE, Vol. 115, No. GT4, pp. 553-573.

Shields, D.H., Scott, J.D., Bauer, G.E., Deschemes, J.H. and Barsvary, A.K., (1977). "Bearing Capacity of Foundations Near Slopes." *Proceedings of the 9th International Conference on Soil Mechanics and Foundation Engineering*, Vol. 1, pp. 715-720.

Shields, D.H., Chandler, N. and Garnier, J.(1990),. "Bearing Capacity of Foundation in Slopes". *Journal of Geotechnical Engineering*, ASCE, Vol. 116, No. GT3, pp. 528-537.

Tatsuoka, F., Huang, C.C., Morimoto, T. and Okahara, M. (1989),"Discussion of Stress Characteristics for Shallow Footings in Cohesionless Slopes. *Canadian Geotechnical Journal*, Vol. 26, No. 4, pp. 748-755.

Terzaghi, K (1943), *Theoretical Soil Mechanics*, John Wiley and Sons, New York

Vesic, A.S. (1973), "Analysis of Ultimate Loads of Shallow Foundations", Journal of the Soil Mechanics and Foundations Division, ASCE, Vol. 99 No. SM1, January, pp.45-73

Brinkgreve, R.B.J., "Plaxis™ User Manual"., A.A. Balkema Publishers, Netherlands, 2002